

Oxide pigments in water : the colloidchemical point of view

Citation for published version (APA):

Heijman, S. G. J. (1993). *Oxide pigments in water : the colloidchemical point of view*. [Phd Thesis 1 (Research TU/e / Graduation TU/e), Chemical Engineering and Chemistry]. Technische Universiteit Eindhoven.
<https://doi.org/10.6100/IR398131>

DOI:

[10.6100/IR398131](https://doi.org/10.6100/IR398131)

Document status and date:

Published: 01/01/1993

Document Version:

Publisher's PDF, also known as Version of Record (includes final page, issue and volume numbers)

Please check the document version of this publication:

- A submitted manuscript is the version of the article upon submission and before peer-review. There can be important differences between the submitted version and the official published version of record. People interested in the research are advised to contact the author for the final version of the publication, or visit the DOI to the publisher's website.
- The final author version and the galley proof are versions of the publication after peer review.
- The final published version features the final layout of the paper including the volume, issue and page numbers.

[Link to publication](#)

General rights

Copyright and moral rights for the publications made accessible in the public portal are retained by the authors and/or other copyright owners and it is a condition of accessing publications that users recognise and abide by the legal requirements associated with these rights.

- Users may download and print one copy of any publication from the public portal for the purpose of private study or research.
- You may not further distribute the material or use it for any profit-making activity or commercial gain
- You may freely distribute the URL identifying the publication in the public portal.

If the publication is distributed under the terms of Article 25fa of the Dutch Copyright Act, indicated by the "Taverne" license above, please follow below link for the End User Agreement:

www.tue.nl/taverne

Take down policy

If you believe that this document breaches copyright please contact us at:

openaccess@tue.nl

providing details and we will investigate your claim.

Oxide Pigments in Water:
The Colloidchemical Point of View

PROEFSCHRIFT

ter verkrijging van de graad van doctor aan de
Technische Universiteit Eindhoven, op gezag van
de Rector Magnificus, prof. dr. J.H. van Lint,
voor een commissie aangewezen door het College
van Dekanen in het openbaar te verdedigen op
woensdag 16 juni 1993 om 16.00 uur

door

SEBASTIAAN GERARD JOZEF HEIJMAN

Geboren te Heerlen

Dit proefschrift is goedgekeurd
door de promotoren
prof. dr. H.N. Stein
en
prof. ir. E.L.J. Bancken

CONTENTS

INTRODUCTION	0-1
--------------	-----

CHAPTER 1:

CHARACTERIZATION OF A THREE COMPONENT COLLOIDAL SYSTEM: TITANIUM DIOXIDE/POLYELECTROLYTE/WATER.

1.1	Introduction.	1-1
1.2	Titanium dioxide samples	1-1
1.3	Titration curves of the oxide/water system.	1-3
1.4	The polyelectrolyte samples.	1-8
1.5	Titration curves of the polyelectrolyte/water solution.	1-8
1.6	Mobility measurements with the three component system: PAA/oxide/water.	1-12
1.7	Titration experiments with the three component system: polyelectrolyte/oxide/water.	1-15
1.8	The adsorption of PAA on the oxide surface.	1-16
1.9	Theoretical approach of the three component system	1-18

CHAPTER 2:

THE CHANGE IN CHARGES OF TITANIUM DIOXIDE AND POLYACRYLIC ACID DUE TO THE ADSORPTION OF THE POLYMER ON THE OXIDE SURFACE.

2.1	Introduction	2-1
2.2	Experimental procedures	2-3
2.3	Results and discussion	2-5
2.4	Conclusions	2-15

CHAPTER 3:

THE HYDRODYNAMIC LAYER THICKNESS OF ADSORBED POLYACRYLIC ACID ON TITANIUM DIOXIDE.

3.1	Introduction	3-1
3.2	Experimental procedures	3-2
3.2.1	Materials and reagents	
3.2.2	Experimental methods	
3.3	Theory	3-4
3.3.1	The electroviscous effect	
3.3.2	Calculation of the hydrodynamic layer thickness from experimental data.	
3.4	Results and discussion	3-16
3.5	Conclusions	3-24

CHAPTER 4:

MONODISPERSE PIGMENT PARTICLES.

4.1	Introduction	4-1
4.2	Materials and methods	4-2
4.3	Results and discussion.	4-11
4.4	Conclusions	4-12

CHAPTER 5:

WETTING BEHAVIOUR OF OXIDES IN WATER.

5.1	Introduction	5-1
5.2	Theory	5-1
5.2.1	The theory of wetting of a sessile drop.	
5.2.2	The theory of the wetting of powders.	
5.2.3	The theory of wetting of a packed bed.	
5.3	Results and discussion	5-12
5.4	Conclusions	5-15

CHAPTER 6:

THE STABILITY OF TITANIUM DIOXIDE/WATER DISPERSIONS.

6.1	Introduction	6-1
6.2	Stability of dilute titanium dioxide suspensions.	6-2
6.4	Stability of TiO ₂ dispersions at high volume fractions ($\phi=0.16$).	6-7
6.5	The influence of a thin polymer layer on the colloidal stability.	6-16
6.6	Consequences for dispersion process of pigments in water.	6-21
6.7	Conclusions	6-22

CHAPTER 7:

POSSIBLE IMPROVEMENTS IN THE DISPERSION PROCESS OF PIGMENTS IN WATER: PRELIMINARY INVESTIGATION.

7.1	Introduction	7-1
7.2	Theoretical considerations	7-4
7.3	Experimental set up	7-6
7.4	Materials	7-10
7.5	Equipment	7-11
7.6	Results and discussion	7-12
7.7	Conclusions	7-14

CHAPTER 8:

THE INFLUENCE OF THE DISPERSING AGENT POLYACRYLIC ACID ON TITANIUM DIOXIDE IN WATER-BASED PAINTS.

8.1	Introduction	8-1
8.2	The wetting of the dry aggregate by the water phase.	8-2
8.3	The milling process.	8-3
8.4	The stabilization of the pigment during the dispersion process.	8-4
8.5	Bridge forming properties of polyacrylic acid.	8-7
8.6	Coagulation under influence of brownian motion	8-9
8.8	Coagulation during the drying process of a paint film.	8-9
8.9	Conclusions	8-11

LIST OF SYMBOLS

DANKWOORD

CURRICULUM VITAE

SUMMARY

SAMENVATTING

INTRODUCTION

This introduction can be used as a guideline for this thesis. Each chapter is briefly discussed in terms of scope and outcome. At the end of this introduction I will spend some lines on the influence of my present job on the multiplication of this thesis.

Chapter 1: In this chapter the titanium dioxide and polyelectrolyte samples as used in our experiments are characterized in a colloidchemical way.

→ **Chapter 2:** In adsorption experiments of polyacrylic acid on titanium dioxide an increasing amount adsorbed is found with increasing equilibrium concentrations. The zeta potential is constant in the same concentration range. This phenomena can be explained by a simultaneous adsorption of H^+ -ions. Additional measurements support this theory.

Chapter 3: The hydrodynamic layer thickness of adsorbed charged polyelectrolytes is thin compared to layers found for uncharged polyelectrolytes. To measure this rather thin layer the decrease in permeability of a packed bed of titanium dioxide is measured. Different approaches resulted in a layer thickness of about 3 nm (0.01 M KNO_3).

Chapter 4: In order to obtain monodisperse pigment particles from a polydisperse sample a so called "counter flow centrifugation method" was used. The method is suited for the fractionation of particles with a radius of 0.1 to 10 μm .

Chapter 5: The dispersion process of pigment in water might be improved by decreasing the contact angle titanium dioxide /solution/air. Theory and experiments are not promising with respect to this possibility.

Chapter 6: The stability in dilute titanium dioxide suspensions is measured using the increase in light-transmission of the dispersion during coagulation. The stability of dispersions with a high volume fraction of solids is measured using viscosity

measurements. The increase in viscosity of a stable suspension of pigment particles can be explained by a hydrodynamic layer thickness of 1 to 5 nm surrounding the particles.

A thin polymer layer of polyacrylic acid increases not only the steric stabilization but also increases the electrostatic stabilization. The charges determining the zeta potential are no longer situated on the oxide surface but are situated about 3 nm from the surface. The influence of the attraction force is declining very rapidly at this distance.

Chapter 7: Knowledge about a three component system is difficult to translate to experiments with full paint systems. In this chapter a first move in this direction has been done.

Chapter 8: In this chapter all colloidchemical events are discussed starting from the dispersion process till the dry paint film.

In my present job I try to find solutions for the waste problem of the drinking water companies in the Netherlands. Every year a huge amount of money is spend to get rid of sludges and other waste materials. And even with the input of all this money the solution found is not satisfactory: the sludge is transported to a landfill and dumped with other waste materials. One concept of dealing with waste materials has proven itself many times: The concept of the three R's:

- Reduction (of waste materials)
- Recycling (in the process itself)
- Reuse (in another process)

Not only can this concept save (a part of) the environment but it can in some cases also save money. For these two reasons I used this concept to make choices for the multiplication of this thesis:

Reduction: The number of books is estimated carefully. If there occurs a shortage, additional books are printed without extra costs.

Reduction: The books are printed in A5-size. In this way four pages are printed on one sheet. With a traditional sized thesis only two pages are printed on one sheet. In this case about 40% of the paper is wasted and the printing costs increase.

Recycling: Laminose paper can not be recycled at this moment and a laminose cover was more expensive compared to a normal cover.

Reuse: To bleach the paper often chlorines are used. The paper for this book is bleached without the aid of chlorine. Chlorine is a problem is the waste water of the paper mill, because the waste water is disposed of to surface water and surface water is used to produce drinking water. Another part of the chlorine is left behind in the paper and contributes to pollution in flue gas of furnaces.

Despite of the extra costs of the chlorine free bleached paper the printing costs of this book is about 50% to 70% of the normal costs of printing a thesis.

CHAPTER 1:

CHARACTERIZATION OF A THREE COMPONENT COLLOIDAL SYSTEM: TITANIUM DIOXIDE/POLYELECTROLYTE/WATER.

1.1 Introduction.

In this investigation we studied some basic problems met during the development of water-based paints. The experiments described in this thesis are almost all restricted to a system with three components: titanium dioxide, a polyelectrolyte and water. The choice of such a system is in fact a compromise between the very complex system of a complete water-based paint and the simplicity needed for fundamental research.

In this chapter the different samples of titanium dioxide and the polyelectrolyte samples as used in our experiments are described. Also the characteristics of both titanium dioxide/water dispersions (surface charge, zeta potential) and polyelectrolyte /water solutions (net charge on polyelectrolyte) are discussed before we consider some characteristics of the three-component system.

1.2 Titanium dioxide samples

All samples had the crystal structure of rutile. The home-made sample (A) was checked by measuring the röntgen diffraction pattern using a powder diffractometer. The three pigment particle samples (B,C,D) were checked by the supplier (Tiofine) using a powder diffractometer.

The home-made titanium dioxide sample was prepared starting from

TiCl₄ (Flucka P.A.) following a synthesis described by Bérubé and de Bruyn¹. Electron microscopic pictures showed needles of 15x150 nm. The pigment particles however were ovals with a radius of 100 to 150 nm. Pigments B and C were taken from the production process of Tiofine pigments R80 respectively R85 (sulfate process) after the inorganic coating was added but before the addition of an organic coating. These pigments were washed several times at pH 11 followed by a reduction of the electrolyte concentration in the dispersion by washing at the isoelectric point. Pigment D was taken from the 'burner discharge' (chloride process) before the inorganic and organic coatings were added.

Surface charges at the rutile/water interface were determined by titration. The titration experiments were carried out under CO₂-free conditions. The pH was measured using a van Laar salt-bridge², a Schott glass-electrode and a Radiometer research pH-meter. The titration-steps were regarded to be in equilibrium when the acid and the hydroxide titration overlapped within the accuracy of the burettes (0.002 ml) and the pH-measurement (0.01 pH-unit). The titration-curves were calculated by comparing the titration of a sample with the titration of a blank solution under the same conditions. Titrations were carried out at three electrolyte concentrations: ±0.001 M, 0.01 M and 0.1 M KNO₃. The pH where the titration curves coincide is defined as the point of zero charge (P.Z.C.).

The electrophoretic mobility of the particles was measured with a Zetasizer III (Malvern). The pH was measured as described above, allowing 90 minutes equilibrium-time after the pH was adjusted. The curves were fitted to a polynome. The pH where the polynome crosses the x-axis is the iso electric point (I.E.P.). Unless another temperature is stated the experimental temperature was 25 ±0.1 °C. The B.E.T. surface area was measured using a Flow Sorb Area Meter at three N₂-pressures: 0.05, 0.148 and 0.246 (P/P₀).

	coating	I.E.P.	P.Z.C.	B.E.T. surf. m ² /g	density kg/m ³
A	none	5.7	5.7	28.3	4260
B	alumina	7.9	8.0	22.2	4000
C	alum./silica	6.5	7.6	21.5	4000
D	none	6.0	?	7.8	4260

Table 1: Some properties of the titanium dioxide samples as used for our experiments.

1.3 Titration curves of the oxide/water system.

There are four different theoretical approaches in describing the surface-charge density as a function of the pH:

- 1) The site binding model introduced by Yates e.a.³.
- 2) The porous gel model introduced by Lyklema⁴.
- 3) The stimulated adsorption model introduced by Siskens, Stein e.a.⁵.
- 4) The Gouy-Chapman theory extended with a Stern layer⁶.

It is beyond the scope of this thesis to compare these models on their validity especially as the value of such models in more complex systems has not yet been investigated.

Because the Gouy-Chapman theory is the most common theory in colloid chemistry we shall discuss the charge-pH curves of the pure titanium dioxide in terms of this theory:

With the Gouy-Chapman theory (the surface is regarded as a flat plate) a charge is calculated in the diffuse layer starting with a potential at the beginning of the diffuse layer. Between the

diffuse layer and the surface a layer of about the radius of the hydrated ions, called the Stern layer is free of charge. The Stern layer can be regarded as a capacitor with a capacity C_s . This capacitance is defined as the charge on one of the "plates" divided by the potential drop in the Stern layer. As a first approximating this capacitance is regarded as independent from the surface charge:

$$C_s = \frac{\sigma_0}{(\psi_0 - \psi_d)} \quad (1)$$

with σ_0 : surface charge (C/m^2) ψ_0 : surface potential (V)
 ψ_d : diffuse double layer potential (V)

The potential at the oxide surface is called the surface potential. Because the surface potential of the oxide can not easily be measured a Nernst behavior of the hydrogen ions is assumed in order to calculate the surface potential starting from the pH of the bulk solution:

$$\psi_0 = -2.303 \frac{RT}{F} (pH - PZC) \quad (2)$$

with PZC: point of zero charge

The surface charge can be measured by titration but if the diffuse double layer potential is known the surface charge can also be calculated by integration of the charge densities of the positive and negative ions in the diffuse double layer:

$$\sigma_0 = -\sigma_d = \sqrt{8 n_0 \epsilon_r \epsilon_0 kT} \sinh \left(\frac{ze\psi_d}{2kT} \right) \quad (3)$$

with σ_d : diffuse charge, n_0 : concentration of bulk electrolyte

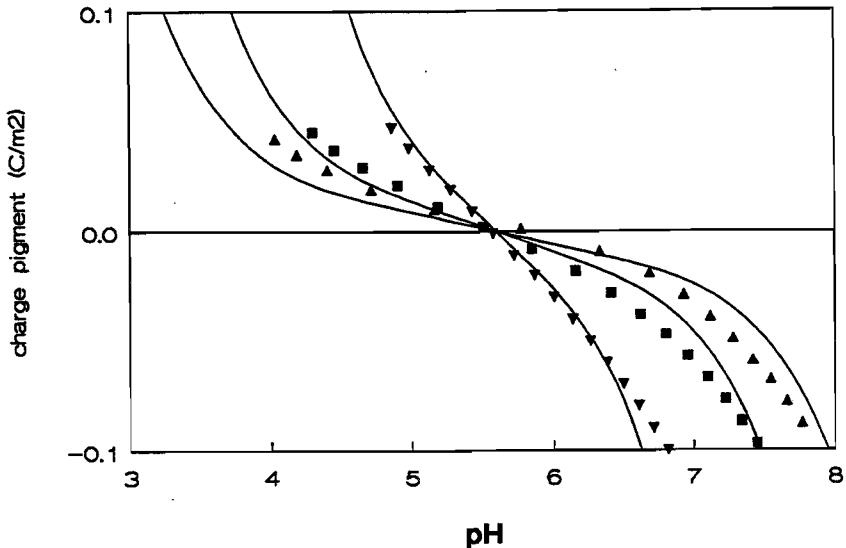


Figure 1: measured and calculated surface charge as a function of the pH. Titanium dioxide: Δ 0.004 M KNO_3 \blacksquare 0.01 M KNO_3 ∇ 0.1 M KNO_3
 On comparing the calculated charges with the experimental values a Stern layer capacitance of 4.7 F/m^2 gave the best fit.

With formula 1,2 and 3 the surface charge can be calculated at a certain pH. These calculated charge-pH curves can be compared with the measured titration curves (see figure 1). The only adjustable parameter in this calculation is the capacitance of the Stern layer (assumed to be constant in the investigated pH-range).

The result of this exercise is a capacitance of the Stern layer of 4.7 F/m^2 . Fokkink⁷ observed a capacitance of 4.5 F/m^2 with a titanium dioxide sample synthesized following the same procedure. The discussion whether such rather high values for Stern layers

obtained with oxide/water surfaces is a realistic value still continues: The value is about 10 times higher compared to the value obtained for Hg/water and AgI/water interfaces. It is noted that on the basis of the stimulated adsorption model such a difference between a non-conducting oxide and conducting solids is expected.

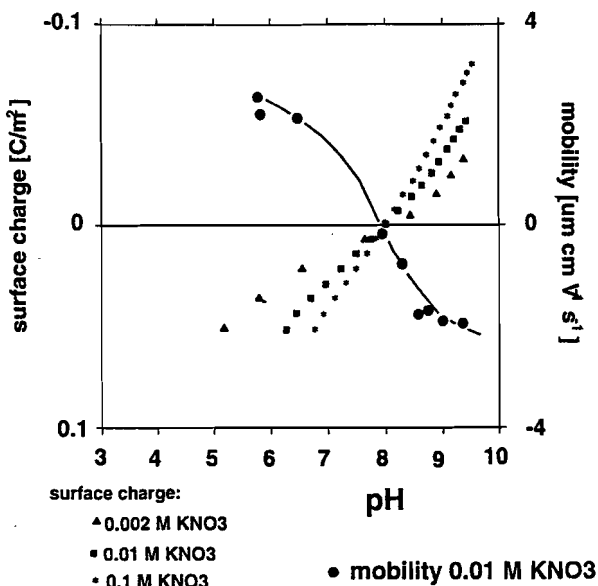


Figure 2: Titration curves of titaniumdioxide sample B: Because a coating of alumina is covering the surface the point of zero charge of this pigment resembles the p.z.c. of alumina.

For oxide samples B several washing steps at high pH were necessary before the P.Z.C. and the I.E.P. coincided. Titration experiments with the original sample resulted in rather straight titration curves with only small differences between the different

electrolyte concentrations. The P.Z.C. of the original sample was 5.8 whereas the I.E.P. was 8.4 indicating specific adsorption of positive ions. Washing at high pH probably causes a solvation of the outer layer of the aluminium oxide coating leaving a fresh and clean alumina surface.

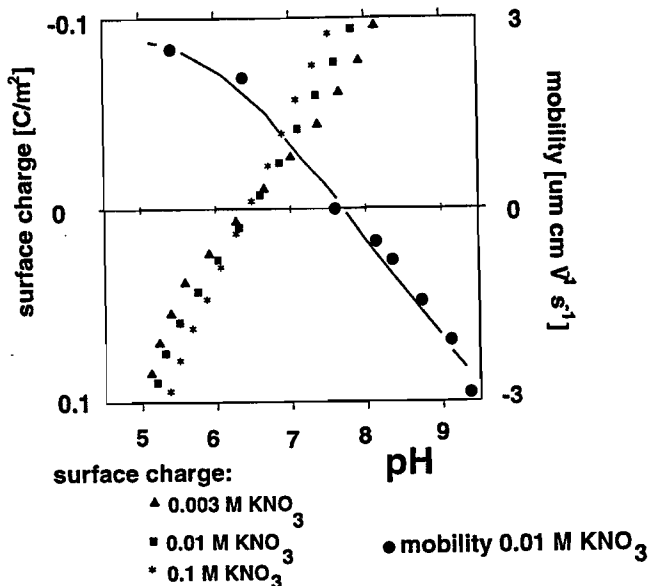


Figure 3: Surface charge and mobility of titaniumdioxide sample C: This pigment is coated with both alumina and silica. Washing procedures did not result in an equal value for P.Z.C. and I.E.P.

With the heterogeneous surface of pigment C the I.E.P. and P.Z.C. did not coincide. The alumina and silica can be arranged at random or patchwise on the surface. We preferred to use pigment B (only alumina coating) for our experiments because with a heterogeneous surface we would be introducing an extra uncertainty⁸ into our system.

1.4 The polyelectrolyte samples.

	supplier	counter ion	Molecular weight	active component
A	Janssen Chemica	H ⁺	2,000	homo polymer of PAA
B	Servo FX 504	NH ₄ ⁺	10,000	homo polymer of PAA
C	Servo FX 508	NH ₄ ⁺	11.000	copolymer of PAA (90%) and polystyrene (10%)
D	Janssen Chemica	Na ⁺		polystyreen sulphonic acid

Table 2: polyelectrolytes as used in our experiments.

The polymers are used as supplied. The concentration in g/l was always recalculated as the polymer with the H⁺ ion as the counter ion.

1.5 Titration curves of the polyelectrolyte/water solution.

The charge of polymers A,B and C is the result of the dissociation of the weak carboxylic acid groups in the polymer chain. The charge of the polymer is zero at about pH 2 and increases over the pH-range 2 to 11. As the number of negative charges increases the mutual repulsion between the charges on the chain hinders the dissociation process.

In order to describe the titration curve of the polyacrylic acid we can assume a Boltzmann distribution for the ions surrounding the charged chain:

$$[\text{H}^+]_{\text{pa}} = [\text{H}^+]_{\text{bulk}} e^{-\frac{e\psi}{kT}}$$

$$\text{or } -\ln[\text{H}^+]_{\text{bulk}} = -\ln[\text{H}^+]_{\text{pa}} - \frac{e\psi}{kT} \quad (4)$$

Here e is the charge of an electron, ψ is the potential at an adsorption/desorption site, k is the Boltzmann constant and T the absolute temperature.

For the dissociation of carboxylic acid groups on the polymer chain we can define a dissociation constant K_a :

$$K_a = \frac{[\text{COO}^-][\text{H}^+]}{[\text{COOH}]} = \frac{\alpha[\text{H}^+]}{1-\alpha} \quad (5)$$

Where α is the degree of dissociation of the chain. The combination of equations 1 and 2 gives an equation that relates the pH of the bulk solution with the dissociation constant of a monomer acrylic acid and the degree of dissociation of the chain. Some authors start from other dissociation constants but for a simple description of the titration curve the dissociation constant of the monomer is satisfactory. The only unknown term is the potential at a certain desorption site on the chain.

$$\text{pH} = \text{p}K_a - 0.434 \ln\left(\frac{\alpha}{1-\alpha}\right) - \frac{e\psi}{2.303 kT} \quad (6)$$

We can give an estimation for this potential when using the Debye-Hückel equation for the potential at a certain distance from a free ion in an electrolyte solution. The polymer is regarded as a straight line with an infinitely small volume following the approximation of the point charges of the Debye-Hückel approach.

From the dissociation degree α we can calculate an average distance (r) between two charged groups on the chain and an uncharged group in the middle. At $\alpha=0.5$ the distance between the charged groups and the uncharged carboxylic acid group in the middle is 2.5 Å. So $r=1.25/\alpha$ Å. The potential which we calculate with the Debye-Huckel approximation at distance r from the charge, must be multiplied by two because there are two charged groups at either side of one uncharged group. Of course there is also an attraction of the carboxylic acid group itself to the proton that is dissociating. But this attraction is already incorporated in the dissociation constant of the carboxylic acid. The potential is calculated from the Debye-Hückel potential:

$$\psi = \frac{2 e}{4 \pi \epsilon_0 \epsilon_r (1+\kappa a)} e^{-\kappa(r-a)} \quad (7)$$

$\epsilon_0 \epsilon_r$ is the dielectric constant of the solution and κ is the reciprocal Debye length., defined as:

$$\kappa = \sqrt{\frac{2 n_0 z^2 e^2 N_{av}}{\epsilon_0 \epsilon_r kT}} \quad (8)$$

Because we do not know the exact value of the radius of the charged group we assume that $a \ll r$ which is probably valid for the lower values of α but is certainly not valid at α -values above 0.5 ($r < 2.5$ Å). This is probably the reason that the model overestimates the charge at the higher pH-values. From figure 4 it is clear that PAA buffers in the range of pH 2 to 11 whereas the monomer only buffers in the range of pH 2 to 6. The salt concentration has only a minor effect on the titration curve of PAA.

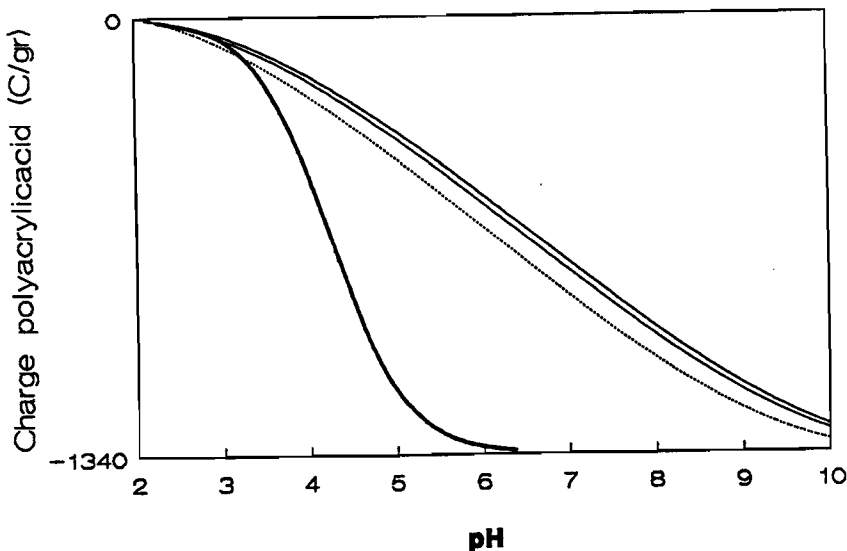


Figure 4: Theoretical titration curves for:
 — the acrylic acid monomer.
 — polyacrylic acid 0.001 M electrolyte
 — polyacrylic acid 0.01 and 0.1 M electrolyte

Leyte and Mandel⁹ observed a conformation transition of the coiled polymer in titration curves of polymethacrylic acid but not for polyacrylic acid.

If we compare the calculated curve with the experimental one we may conclude that the theory is able to predict the experiments until about 80% of the carboxylic acid groups are dissociated. At higher pH's the calculation overestimates the real charge of the polymer.

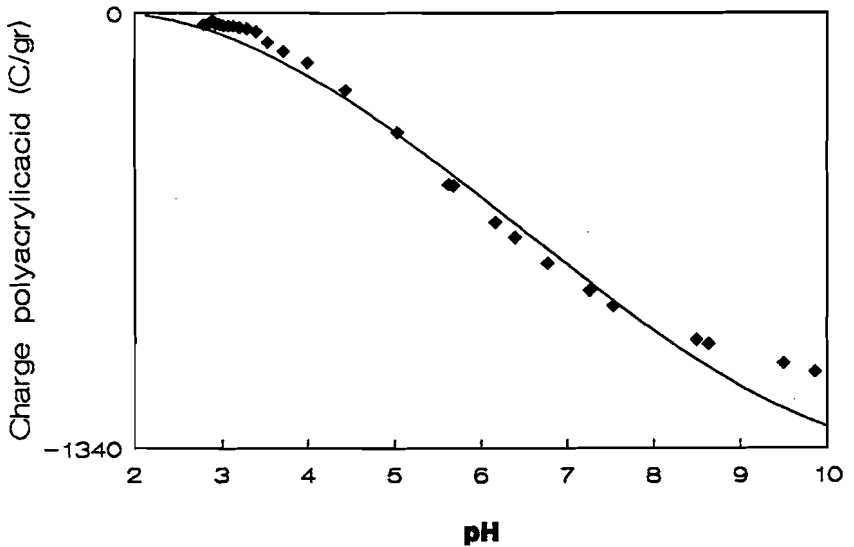


Figure 5: The theoretical titration curve ($pK_a=4.25$) and the experimental titration curve (PAA sample A, 0.01 KNO_3).

1.6 Mobility measurements with the three component system: PAA/oxide/water.

One of the characteristics of the adsorption of a polymer on a solid/liquid surface is that the adsorption is fast but the desorption is a slow process. This is explained by the consideration that a polymer is adsorbed with more segments on the surface and a desorption is only effective when all the segments are desorbed at the same time. The more segments of one polymer

are adsorbed on the surface the smaller the chance that desorption will happen within a certain period of time. From an experimental point of view this slow desorption of polymers is difficult to handle because it influences the equilibrium time. In our mobility measurements there was a striking difference in measuring the mobility after an increase or a decrease of the pH (see figure 6).

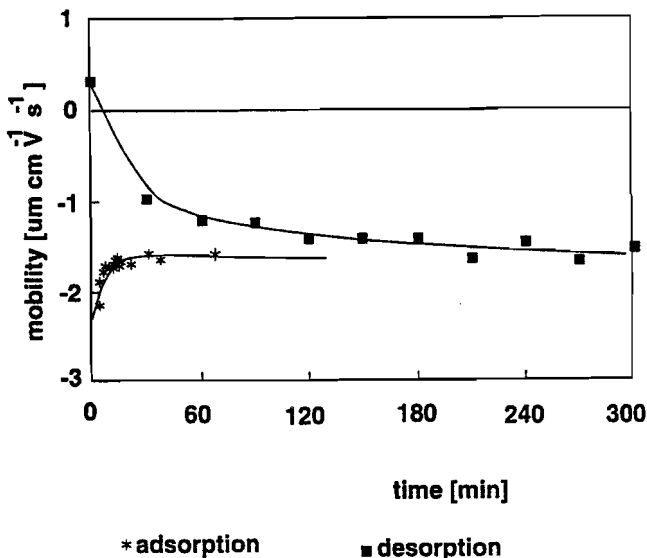


Figure 6: The time effect of adsorption and desorption on the mobility of titaniumdioxide(A) particles with $3 \times 10^{-3} \text{ g/m}^2$ PAA(A). 0.01 M KNO_3 .
 ■ pH=4 suddenly increased to pH=6.5.
 * pH=9 suddenly decreased to pH=6.5

In our view this phenomenon can be explained by the fact that at a low pH the amount PAA adsorbed on the oxide surface is large compared to the amount adsorbed at higher pH. So the effect of decreasing the pH is adsorption of PAA whereas after an increase

of the pH the PAA is forced to desorb. From the above experiment we concluded that the titrations of oxide suspension in the presence of polyacrylic acid should be started at a high pH and only after an equilibrium time of at least six hours.

Figure 7 shows the measured zeta potentials of samples drawn from a dispersion during a titration.

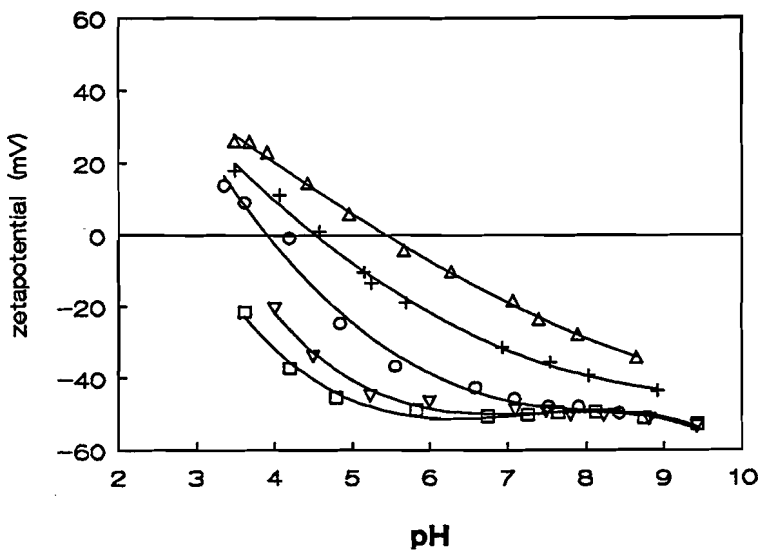


Figure 7: Zeta potential as a function of the pH. Titanium dioxide sample=A, PAA=C The total PAA concentration is constant during a titration. The concentration is presented proportionally to the surface area of oxide in the dispersion.

1.7 Titration experiments with the three-component system: polyelectrolyte/oxide/water.

At very low concentrations of PAA the titration of the surface charge of titaniumdioxide is possible. But at medium and high concentrations of PAA the majority of the acid added to the suspension is needed for the protonation of the carboxylic acid groups of the polymer itself. The amount of acid needed to change the surface charge vanishes in the total amount of acid added. The only way to quantify the influence of an adsorbed polyelectrolyte on the surface charge of the oxide is to use a polyelectrolyte with a fixed charge. Figure 8 is the result of an experiment with such a polyelectrolyte (polysulphonic acid).

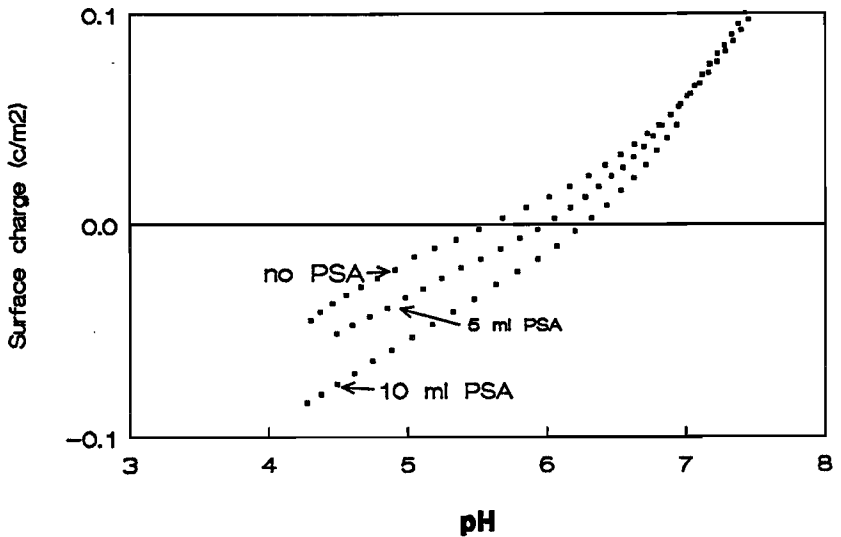


Figure 8: Titration of titaniumdioxide(A) in the presence of respectively 0, 0.6×10^{-4} and 1.2×10^{-4} g/m² polystyrenesulphonic acid. The maximum possible charge of the polymer is 435 C/g

The common intersection point at pH=7 is in fact the pH where the repulsion of the negative surface is high enough to prevent the negative polymer from getting adsorbed. At pH's between 7 and 6 the adsorption increases as a result of the decreasing surface charge. At pH's below 6 almost all the polysulphonic acid is adsorbed and the influence on the surface charge is constant. In general the charge of the adsorbed polysulphonic acid is compensated by the surface charge.

1.8 The adsorption of PAA on the oxide surface.

The adsorption of PAA is strongly dependent on the pH. There are three reasons for the larger amount of PAA being adsorbed at lower pH's (see figure 9):

- 1) The oxide charge is more positive at lower pH's
- 2) The charge of the PAA is lower at lower pH's and consequently more PAA is necessary to (over)compensate the surface charge.
- 3) At lower pH's the PAA resembles an uncharged polymer rather than a charged polymer. Uncharged polymers are adsorbed in loops and tails on the surface. Charged polyelectrolytes on the other hand are adsorbed rather flat and in smaller amounts on the surface.

In theory an increase in electrolyte concentration can either increase or decrease the amount adsorbed.

- 1) The attraction between surface charges and polymer charges declines at higher salt concentrations as a result of the shielding of the charged groups by counter ions. The result is a decrease of the amount adsorbed as the electrolyte concentration increases.
- 2) The mutual repulsion between the charged groups on the polymer chain declines as a result of the shielding of the charged groups

by counter ions. The polymer acts like an uncharged polymer. The result is an increase in adsorption with increasing electrolyte concentrations.

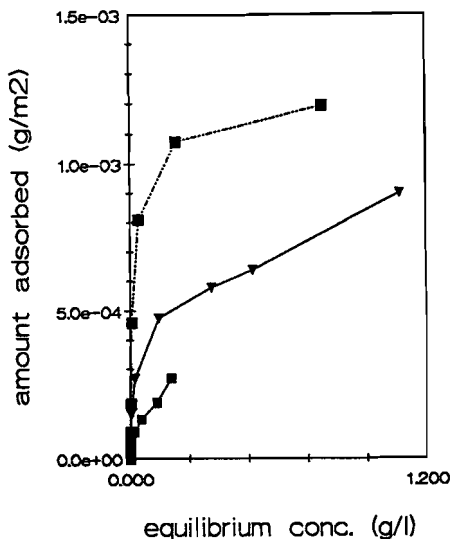


Figure 9: The amount of PAA adsorbed on the oxide surface (A) as a function of the measured equilibrium concentration in the bulk.

—■— pH: 4.2, -V- pH: 5.3, -■- pH: 6.5.
Electr.conc.=0.01 M KNO_3

From figure 10 it is clear that the second process dominates: the adsorption increases with increasing salt concentrations.

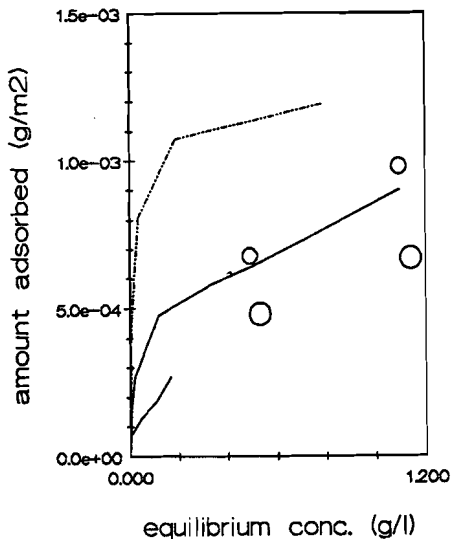


Figure 10: The influence of the electrolyte concentration on the adsorption of PAA (A) on titanium dioxide (A). Drawn lines: same as figure 9. Small circles: 0.1 M KNO_3 Large circles: 0.001 M KNO_3 . The adsorption increases with increasing electrolyte concentration.

1.9 Theoretical approach of the three component system

The titanium dioxide/polyacrylic acid/electrolyte system is very difficult to describe with an available theory.

The pH as well as the electrolyte concentration influences the:

- the charge of polyacrylic acid
- the charge of titanium dioxide

- the repulsion of charged groups of both polyacrylic acid and titanium dioxide
- the attraction of oppositely charged groups of polyacrylic acid and titanium dioxide
- the amount adsorbed

Experiments show that the charges of polyacrylic acid and titanium dioxide change as a consequence of the adsorption of the polymer on the surface (see chapter 2 of this thesis). The distribution of the remaining charge is not necessarily homogeneous in the polymer layer on the oxide surface.

A model in order to calculate a hydrodynamic layer thickness from surface and polymer properties at a given pH and electrolyte concentration is necessarily build on many parameters or assumptions. One way to reduce the number of parameters is to use the experimental results from the polymers in solution and add some extra interactions between surface and polymer to these. The theoretical approach of T.J. Odijk¹⁰ can probably be extended for this purpose. The properties of polymers in solution can be used to predict the behavior of the polymer near the surface. Unfortunately the polymers used for our experiments are typical low molecular whereas the theory is dealing with larger polyelectrolytes. For a theoretical model more experiments with a larger range of molecular weights are necessary to support the theory.

With these polyelectrolytes influence of tail effects is to be expected. In the theoretical approach of J. Scheutjens e.a.¹¹ the segmental ranking number is explicitly account for.

We may conclude that a theoretical approach is an interesting research topic for the future especially as it is supported by a systematic series of experiments with a range of molecular weights.

- ¹Bérubé Y.G. and Bruyn P.L. de, Adsorption at the rutile solution interface. 1 Thermodynamic and experimental study, J. of Colloid and Interface Science, Vol 27, no 2 (1986).
- ²Laar J.A.W. van, Het ladingsnulpunt van zilverjodide, Thesis, Utrecht, 10 juli 1952.
- ³Yates D.E., Levine S. and Healy T.W., J. Chem. Soc. Faraday Trans. I,70, 1807 (1974)
- ⁴Lyklema J., Croat.Chem.Acta.,43,242 (1971).
- ⁵Siskens C.A.M., Stein H.N., Stevels J.M., J.Coll.Interface Sci., Vol 52,251(1975).
- ⁶Verwey E.J.W. and Overbeek J.Th.G., Theory of the stability of lyophobic colloids, Elsevier Publishing Company, inc. (1948).
- ⁷Fokkink L.G.J., Thesis, Wageningen, The Netherlands, may 1987.
- ⁸Kuo J.F. and Yen T.F., J. Coll. Interface Sci. Vol 121, no. 1,(1988) p220.
- ⁹Leyte J.C., Mandel M. Journal of Polymer Science, Part A, Vol. 2 (1964) p1879.

¹⁰Odijk T.J., On the statistical physics of polyelectrolytes in solution, thesis february 1983, Leiden.

¹¹Scheutjens J.M.H.M., Fleer G.J., Cohen Stuart M.A., End effect in polymer adsorption: a tale of tails, Colloids and Surfaces, 1986.

CHAPTER 2:

THE CHANGE IN CHARGES OF TITANIUM DIOXIDE AND POLYACRYLIC ACID DUE TO ADSORPTION OF THE POLYMER ON THE OXIDE SURFACE.

2.1 Introduction

The subject of our investigation is the influence of polyacrylic acids on the stability of TiO_2 /water dispersions. There are two major application areas for the use of polyacrylic acids in combination with oxide particles. The first encompasses waste water treatment, selective flocculation, flotation separation and soil-conditioning. In this area the polyacrylic acid acts as a bridge forming polymer when adsorbed on two positively charged oxide particles. The polyacrylic acids used for this purpose have relatively large molecular masses (MW:100,000-2,000,000). The second area includes the use of polyacrylic acids as dispersing agents for oxide pigments in water based paints. Here the oxide particles are stabilized against flocculation as the polyacrylic acid is adsorbed on the surface. The molecular masses of the polyacrylic acids used are typically low (2000-20,000). For this application area it is very important to know whether the stabilization mechanism is purely electrostatic or whether there is also a steric component.

If we compare the adsorption of charged polymers with the adsorption of neutral polymers we find two important differences¹:

- 1) The amount of charged polymer adsorbed in the plateau of an adsorption isotherm is much less than the adsorbed amount of a neutral polymer. This is caused by the mutual repulsion between the adsorbed loops and tails. This repulsion is absent between

trains because the charge of the trains is compensated by the surface charge. So the polyelectrolyte is predominantly adsorbed in trains rather than in loops and tails.

2) The amount of charged polymer adsorbed is not strongly influenced by the molecular mass of the polymer. This is also a consequence of the rather flat adsorption of the polyelectrolyte. It is important to distinguish three different types of experiments:

1) The adsorption of a polyelectrolyte with a fixed charge on a surface with a variable charge².

2) The adsorption of a polyelectrolyte with variable charge on a surface with a fixed charge³.

3) The adsorption where both the charge of the polyelectrolyte and the charge of the surface depend on the pH, salt concentration and the amount adsorbed⁴.

In the first case the surface charge is of course very important for the maximum amount of polyelectrolyte adsorbed. The adsorption is almost proportional to the surface charge. In the second case the amount adsorbed depends on the charge of the weak polyelectrolyte. The polyelectrolyte is adsorbed in small amounts when it is highly charged. At low pH's where the polyelectrolyte is not charged (in the case of a negative polyelectrolyte) the polymer behaves like an uncharged polymer and the adsorption is larger than at a high pH. In the third case both the charge of the surface and of the polyelectrolyte are important for the amount adsorbed. Gebhardt et al.⁴ report an adsorption proportional to the surface charge on rutile and hematite. The adsorption is a linear function of the pH with a zero adsorption at a pH 7 for rutile and pH 9 for hematite. The slope of the linear function is three times larger for the adsorption on hematite than for the adsorption on rutile. In the literature there is no agreement about the conformation of the polyacrylic acid as a function of

the pH. The amount adsorbed is larger at a low pH. So from this point of view the polymer layer is thicker at a low pH. According to Lyklema and Fleer¹ the polyacrylic acid behaves more like an uncharged polymer at a low pH. Uncharged polymers are able to adsorb with loops and tails and the polymer layer is more extended. But Somasundaran⁵ concludes from flocculation experiments as well as from conformation experiments with pyrene-labeled polyacrylic acids that the polymers are adsorbed perpendicular to the surface when the overall charge of the surface (ζ -potential) is of the same sign as the charge of the polymer. So at a high pH the polymer layer is extended but not very dense. At a low pH the polyacrylic acid is coiled and not so extended.

According to the available literature it is not clear what happens to the charge of a weak polyelectrolyte when it is adsorbed on a surface. This is nevertheless an important factor in the adsorption mechanism because it is possible that the weak polyelectrolyte loses most of its charge due to the adsorption and in this way resembles the adsorption of an uncharged polymer rather than a strong polyelectrolyte. In this project we measured the charge of the polyacrylic acid as well as the charge of titanium dioxide as a function of the polyacrylic acid equilibrium concentration using pH-titration experiments and adsorption experiments.

2.2 Experimental procedures

Materials and reagents

The titanium dioxide used in this investigation was made starting from TiCl_4 (Fluka P.A.) and was pure rutile⁶. Electron microscopic photos showed that the particles were needles of 15x150 nm. The

surface area was $28 \text{ m}^2/\text{g}$ using the B.E.T. method with nitrogen as the adsorbate. The P.Z.C. and the I.E.P. of the pure sample coincided at pH 5.7. The polyacrylic acid (Janssen chem.) had a molecular weight of 2000. All other chemicals were P.A.-grade (Merck).

Experimental methods

The **titration** experiments were carried out under CO_2 -free conditions. The pH was measured using a van Laar salt-bridge⁷ and a glass-electrode. The titration-steps were regarded to be in equilibrium when the acid and the hydroxide titration overlapped within the accuracy of the burettes and the pH-measurement. The titration-curves were calculated by comparing the titration of a sample (TiO_2 or PAA) with the titration of a blank solution under the same conditions.

The **electrophoretic mobility** of the particles was measured with a Zetasizer III (Malvern). The pH was measured as described above, allowing 90 minutes equilibrium-time after the pH was adjusted.

The **pH-stat** experiments were performed with the same equipment as the titration experiments. Diluting the polyacrylic acid solution in a 0.01 M KNO_3 - solution of the same pH did not change the pH of the solution.

The **adsorption isotherms** were obtained by adding a solution of polyacrylic acid with the required pH and ionic strength to a suspension of TiO_2 with the same pH and ionic strength. After one hour of agitation the pH was adjusted. After 20 hours agitation at 25°C the suspension was centrifuged and the concentration of the polyacrylic acid was measured in the supernatant using a T.O.C.-analyzer. Blank tests indicated very little organic species from the solid (<0.1 ppm in the equilibrium solution). The pH of the supernatant was always in a range of ± 0.1 pH-unit from the desired pH. The electroforetic mobility of the particles was

measured by resuspending a small part of the sediment in the supernatant.

2.3 Results and discussion

Titration experiments

In figure 1 the charges of both titanium dioxide and polyacrylic acid are plotted as a function of the pH. These charges were obtained in two different experiments, so there was no adsorption of the polymer on the oxide. The P.Z.C. as well as the absolute charge of the oxide corresponded with other experiments^{1,8}. The charge of polyacrylic acid increases over the whole pH-range from pH 3 where the polymer is uncharged to pH 10 where the charge is about -1000 C/g polymer. The theoretical maximum charge of the polyacrylic acid is -1340 C/g (Faraday's constant divided by the molecular weight of a monomer-unit). This theoretical value is only reached when all monomer units are indeed acrylic acid monomers and all the groups are dissociated.

Electrophoretic experiments

The zeta potential is calculated from the electrophoretic mobility using the calculations of Wiersema⁹. In these experiments we dealt with packages of needles of about 0.2 to 0.7 μm in diameter when the dispersion was electrostatically stabilized. Around the i.e.p. larger flocks were formed but these flocs were resuspended ultrasonically just before the measurement. The zeta potential was measured as a function of the pH at the same initial concentration (figure 2).

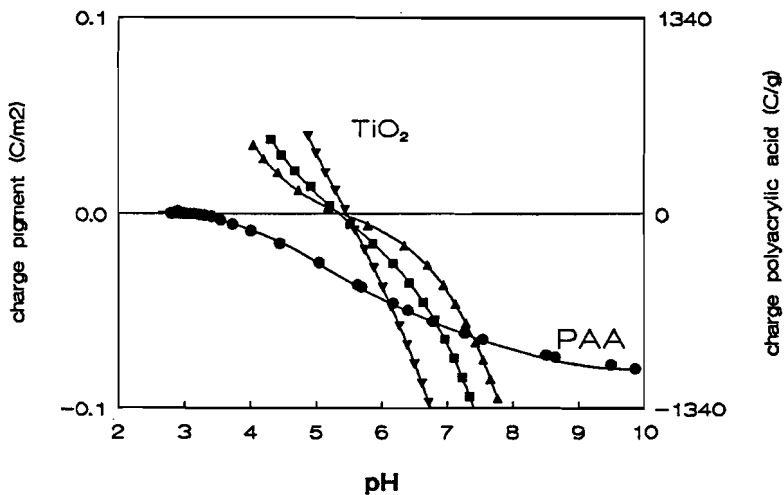


figure 1
 The surface charge of titaniumdioxide as a function
 of the pH. 0.003(Δ), 0.01(\blacksquare) and 0.1(∇) M KNO_3 (l.axis)
 The charge of polyacrylic acid as a function of the pH.
 Electrolyte concentration: 0.01(\bullet) M KNO_3 (right axis)

The initial concentration is reported as the concentration of the polymer divided by the total surface area of the solid in order to achieve a better comparison with other experiments. The equilibrium concentration and the amount adsorbed vary during this experiment. The zeta potential becomes more negative over the whole pH range as a result of the adsorption of the polyacrylic acid on the TiO_2 -surface. In spite of the very large negative surface charge of the oxide at pH 9 there must be some residual adsorption of the highly charged polyacrylic acid at this pH. At

higher concentrations of the polyacrylic acid the zeta potential is constant in the range pH 6 to 9 and does not change at higher polymer concentrations. At pH values below pH 6 the zeta potential decreases as a result of the decreasing charge of polyacrylic acid.

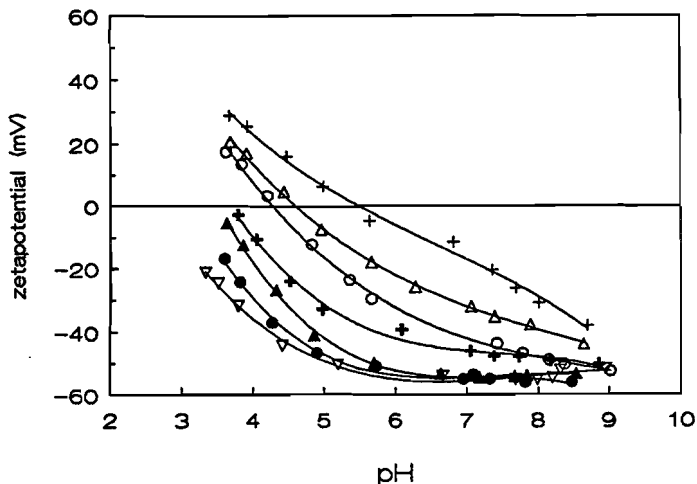


Figure 2
 Zeta potential as a function of the pH.
 Electrolyte concentration: 0.01 M KNO_3
 Initial concentration polyacrylic acid respectively:
 0(+), 0.09(Δ), 0.35, 0.71, 1.4, 2.8, 10(∇) [$\times 10^{-4} \text{g/m}^2$]

Adsorption isotherms

The adsorption isotherms at pH 4.2, 5.3 and 6.5 show a high affinity and a low affinity part (figure 3). Gebhardt⁴ did not find a low affinity part of the adsorption isotherm, the adsorption plateau was about 10 times less than the plateau we found. The difference may be explained by the very large molecular mass

(2,000,000) used by Gebhardt. The rearranging process of the polymer on the solid surface that is probably necessary for the low affinity part of the isotherm is absent in the case of very large polymer molecules.

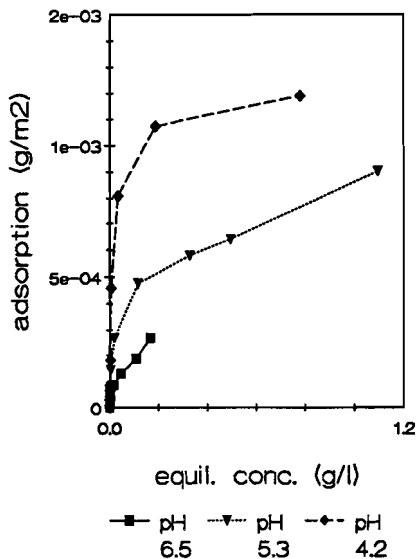


figure 3
Amount of adsorbed polyacrylic acid versus equilibrium concentration. Electrolyte concentration 0.01 M KNO₃, pH :4.2 (◆), 5.3 (∇), 6.5 (■).

If the zeta potential is measured in the same experiment it appears that the zeta potential becomes more negative in the high affinity part of the isotherm and remains at a constant negative value in the low affinity part of the isotherm (figure 4). These zeta potentials correspond with the zeta potential at the highest polymer concentrations in figure 2. If we want to explain why the adsorption still increases whereas the zeta potential becomes

constant it is illustrative to compare the charges in the diffuse part of the double layer calculated from both experiments. From the zeta potential the diffuse charge behind the electrokinetic slipping plane can be calculated by integrating the Poisson-Boltzmann equation from the slipping plane ($\psi = \zeta$) to infinity ($\psi = 0$). From the titration experiments we know the charge of the oxide and the polyacrylic acid.

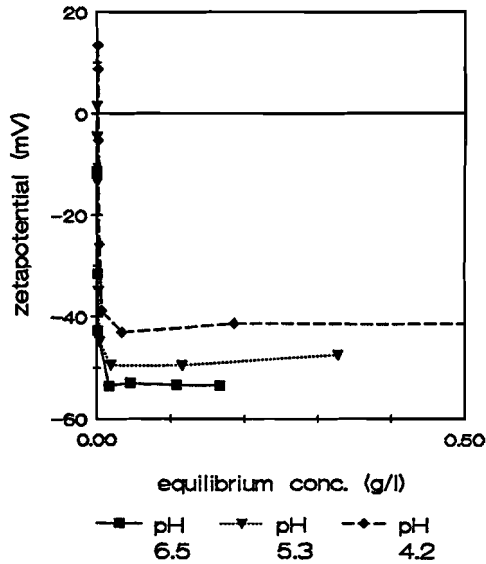


Figure 4
Zeta potential as a function of the equilibrium concentration polyacrylic acid. Same conditions as the experiments of figure 3.

If we assume (zeroth-order approximation) that the charge of the oxide and the charge of the polymer do not change as a result of the adsorption, we can calculate the total charge in the diffuse double layer:

$$\sigma_d = -\sigma_0 - \sigma_{PAA}$$

The surface charge of the oxide and the amount and the charge of the polyacrylic acid at a certain pH is known from independent experiments so we can compare them with the charge calculated from the zeta potential. The result is that the charge behind the electrokinetic slipping plain becomes constant while the total calculated charge on the surface still increases (figure 6 and 7). From this calculation we conclude that the assumption that neither the polyacrylic acid charge nor the titanium dioxide charge changes as a result of the adsorption is incorrect.

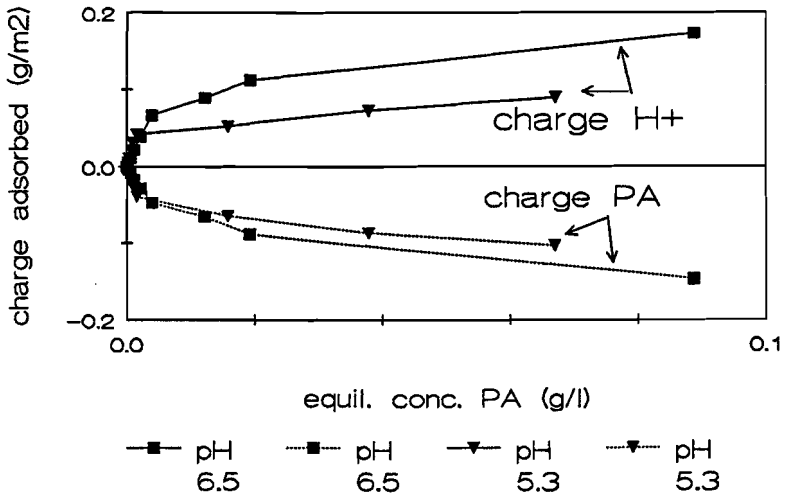


Figure 5: Adsorbed charges:
Charge of polyacrylic acid, calculated from adsorption isotherms and titration.
 ——Charge of H⁺, calculated from pHstat experiment. pH 6.5(■) and pH 5.3(▼)

From an experimental point of view we can not distinguish between the change in the surface charge and the charge of the polyacrylic acid as a result of adsorption. On the other hand we can measure the change of the sum of both charges by a pH-stat experiment. These experiments showed that H^+ addition was always necessary to keep the pH constant after an adsorption of polyacrylic acid on the TiO_2 -surface. From this experiment we can calculate a H^+ -consumption per square meter oxide surface at a certain initial concentration of polyacrylic acid. From the initial concentration we can calculate the equilibrium concentration of polyacrylic acid by iterative interpolation in the adsorption isotherm. Now we can recalculate the total charge on the surface with the correction of the pHstat-experiment:

$$\sigma_d = -\sigma_0 - \sigma_{PAA} + \sigma_{pHstat}$$

The pHstat experiment shows an almost equal adsorption of negative charge as a result of the adsorption of the polymer and an adsorption of positive charge due to the adsorption of H^+ -ions (figure 5).

If we start with a positive surface the surface charge is overcompensated by the negative charge of the polymer at low equilibrium concentrations (high affinity part of the isotherm).

equil conc. g/l	pH	calculated diffuse charge C/m^2		%
		from zetapotential	from adsorption	
0	5.3	-0.0004	-0.007	94
0.2	5.3	0.013	0.018	28
0	6.5	0.003	0.032	91
0.2	6.5	0.015	0.019	21

tabel 1
comparison of the calculated diffuse charge behind the electrokinetic slipping plane and the total diffuse charge calculated from adsorption, titration and pHstat experiments.

At higher equilibrium concentrations (low affinity part of the isotherm) both the diffuse layer charge, calculated from adsorption and surface charge, and the calculated net charge behind the electrokinetic slipping plane, calculated from the zeta potential, are independent of the polyacrylic acid concentration. The charge calculated from the zeta potential is now about 25% of the total diffuse charge (see also table 1).

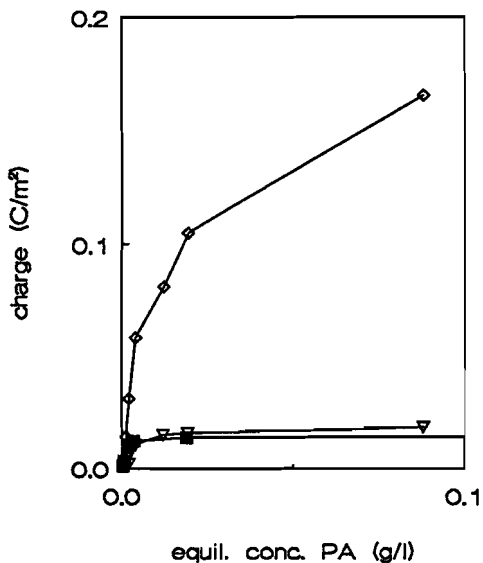


figure 6

Diffuse charges at pH 5.3:

- Charge behind the electrokinetic slipping plane
- ◇ Charge of the oxide + polyacrylic acid₊
- ▽ Charge of oxide, polyacrylic acid + H⁺ (pHstat)

The remaining difference is the diffuse charge in the layer between surface and slipping plane. In figure 7 the pure oxide has a positive diffuse charge (the surface charge is negative) which is about 10 times higher than the charge calculated from the zeta

potential. The same, rather strange effect, occurs at pH5.3: The pure oxide has a charge behind the electrokinetic slipping plane (calculated from the zeta potential) which is about 10% of the total diffuse charge ($=-\sigma_0$ oxide). Both charges are negative because the surface charge of the oxide is positive. As a result of the adsorption of polyacrylic acid both diffuse charges become positive and the charge behind the electrokinetic slipping plane is about 80% of the total diffuse charge. When explaining this it is important to keep in mind that the situation at a higher polymer concentration proves the theory better than the situation of the pure rutile sample.

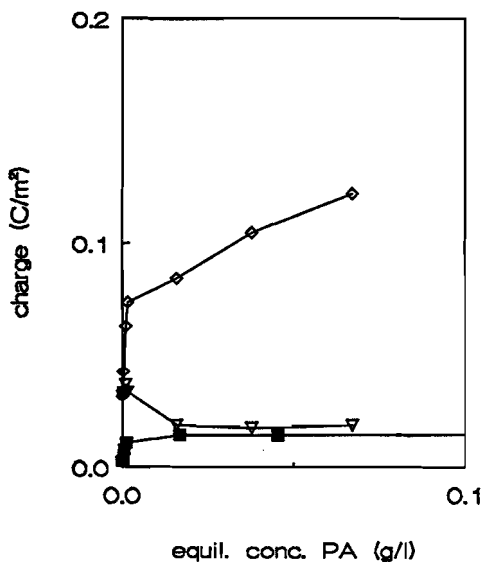


Figure 7
Diffuse charges at pH 6.5:
 ■ Charge behind the electrokinetic slipping plane
 ◇ Charge of the oxide + the polyacrylic acid.
 ▽ Charge of oxide, polyacrylic acid + H⁺ (pHstat)

In fact phenomena at oxide/electrolyte solution interfaces were always very difficult to explain by the diffuse double layer theory. The best fit was obtained by assuming a stern layer capacity of about 10 times the Stern layer capacity found for the AgI/water interface⁸.

A large potential drop in the layer (or a large capacity) between oxide the surface and the electrokinetic slipping plane can be explained in two ways:

1) The first layers of water on the oxide surface may have an ice-structure or are at least more structured than water molecules in the bulk solution. In this case the hydroxyl groups on the surface impose an orientation to the first layer of water molecules. The diëlectric constant of this "ice-layer" is less then the diëlectric constant of the bulk solution. In order to explain the difference between oxides and other surfaces like AgI we must assume a higher structuration of the water layers surrounding the oxide than the water layers surrounding other surfaces. The assumption of a very structured layer of water molecules is supported by the findings of Parfitt¹⁰. The adsorbed molecular water is only removed at an outgassing temperature higher than 150 °C. Morterra¹¹ can distinguish between coordinated water and surface hydroxyl groups during the dehydration process. The coordinated water is desorbed between 100 and 300 °C (vacuum) whereas the hydroxyl groups are removed by condensation of two hydroxyl groups between 200 and 550 °C.

In the case of an adsorbed polyacrylic acid the negative carboxyl groups are probably located just outside this ice layer. So in the case of the adsorbed charges being more important than the charge of the oxide surface groups, the diëlectric constant of the "Stern layer" more resembles the diëlectric constant of the solution.

2) The second explanation is based on the difference in conducting

properties of titanium dioxide and silver iodide. In the case of a conducting material like AgI, a charge at a certain place at the surface is smeared out because the electrons in the solid phase are either attracted by the positive charge or repelled by a negative charge. The charge of a surface group on a non-conducting surface is fixed on one spot. For this reason the potential profiles close to the surface are different for both materials. For AgI a smeared out potential is to be expected, but for TiO_2 a more local potential with a spherical potential profile is more likely. With a local potential a stronger attraction of the counter ions causes a better screening of the surface charge. Such a local potential was used by Van Diemen and Stein¹² to explain co-adsorption of cations and anions on calcium silicates.

If the surface is covered with polyacrylic acid molecules the negative charge is further away from the surface and there is no insulating layer just underneath the negative groups.

2.4 Conclusions

As the polyacrylic acid is adsorbed on the oxide surface first the charge becomes more negative in the case of a negative surface. In the case of a positive surface the positive charge is overcompensated. But the charge on the surface is restricted to a certain value. If this amount of charge is attained the polymers are adsorbed as neutral species on the oxide surface. The results obtained in the experiments in this chapter correspond with the theory. A phenomenon which is not so easy to explain is that the capacity of the Stern layer of an uncovered oxide particle is very high (as also reported in the literature) whereas the capacity of the Stern layer of a PAA covered particle is moderate.

Literature

¹Lyklema J. and Fler G.J., Electrical contributions to the effect of macro molecules on colloid stability, *Colloid and Surfaces*, 25 (1987) 357-368.

²Lyklema J., Fler G.J., Electrical contributions to the effect of macromolecules on colloid stability, *Colloid and Surfaces*, 25 (1987) p361 figure 1.

³Blaakmeer J., The adsorption of weak polyelectrolytes and polyampholytes: an experimental study. PHD-Thesis, chapter 2, Wageningen 1990

⁴Adsorption of polyacrylic acid at oxide/water interfaces, J.E. Gebhardt, D.W. Fuerstenau, *Colloids and Surfaces*, 7(1983), 221-231.

⁵Fundamental research on solid/liquid separation, Somasundaran, Annual Report (ARR-14-04), (1988).

⁶Berube Y.G. and Bruyn P.L. de, Adsorption at the rutile solution interface. 1 Thermodynamic and experimental study, *J. of Colloid and Interface Science*, Vol 27, no 2(1968)

⁷Laar J.A.W. van, Het ladingsnulpunt van zilverjodide, PHD-Thesis, Utrecht, 10 juli 1952.

⁸Fokkink L.G.J., Ion adsorption on oxides, Surface charge formation and cadmium binding on rutile and hematite, PHD-Thesis, Wageningen 22 mei 1987.

⁹Wiersma P.H., Loeb A.L., Overbeek J.Th.G., Calculation of the electrophoretic mobility of a spherical colloid particle, J. of Colloid and Interface Science 22, 78-99 (1966).

¹⁰Parfitt G.D., Prog.Surf.Membr.Sci.,11,181 (1976)

¹¹Morterra C., Bolis V., Fiscaro E., On the nature and properties of the hydrated layer and of strong Lewis acidic centers at the surface of pure and sulfate-contaminated TiO₂ (anatase).

¹²Diemen A.J.G. van, Stein H.N., Adsorption and electrokinetic potentials at solid/aqueous solution interfaces characterized by mutually stimulated adsorption of cations and anions, J. of Colloid and Interface Science, Vol.67, No.2, 1978, p213-218.

CHAPTER 3:

THE HYDRODYNAMIC LAYER THICKNESS OF ADSORBED POLYACRYLIC ACID ON TITANIUM DIOXIDE.

3.1 Introduction

Polyacrylic acids are used in the industry to stabilize oxide dispersions. In the paint industry for instance the oxide pigments for water-based paints are treated before the dispersing process with a so-called dispersing agent. The aim of the use of these dispersing agents is to decrease the dispersing time, to achieve an optimal degree of dispersion and to stabilize the primary pigment particles against flocculation during a very long period (months, even years). In many cases the dispersing agent used is a polyacrylic acid of a relatively low molecular weight (MW: 10,000). From literature it is known that polyelectrolytes are adsorbed from an electrolyte solution on a substrate as a thin layer compared to the extended layer of an uncharged polymer under the same conditions. These conclusions were drawn from neutron scattering experiments¹ and from calculations with an extension of the Scheutjens-Fleer theory². The consequence of a thin polymer layer is that the steric stabilization is not as pronounced as in the case of an uncharged polymer. Since the charge of the adsorbed polyelectrolytes increases the zeta potential (in absolute sense) of the particles in most cases, it is concluded that polyelectrolytes stabilize the dispersions in an electrostatic way rather than giving a steric stability to the particles. However this does not explain why the polyelectrolytes are better dispersing agents than adsorbed polyvalent ions even in the case that the zeta potential is changed to the same value.

In this paper we present the results of permeability experiments

with a packed bed of TiO_2 particles and the influence on this permeability of polyacrylic acid adsorbed on the particles. From the permeability reduction we can calculate a hydrodynamic layer thickness of the polymer layer on the particles.

3.2 Experimental procedures

3.2.1 Materials and reagents

The titanium dioxide particles used in this investigation were prepared from TiCl_4 (Flucka P.A.) following a recipe of Bérubé and de Bruyn³. By X-ray powder diffraction no other crystalline structures except rutile could be detected. Electron microscopy showed that the particles were needles of about 15×150 nm. The surface area was $30 \text{ m}^2/\text{g}$ using a four point B.E.T. method with nitrogen as an adsorbent. The TiO_2 sample was outgassed for 12 hours at 300°C while being flushed with nitrogen. The B.E.T. surface was about half the calculated geometrical surface probably caused by some larger rutile crystals. The point of zero charge and the isoelectrical point of the pure rutile sample coincided at pH 5.7. The polyacrylic acid was purchased as a 63 wt% solution in water (Janssen Chem. M.W.=2000). All other chemicals were P.A.-grade (Merck).

3.2.2 Experimental methods

The **electrophoretic mobility** of the particles was measured using a zetazizer III (Malvern) using an AZ4 cell for samples with a medium conductivity (salt concentration $< 0.1\text{M}$) and an AZ3 cell for samples with a high salt concentration ($>0.01\text{M}$).

The **viscosity** of the polyacrylic acid solutions was measured with an Ubbelohde capillary viscosimeter (Schott Oa and Oc with maximum shear rates of resp.: 2100 and 1630 s^{-1}). The viscosity of the

solutions was calculated from the kinematic viscosity using the density of the fluids.

The permeability of the packed bed of TiO_2 -particles was measured using an ISCO LC-5000 syringe pump at ± 100 atmosphere and a flow rate of ± 5 ml/hr. This pump was especially suited for this experiment because the flow was not pulsating even at such low flow rates. The flow was measured separately using a Sartorius L420 S+ balance. The electrical conductivity was measured on-line in the solution after passing the packed bed. In order to measure the conductivity in very small volumes a very small conductivity cell (thermostatically controlled) was constructed. The particles were packed in a thermostatically controlled column with a radius of 12.5 mm and a length of 98.8 mm. To prevent wall effects, the inside wall of the column was provided with a screw-thread. The column was first packed with a concentrated dispersion (20 wt%) of titanium dioxide and then with a well dispersed diluted dispersion (<0.1 wt%) in order to fill the largest channels. After two weeks of packing the permeability reached a constant value and this constant value did not change for two months. The permeability was independent of the pressure exerted on the plug.

After the experiments the pore size distribution of the packed bed was measured using mercury intrusion in some fragments of the packed bed (Micromeretics Pore Sizer 9310). The contact angle of the mercury on the substrate was measured separately using a monocrystalline rutile surface rinsed in a polyacrylic acid solution and dried in the air. The contact angle of a sessile drop of mercury on this surface was 137° .

3.3 Theory

3.3.1 The electroviscous effect

One possible basis of a permeability change of a porous plug is an electroviscous effect in the pores of the plug. The literature distinguished three electroviscous effects in the case of stable suspensions:

When the diffuse double layer of a charged particle is distorted by a shear, there is a tendency for restoration of the original spherical diffuse double layer. The viscosity of the fluid is increased by the tendency of the counter ions to restore the original diffuse layer. This is called the first electroviscous effect. According to Hunter⁴ the apparent increase in viscosity of the electrolyte solution in a slit-shaped capillary of $2h$ width is given by:

$$\eta_r = \frac{1}{\left[1 - \frac{3(\epsilon_0 \epsilon_r \zeta)^2}{h^2 \eta_0 \lambda_0} \right]} \quad (1)$$

with $\epsilon_0 \epsilon_r$: the dielectric constant (F/m) ζ : zeta potential (V)

h : slit width (m) η_0 : real viscosity of the solution (Pas)

λ_0 : electrical conductivity ($\Omega^{-1} \text{m}^{-1}$)

This approximate equation gives an overestimated value for η_r because the ion distribution is modified in capillaries. Especially at low kh (reciprocal Debye length compared with the slit width) and large ζ (absolute value) the overestimation can be significant. In our case the overestimation did not exceed 10% of the measured decrease of the permeability (see figure 11).

The permeability of the packed bed is reduced by this apparent viscosity: $K' = K/\eta_r$. With the Blake-Kozeny equation k (see later)

a theoretical layer thickness can be calculated and defined as the apparent decrease of the capillary radius in the presence of the first electroviscous effect compared to the the capillary radius without the first electroviscous effect:

$$\Delta r = r - r' = 2 \sqrt{\frac{K k}{\epsilon}} - 2 \sqrt{\frac{K' k}{\epsilon}} = (1 - \eta_r^{-1/2}) r \quad (2)$$

In the above approach the shear rate of the fluid is not important. But if the transport of ions caused by a shear rate is faster than the restoration of the diffuse double layer by diffusion of the ions the first electroviscous effect is smaller. So the electroviscous effect is dependent on the shear rate. Another drawback of the above theory is that the packed bed is made of particles instead of slit-capillaries.

Another approach is to calculate a theoretical viscosity of a theoretical suspension with a low volume fraction under the same conditions as occur in the packed bed. The viscosity calculated for this suspension is then compared to the viscosity of the same suspension without the electroviscous effect, from the change in volume fraction a theoretical increase in particle radius is calculated. An equation to calculate such viscosity increases in a dilute suspension (low surface potentials) was given by Russel^{5,6}:

$$\eta_r = 1 + 2.5 \phi \left(1 + \frac{6\epsilon_0 \epsilon_r \psi^2}{(\kappa a)^2 \eta_0 \omega kT (1 + Pe_i^2)} \right) \quad (3)$$

with κ : reciprocal Debye length (m^{-1})

k : Boltzmann constant (J/K) T : absolute temperature (K)

ψ : potential at the surface of the particles.(V)

Pe_i : Péclet number for ions, defined as:

$$Pe_i = \frac{\gamma}{\kappa^2 \omega kT} \quad \text{with } \gamma \text{ being the shear rate (s}^{-1}\text{)}$$

ω : mobility of the ions in the double layer ($m N^{-1} s^{-1}$)

γ can be estimated as the maximum shear rate on the wall of the capillaries in the pores of the packed bed: $\gamma = (4Q)/(\pi r^4)$ with Q the volume rate of flow through a pore in the packed bed and r the mean pore radius of such a pore. The maximum shear rate in the packed bed is in our case about 500 s^{-1} . The Péclet number calculated in our case (electrolyte concentration 0.01-0.4 M KNO_3 , 25°C , ω for K^+ -ions is $4.8 \times 10^{11} \text{ m N}^{-1} \text{ s}^{-1}$) is very low ($\approx 10^{-6}$). The mean shear rate is of course less than the maximum shear rate but then the Péclet number calculated is even smaller. The equation can in the case of low Peclet numbers be reduced to the Booth⁷ formula for low potentials:

$$\eta_r = 1 + 2.5 \phi \left(1 + \frac{6\epsilon_0 \epsilon_r \zeta^2}{(\kappa a)^2 \eta_0 \omega kT} \right) \quad (4)$$

We are not interested in the contribution of the first electroviscous effect on the viscosity of a suspension with a low volume fraction, but we want to make an estimation of the first electroviscous effect in the pores of the packed bed. We therefore calculate an increase in effective particle radius:

$$\begin{aligned} \frac{\eta_r' - 1}{\eta_r - 1} &= \frac{2.5 \phi'}{2.5 \phi} = \frac{2.5 \phi \left(1 + \frac{6\epsilon_0 \epsilon_r \zeta^2}{(\kappa a)^2 \eta_0 \omega kT (1 + \text{Pe}_i^2)} \right)}{2.5 \phi} = \\ &= \frac{(a + \Delta a)^3}{a^3} \end{aligned}$$

$$\Delta a = a \sqrt[3]{1 + \frac{6\epsilon_0 \epsilon_r \zeta^2}{(\kappa a)^2 \eta_0 \omega kT (1+Pe_i^2)}} - a \quad (5)$$

The second electroviscous effect is the apparent increase in viscosity of a fluid as a result of double-layer interactions. In a dilute suspension this interaction changes the trajectory of one particle when passing another particle of the same charge. In a packed bed it is not possible to separate the first and the second electroviscous effects completely. But as a consequence of the overlap of the double layers the increase in viscosity calculated as the first electroviscous effect will be somewhat lower. This second electroviscous effect is only important when the diffuse double layer is large compared to the pore size in the packed bed ($\kappa h < 10$). In our case with electrolyte concentrations of 0.01 M KNO_3 or higher and a mean pore radius of about 40 nm the effect is not important.

The third electroviscous effect is due to a layer of adsorbed polyelectrolyte. The thickness of this polymer layer changes with the electrolyte concentration because the repulsion between the charged groups of the polymer chains and the charged groups on the surface depends on the electrolyte concentration. Lyklema² pointed out that there are two opposing trends in a system with polyelectrolyte being adsorbed from an electrolyte solution on a charged surface: If salt is added to such a system the attraction between the charged groups of the polyelectrolyte and the charged groups on the surface (in our case $-OH_2^+$ groups) is reduced and the adsorption is decreased. On the other hand the mutual repulsion between the charged groups is also reduced so the polyelectrolyte behaves more like an uncharged polymer. An uncharged polymer is

able to form extended loops and tails and so the adsorption is increased. Experiments show either an increase² or a decrease in adsorption⁸ with increasing salt concentrations. If the amount adsorbed is directly related to the layer thickness the layer thickness can increase as well as decrease as a function of the electrolyte concentration. On the other hand if the amount adsorbed is irrespective of the electrolyte concentration the mutual repulsion of the polyelectrolyte chains will, at low salt concentrations, cause an extended layer containing much solvent between the polymer chains and a thin and compact layer at high salt concentrations⁹.

3.3.2 Calculation of the hydrodynamic layer thickness from experimental data.

The permeability of the packed bed is defined according to D'Arcy:

$$K = \frac{Q \eta L}{A \Delta P} \quad (6)$$

with : Q: volume rate of flow (m³/s)
 η : viscosity (Ns/m²)
 L: length of the packed bed (m)
 A: cross section area (m²)
 ΔP : pressure drop over the column (Pa)

The most convenient way to calculate the radius in the pores of the packed bed is introduced by Blake-Kozeny¹⁰:

$$r_c = 2 \sqrt{\frac{K k}{\epsilon}} \quad (7)$$

with : K: permeability (m²)
 ϵ : porosity=void volume/total volume
 k: Kozeny constant (normally + 4.2)
 r_c : radius of capillary

The Kozeny constant is an empirical value which is introduced to bring the theoretically derived equation in line with the experimental data. A packed bed can be approximated as a bundle of capillaries with radius r_c . In each capillary there is a Poiseuille velocity distribution so the volume rate of flow can be calculated for one capillary as:

$$Q_c = \frac{\pi \Delta P r_c^4}{8 \eta L} \quad (8)$$

with : ΔP : pressure drop over the column (Pa)
 r_c : radius of one capillary (m)
 L : length of the column (m)

The number of capillaries of length L in the column can be calculated with:

$$N = \frac{A \varepsilon}{\pi r_c^2} \quad (9)$$

With: A : cross section area of the column (m^2)
 ε : porosity ()

For 6, 8 and 9 the theoretical capillary radius can be calculated:

$$r_c = \sqrt{\frac{8 \eta L Q_t}{\varepsilon \Delta P A}} = 2 \sqrt{\frac{2 K}{\varepsilon}} \quad (10)$$

with Q : total volume rate of flow (m^3/s)

If the particles are spheres a relation can be derived¹⁰ between the capillary radius (r_c) and the particle radius(r_p):

$$r_c = 2 \left(\frac{\text{volume available for flow}}{\text{total wetted surface}} \right) = 2 \left(\frac{\frac{\text{volume of voids}}{\text{volume of bed}}}{\frac{\text{wetted surface}}{\text{volume of bed}}} \right) = \frac{2 \varepsilon}{A_{sp} (1-\varepsilon)}$$

where A_{sp} is the specific surface area (m^{-1}) which is related to the mean particle radius as $A_{sp} = 3/r_p$. So the capillary radius can be calculated from the particle radius with:

$$r_c = \frac{2/3 \epsilon r_p}{1 - \epsilon} \quad (11)$$

with ϵ : void fraction
 r_p : particle radius r_c : mean capillary radius

In the case of non spherical particles equation 11 can be used to calculate an effective particle radius in the packed bed.

If we compare the theoretical equation 10 with the empirical equation 7, it is now obvious that the adjusting parameter is ± 2.1 (=half the Kozeny constant). The difference between theory and experiment (implemented in the Kozeny constant) is explained by the consideration that the pores in a packed bed are not straight capillaries but have narrow and wide passages. Another consideration is that the flow of the fluid through the pores is not straight: The length of the capillaries should be greater than the length of the column due to the tortuosity in the column. With the Blake-Kozeny equation the mean pore radius can be calculated from the permeability if the porosity of the packed bed is known. If there is a reduction of the permeability caused by the third electroviscous effect the hydrodynamic layer thickness is calculated as the difference between the newly calculated radius and the original radius.

The second way to calculate the hydrodynamic layer thickness is to combine the permeability experiments with the mercury-porosimetry experiments. We tackle the problem in the same way as in equations 8 and 9, except that we now calculate a flow through a capillary of each measured pore radius. The bundle of capillaries with equal radii is now transformed into a number of bundles of capillaries

with equal radii. Each bundle is built of capillaries with radii measured by mercury intrusion. These bundles can be placed beside each other (parallel) or behind each other (serial) (see figure 1).

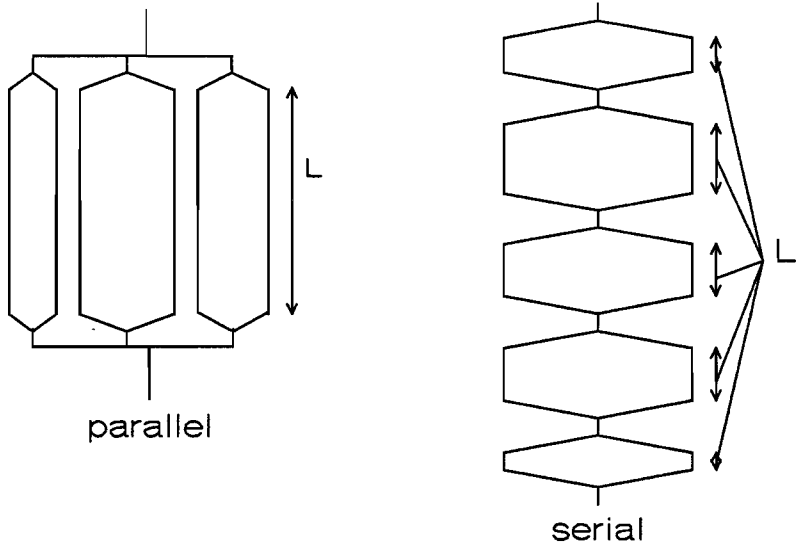


Figure 1: Different pore-sizes determined by mercury porosimetry can be regarded as parallel or serial bundles of capillaries

In the case of serial capillaries the pressure drop over each bundle can be calculated using equation 10. The length of each bundle is proportional to the incremental pore volume determined by mercury porosimetry. The pressure drop over the column is the sum of the pressure drops over the bundles. With the parallel bundles of capillaries the pressure drop over the capillaries and the length of the capillaries are the same for all size categories. The flow in the whole column is the sum of the flow in

the separate classes of capillaries.

In the case of serial bundles of capillaries the small pores in the packed bed are overestimated because the pressure drop over the smallest pores is very high even when the length of that bundle is small compared to larger pores. In the case of the parallel bundles the permeability of each bundle is calculated using equation 10. The cross-section area of each bundle is assumed to be proportional to the incremental pore volume of each radius and the total permeability is the sum of the permeabilities of all bundles. With the parallel bundles the large pores in the packed bed are overestimated. In this approach we do not use a Kozeny constant to adjust the theoretical calculation to the experimental measurements. Instead the range of the capillary radii is adjusted to give an acceptable value for the macroscopic quantity (pressure difference or permeability). For the serial bundles of capillaries the very small capillaries are disregarded. In the case of the parallel bundles of capillaries the very large capillaries are excluded. In this way we can calculate a decrease in the radii of the subsequent pores if the pressure drop is higher at the same flow rate (serial bundles) or if the permeability decreases (parallel bundles). If a homogeneous layer is formed on all capillaries a lower permeability for the packed bed is measured. If we fit the layer thickness to the measured permeability we obtain an overestimation of the layer thickness in the case of the parallel capillaries and an underestimation of the layer thickness in the case of the serial capillaries.

The third way to calculate the hydrodynamic layer thickness is a pore model for a hexagonal closed packed (HCP) bed of equal sized spherical particles. The octahedral holes in a HCP bed are situated above each other in contrast to the tetrahedral holes of a cubic closed packed (CCP) bed¹¹ (see figure 2). To obtain the

right porosity in the bed the particles are placed at a fixed distance from each other (see figure 3).

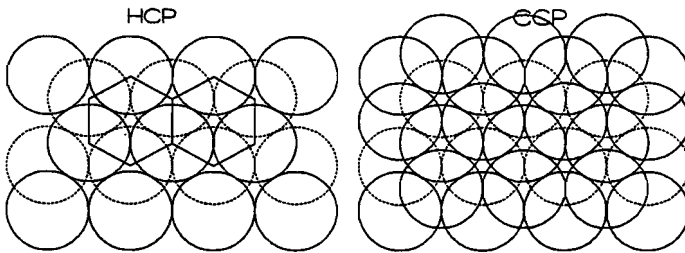


Figure 2: Hexagonal Close Packing a) and Cubic Close Packing b). In the Hexagonal Close Packing a pore can be defined in the middle of a hexagon.

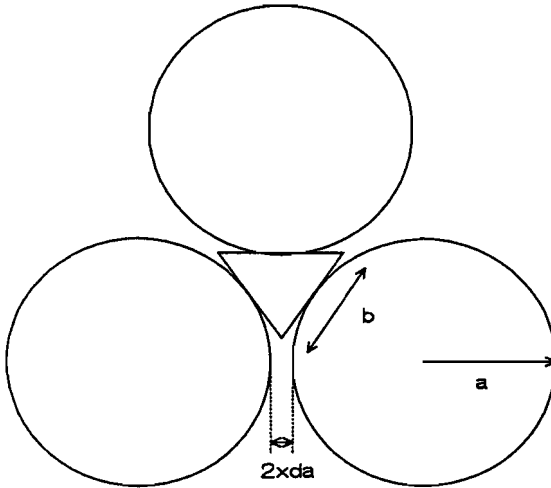


Figure 3: Triangle in the narrowest part of the pore in a HCP-bed. The particles are separated at distance da to obtain the right porosity.

The pore is then approximated by a stack of triangles each fitting into the space between the particles (see figure 4). For an equilateral triangular shaped tube with sides of length b the volume rate of flow is given by¹²:

$$Q = \frac{\sqrt{3} \Delta P b^4}{320 \eta l} \quad (12)$$

with ΔP : pressure drop over the tube (Pa)
 b :triangle side length (m)
 l :length of the tube (m)

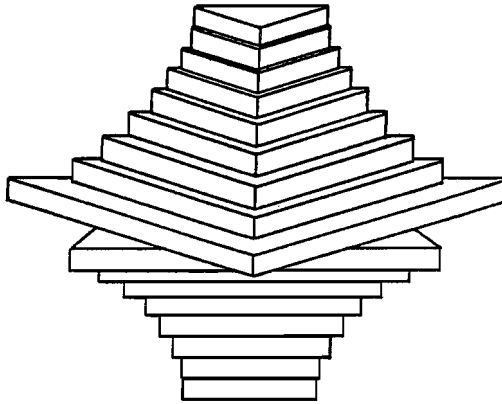


Figure 4: Stacked triangles as an approximation of the pore in an HCP-bed.

The volume rate of flow is the same in all segments of the pore and can be calculated from the total flow rate in the column, using the cross section area of the column and the area of the hexagon (figure 2a):

$$Q_p = Q_t \frac{\text{surface area hexagon}}{A}$$

$$Q_p = Q_t \frac{3.464 (a + da)^2}{A} \quad (13)$$

with Q_p : flow through one pore (m^3/s)
 a : particle radius (m)
 da : distance to be adjusted
for the right porosity (m)
 A : column cross section (m^2)
 Q_t : flow through the packed bed

With the equations 12 and 13 the pressure drop over each triangle can be calculated and the pressure drop over the pore is the sum of all triangle segments in the pore. To calculate the total pressure drop over the column, the pressure differences over the slices of one pore (as drawn in figure 4) are totalled and the result is scaled to the total column:

$$\Delta P_t = \Delta P_p \frac{L}{1.633 (a + da)} = \frac{L}{1.633 (a + da)} \sum \Delta P_i \quad (14)$$

with: ΔP_t , ΔP_p , ΔP_i respectively the pressure drop over:
the column, a pore, a triangle.

L: length of the column.

1.633(a+da): length of a pore as drawn in figure 4

In the narrow part of the pore the pressure drop calculated in this way is overestimated compared to the real pressure drop because the area of the triangle is less than the real void area in the pore. In the wide part of the pore the calculated pressure drop is underestimated because the edges of the triangle reach beyond the hexagon. The underestimation at the wide part of the pore is not as important as the overestimation in the narrow part because the absolute value of ΔP_i is negligible in the wider part (see figure 4). As a result of the overestimation in the narrow part of the pore the calculated pressure drop over the pore is too high and the calculated hydrodynamic layer thickness is underestimated.

3.4 Results and discussion

In figure 5 the influence of both the electrolyte concentration and the polyacrylic acid concentration on the permeability is shown. Higher electrolyte concentrations give higher

permeabilities. The polyacrylic acid concentration is an equilibrium concentration because the column has been washed with these concentrations for 12 hours or more. For the highest electrolyte concentrations (0.4 and 0.1 M KNO_3), the polyacrylic acid concentration has no effect on the permeability.

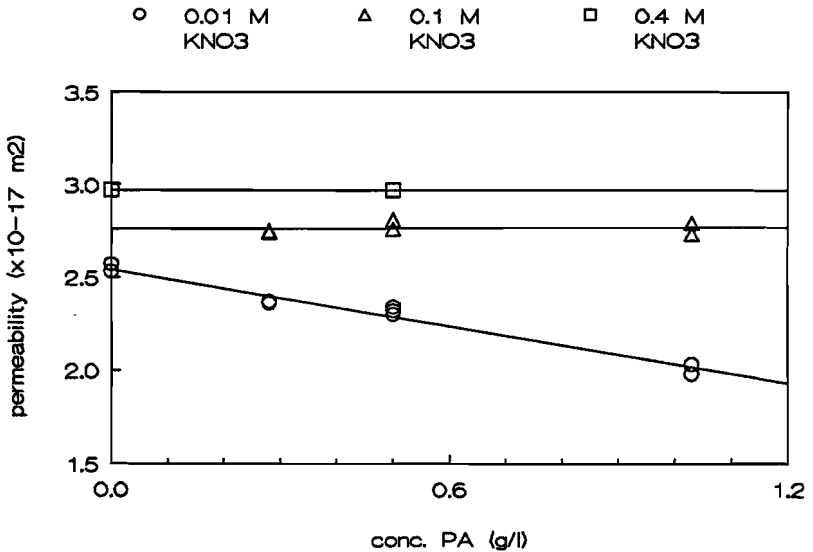


Figure 5: The influence of the salt concentration and the polyacrylic acid concentration on the permeability of the packed bed. The PAA concentration is only important at the lower electrolyte concentrations.

However at a concentration of 0.01 M KNO_3 the permeability decreases with the polyacrylic acid concentration. There are three possible explanations for this effect:

a) At higher concentrations of polyacrylic acid more polymer is adsorbed and the hydrodynamic layer thickness increases. This is not a plausible explanation because the adsorption isotherm

reaches its plateau above an equilibrium concentration of 0.5 g/l polyacrylic acid. The packed bed is flushed with a PAA-solution with an initial concentration of more than 0.5 g/l. The packed bed is flushed until the permeability is constant for 15 hours.

b) The polyacrylic acid solution is shear thinning. The viscosity measured in the Ubbelohde viscosimeter was used to calculate the permeability. But the shear rate in the capillary viscosimeters is different from the shear rate in the pores of the packed bed. This is not probable either because the solutions used are very dilute (the absolute viscosity of the most concentrated solution was 1% higher than the viscosity of water) and showed no difference in measured viscosity in the Oa ($\gamma_{\max} = 2100 \text{ s}^{-1}$) and the Oc ($\gamma_{\max} = 1630 \text{ s}^{-1}$) Ubbelohde Viscometer. The maximum shear rate in the pores of the plug is about 500 s^{-1} (calculated with $\gamma = 4Q/\pi r^3$, where Q is the volume rate of flow through a pore and r the radius of the pore, in our case about 35 nm). So the shear rate in the pores is still a factor 3 lower than in the Oc Ubbelohde. The effect in figure 5 is explained by the fact that a decrease in the shear rate from 1600 to 500 results in an increase in the absolute viscosity of about 20% .

c) Rod-like polymers have a concentration profile in narrow capillaries^{13,14}. The polyacrylic acid molecules have a rod-like structure at low salt concentrations and are probably coiled at higher salt concentrations. This appears to be the most probable explanation.

In order to avoid these polymer concentration effects at lower electrolyte concentrations we can extrapolate to polymer concentration zero. Another and shorter way to avoid this problem is to wash the column alternately with solutions with polyacrylic acid and without polyacrylic acid at a one electrolyte concentration. In this way the solution at a certain distance from the particle surface is close to zero and the polymer layer at the

particle surface will be unchanged because the desorption process is very slow. The permeabilities obtained after washing with only the electrolyte are plotted in figures 6 and 7.

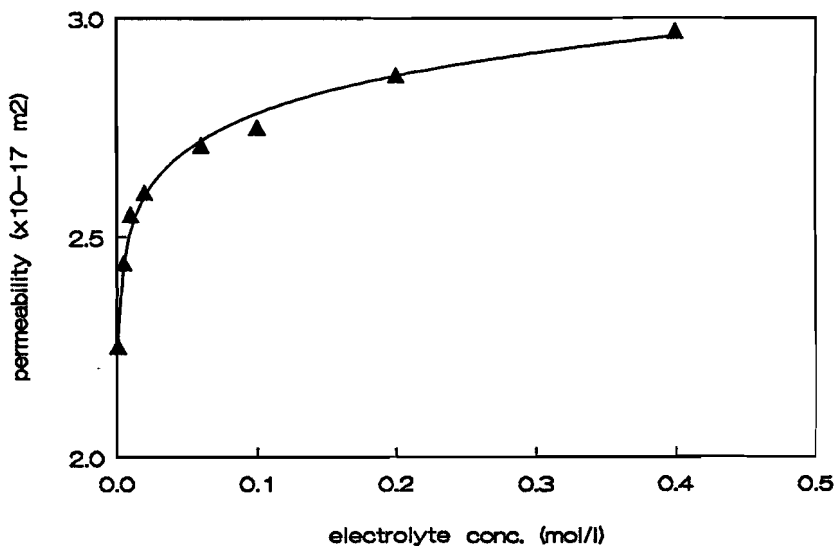


Figure 6: The permeability of the packed bed of titanium dioxide at different electrolyte concentrations.

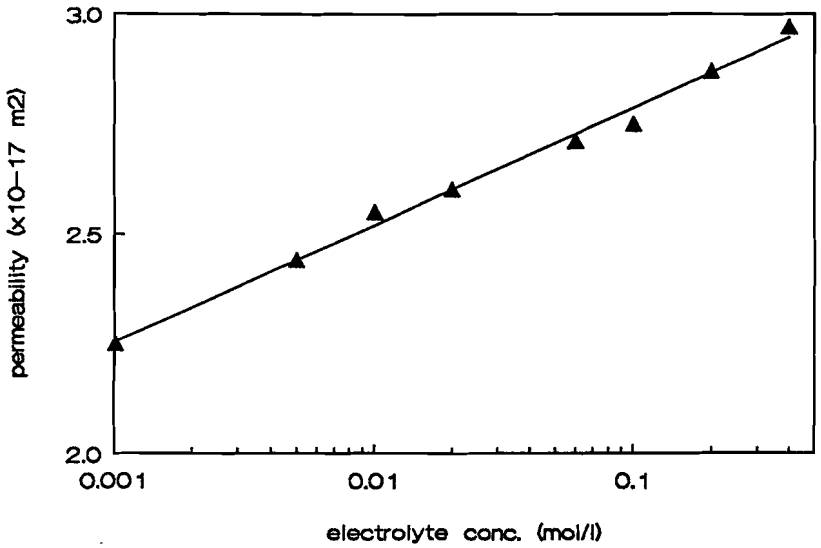


Figure 7: The linear dependency of the permeability of the $\log(\text{electrolyte conc.})$ as used for the calculations of the layer thickness.

To get an idea of the validity of the three models mentioned, we performed some calculations with a well defined packed bed of glass spheres (diameter= $64.3 \pm 7.6 \mu\text{m}$, $K= 3.9 \times 10^{12} \text{ m}^2$, $\epsilon=0.375$, median pore diameter(volume) from mercury porosimetry= $18.60 \mu\text{m}$). The results of these calculations are shown in table 1:

Table 1: Parameters as used with the 4 different models in order to fit the permeability data of a packed bed of monodispersal glass particles.

model	radius used	calibration param.
Kozeny	32.2 μm sphere	2.08
HCP	32.2 μm sphere	2.75
parallel	pore < 100 μm	--
serial	pore > 0.2 μm	--

The calibration parameter obtained with the Kozeny model is the kozeny constant ($k=2 \times 2.08=4.16$) normally found for packed spheres. The model which uses mercury porosity data seems to fit well with the measurements. The pores used for the calculation of the serial and the parallel bundles of capillaries form the majority of the pores in the packed bed (see figure 8).

The HCP model underestimates the permeability because the pressure drop in a narrow part of the pore is overestimated (see theory).

We performed the same calculations for the packed bed of rutile particles which were of course far from ideal for this kind of calculation (polydisperse needles):

Table 2: Parameters as used with the different models to fit the permeability data of a packed bed of titanium dioxide particles.

model	radius used	calibration param.
Kozeny	75 nm sphere	2.08
HCP	75 nm sphere	2.55
HCP	116 nm sphere	1
parallel	pores < 100 nm	--
serial	pores > 20 nm	--

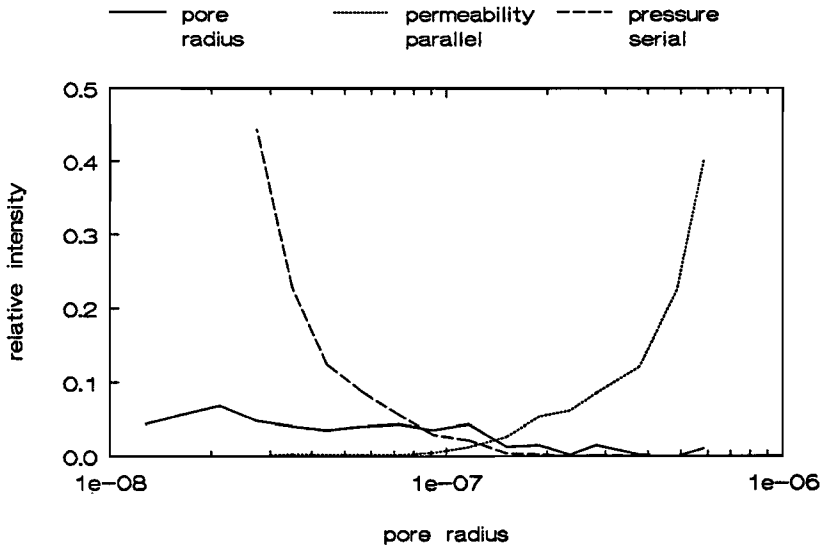


Figure 8: The relative intensity of different parameters obtained from mercury porosimetry (heterodisperse titanium dioxide particles):

- intensity of the pore radius
- calculated relative importance of the pore radius in the parallel model
- calculated relative importance of the pore radius in the serial model.

Because the particles are heterodisperse and the bed is heterogeneous packed the two calculated intensities do not match the pore size distribution.

In the case of the Kozeny theory we adjusted the sphere diameter to match the experimental data using a Kozeny constant of the usual value. Electron microscopy showed that the needles were bundles of parallel packed needles, so a discription as packages with a radius of 150 nm is quite satisfactory. For the HCP-model

the same radius for the spheres is used as was found for the Kozeny model. When a radius of 110 nm was chosen for the particles the model fitted the experiments precisely. In the model using the mercury porosity measurements the large pores are excluded in the parallel variant. The number of large pores measured with mercury porosity is low but they contribute substantially to the porosity in the parallel model.

The result of the calculations with the three models is plotted in figure 10. Although the results of these calculations differ a factor 4, it is clear that the hydrodynamic layer thickness does not exceed 10 nm.

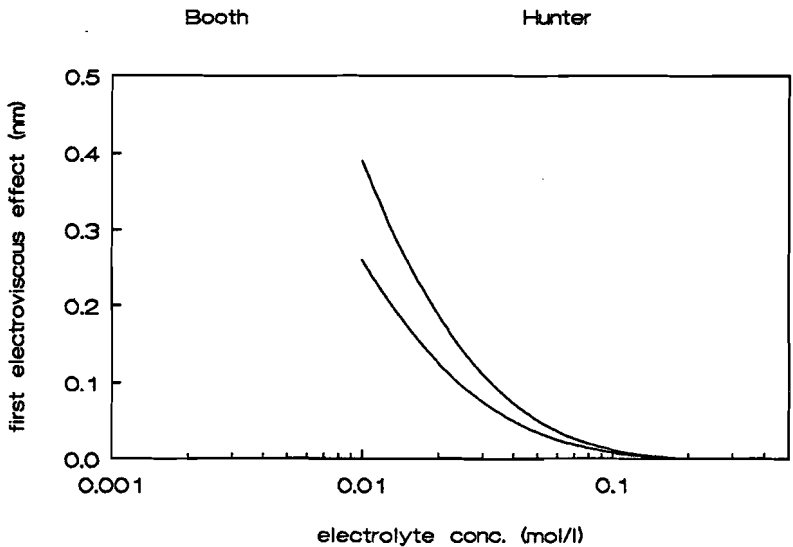


Figure 9: Calculated apparent increase in layer thickness as the result of the first electroviscous effect.

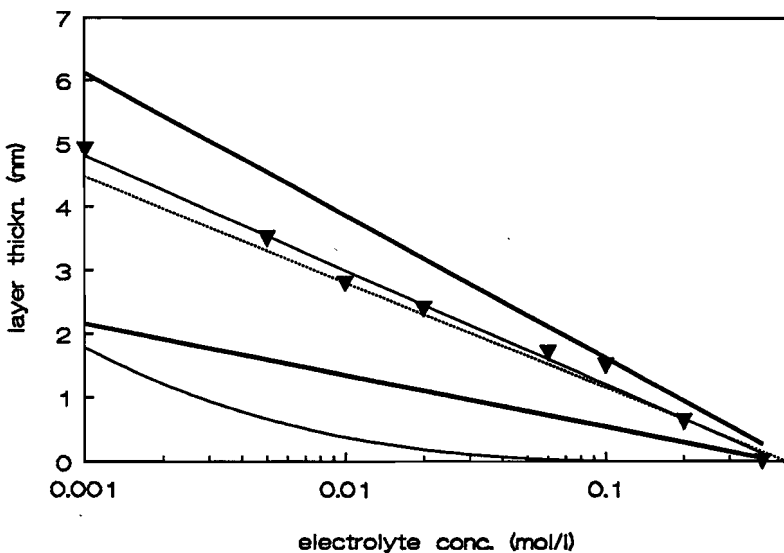


Figure 10: Calculated layer thickness with the four models:
 — over and underestimation (mercury por.)
 — Blake/Kozeny model
 - - - HCP-model
 For comparison the calculated contribution of the first electroviscous effect is also shown

3.5 Conclusions

- In a packed column of titanium dioxide particles a decrease in permeability is observed after the column is flushed with a PAA solution.
- The decrease in permeability can be explained by a polymer layer on the oxide surface.
- A hydrodynamic layer is calculated varying from 0 to 5 nm depending on the electrolyte concentration.

- ¹T. Cosgrove, T.M. Obey, B.Vincent, J.Colloid Interface Science,111(1986) 446.
- ²J.Lyklema, G.J. Fler, Electrical contributions to the effect of macromolecules on colloid stability, Colloids and Surfaces,25 (1987) 3357-368.
- ³ Y.G. Bérubé and De Bruyn, Adsorption at the Rutile-Solution Interface, I Thermodynamic and Experimental study, J. of Colloid and Interface science, Vol. 27, no. 2,(1968), P. 305-318.
- ⁴R.J. Hunter, Zeta potential in colloid science, Academic Press Inc., London(1981), p. 181.
- ⁵W.B. Russel, The rheology of suspensions of charged rigid spheres, J. Fluid Mech. Vol. 85, 1978, p.209-232
- ⁶W.B. Russel, Bulk stresses due to deformation of the electrical double layer around a charged sphere, J.Fluid Mech.(1978), vol 85, part 4, p 673-683.
- ⁷F. Booth, The electroviscous effect for suspensions of solid spherical particles, Proc. Roy. Soc. Vol.A 203, (1950), p. 533-551.
- ⁸T.K. Wang, R Audebert, Adsorption of cationic copolymers of acrylamide at the silica-water interface: Hydrodynamic layer thickness measurements. J. of Colloid and Interface Science Vol 121, No.1,(1988), p 32-41

⁹R. Buscall, Properties of polyelectrolyte-stabilized dispersions, J. Chem. Soc. Faraday Trans. I Vol 77(1981),909-917.

¹⁰R.B. Bird, W.E. Steward, E.N. Lightfoot, Transport Phenomena, New York 1960, Willk & Sons Inc..

¹¹F.A. Cotton and G. Wilkinson, Basic Inorganic Chemistry, J. Wiley & sons, inc., New York (1976), ISBN 0-471-17539-0.

¹²J. Happel and H. Brenner, Low Reynolds number hydrodynamics, (1986) Martinus Nijhof Publishers,Dordrecht,The Netherlands, ISBN 90-247-2877-0, p 39.

¹³G. Chauveteau, M. Tirrell, A. Omari, 2nd Colloque Europeen, Récupération assistée du Pétrole, Paris, November 8-10, 1982, p.163, Technip Ed.,Paris, 1982.

¹⁴D.A. Hoagland, Concentration profiles of rod-like polymers in narrow channels, J. of Colloid and Interface Science, Vol.123, No 1,(1988).

CHAPTER 4:

MONODISPERSE PIGMENT PARTICLES.

4.1 Introduction

In colloid chemical experiments monodisperse particles are often preferred to poly disperse samples. The theoretical interpretation of the experiments with monodisperse particles is easier. In dynamic light scattering experiments (or Photon correlation Spectroscopy) the polydispersity of the sample is very important. With dynamic light scattering a correlation function for the decrease of the intensity of the scattering of a particle in time is found. For a monodisperse sample an exponential function can be matched to the correlation function. The result of the matching procedure is a diffusion constant from which a particle radius can be calculated. For a heterodisperse sample for each class of particle size a theoretical exponential function is calculated and the summation of the exponential functions at each radius is fitted to the correlation function. In this way a diffusion constant of several size classes and the accompanying particle radii can be found. For samples with a relatively low polydispersity this procedure gives a reasonably good result. But if the sample is more polydisperse the number of variables in the fitting procedure increases and the result is no longer reliable. Often a bimodal size distribution is found in samples with a continuous size distribution.

Mono disperse particles are often obtained by a special synthesis. Organic particles can be synthesized by an emulsion polymerization. Mono disperse titanium dioxide particles can be synthesized also¹. But the particles synthesized in this way have

some drawbacks:

- 1) The specific surface area obtained with the B.E.T.-method is very large and the density is very low, indicating that the particles are porous.
- 2) The yield of one batch of this synthesis is only a few grams of monodisperse particles.

For the industry it is also important that the particles have had the same treatment as the particles used in their products, so the same synthesis and the same coatings on the particles are preferred. The only way to achieve a monodisperse sample meeting these requirements is to separate a monodisperse fraction from a heterodisperse sample. The most appropriate method for fractionation of a heterodisperse sample is sedimentation: a suspension is stirred in a large cylinder and is allowed to sediment for a fixed time. After this time a sample is taken at a certain height in the cylinder and this procedure is repeated until enough particles have been collected. This method is not only laborious and time consuming but for particles with a radius smaller than 1 μm sedimentation is also very slow and the diffusion causes a broadening of the band with the monodisperse particles. In order to fractionate particles with a radius of between 0.1 and 1 μm we investigated the possibility of using a counter flow centrifugation method.

4.2 Materials and methods

For the testing of the apparatus we used Potters Ballotini glass particles (soda lime glass) with a diameter of about 1 to 10 μm . The glass particles had a zeta potential of about -70 mV at pH 11, no electrolyte was added.

As titanium dioxide particle a so called 'burner discharge' was

used from Tiofine. The burner discharge contains titanium dioxide particles produced with the reaction between TiCl_4 and O_2 in the 'burner'. The particles formed in the 'burner' have their ultimate shape and diameter and no other treatments are applied.

To fractionate the particles we used a Heraeus Varifuge F with a special counter flow rotor (speed 0-3000 \pm 3 rpm). The rotor is designed in such a way that the incoming and outgoing tubes are not strangled while the rotor is turning. No use was made in this construction of a sliding-contact to transport the fluids. The purchased rotor was developed for the fractionation of blood cells with four cuvettes on the rotor, four supplying tubes and four discharging tubes. The fractionation of the original equipment was semi-continuous: At a certain rotor speed the cuvettes were flushed with the dispersion until enough particles of one diameter had gathered in the cuvette. To harvest the required fraction the rotor speed was decreased.

In order to make a full continuous process we designed two new cuvettes each with two outlets and one inlet (see figure 1).

The cuvettes were used in series to obtain a separation into three fractions in one run: The polydisperse sample is pumped into the inlet (1). In the first cuvette the largest particles are centrifuged away from the axis of the rotor and are discharged at one outlet (2). The smallest particles are taken with the flow of the liquid to the second cuvette. The radius of the second cuvette is larger than that of the first cuvette and the velocity of the mainstream is lower. In this cuvette a mid fraction is separated and discharged by an outlet (3). The mainstream with the smallest particles is discharged through the last outlet (4).

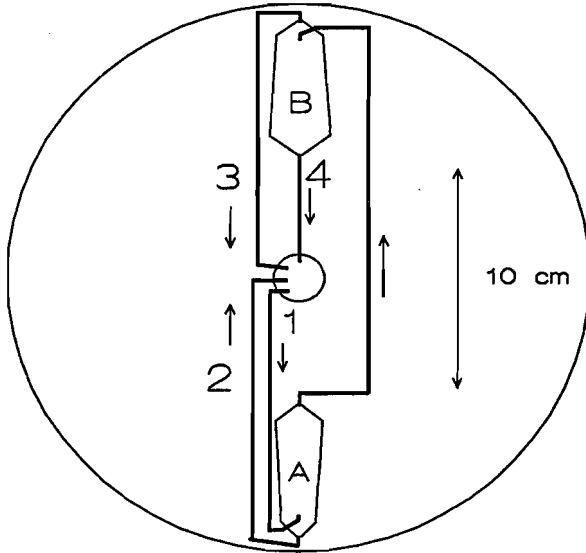


Figure 1: Rotor with two serial cuvettes. With this setup it was possible to obtain three fractions of particles out of a polydisperse sample in one run

The velocity in the cuvette is related to the volume rate of flow as:

$$v_1 = \frac{Q}{\pi r_c^2} \quad (1)$$

with: Q : volume rate of flow (m^3/s)
 r_c : radius of the cuvette (m)
 v_1 : velocity of the liquid in the cuvette (m/s)

The velocity of a particle in a centrifugal field is calculated with:

$$v_p = \frac{2 r_p^2 (\rho - \rho_0) \omega^2 x}{9 \eta_0} \quad (2)$$

with r_p : particle radius
 ρ, ρ_0 : density of the particle resp.
the fluid. (kg/m³)
 ω : rotor speed (s⁻¹)
 x : distance to the rotor axis (m)
 η_0 : viscosity fluid.

The cuvettes are designed to give a constant value to the ratio of the centrifugal force on a particle to the drag force of the liquid on a particle at any place in the cuvette, so near the axis of the rotor the radius of the cuvette is wider and the velocity of the liquid is lower than at a greater distance from the axis where the radius is smaller and the velocity of the fluid is high (see figure 1). The radius of the separated particles can be calculated if we assume that the velocity of the fluid and the sedimentation of the particles are equal ($v_l = v_p$). The particles with this radius do not move in the cuvette. Combining formula 1 and 2 we obtain:

$$r_p = \sqrt{\frac{9 \eta_0 Q}{2 \pi r_c^2 (\rho - \rho_0) \omega^2 x}} \quad (3)$$

The calculated particle sizes of six different experiments and the measured particle size are compared in figure 2: The measured size and the calculated size are of the same order of magnitude. There

is only a difference between measured and calculated sizes for the largest particles, probably caused by sedimentation during the experiment.

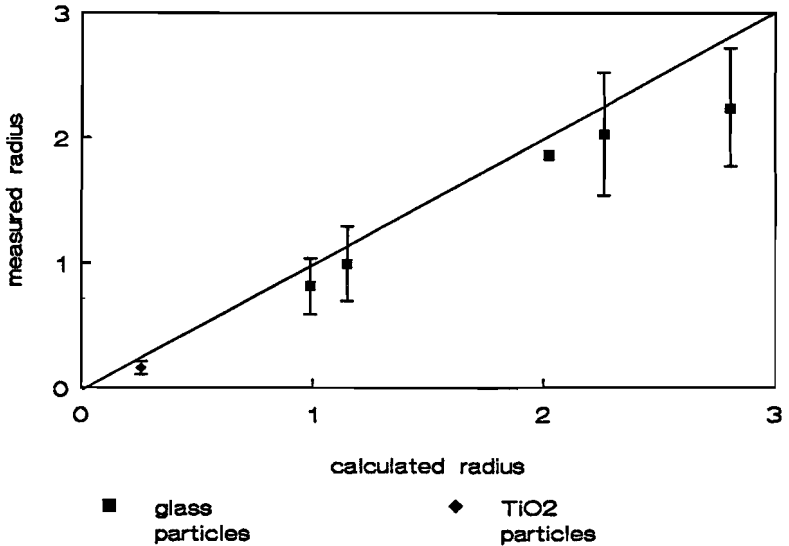


Figure 2: The calculated (formula 3) and measured particle radii of six experiments with the counter flow centrifugation equipment. For this graph data from table 1 are used.

The particle size distribution of the original samples and of the fractioned samples were measured using four methods:

1) For the glass particles above 1 μm a **Coulter Counter** (Coulter Counter ZM, Coulter Counter Channelyzer 256, Coulter range expander) was used. The particle size distribution was measured using a tube with an opening of 30 μm . With this equipment

particle sizes of 1 to 10 μm were measured accurately. An example of the original sample and the fractioned sample is shown in figure 3.

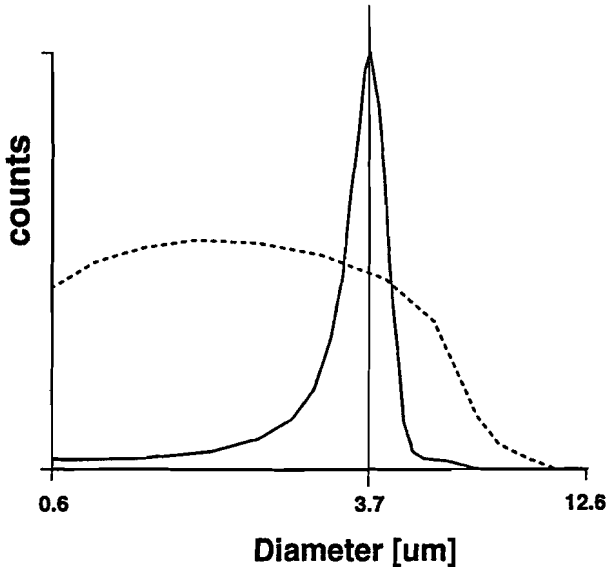


Figure 3: Measured particle size distribution of the original and the fractioned glass particles.

2) For the titanium dioxide particles with a size of less than 1 μm a **disc centrifuge particle sizer** (Brookhaven Instruments Corporation DCP-particle sizer) was used. The spin fluid (fluid with a known viscosity and density in which the sedimentation of the particles is measured) was a 10 wt% solution of sucrose in water (12 ml). As a buffer layer (layer on top of the spin fluid in which the particles are injected) 2 ml of water was used. The disc speed was in all cases 1500 rpm and the particle concentration was about 0.05 wt%. In figure 4 the results of an

original and a fractioned sample are shown.

3) **Dynamic light scattering** is a technique which only gives a reliable result in the case of more or less monodisperse spherical particles with a diameter of less than 1 μm . The technique was tested with a monodisperse latex dispersion of 200 nm and the result was within 1% accuracy the same as the result of an electron microscopic picture. The measurements were performed on a zetasizer III, with a round cell(AZ10). The correlation function was measured 20x10 seconds. This procedure was repeated at six angles (45,60,75,90,105,120^o). The correlation functions were

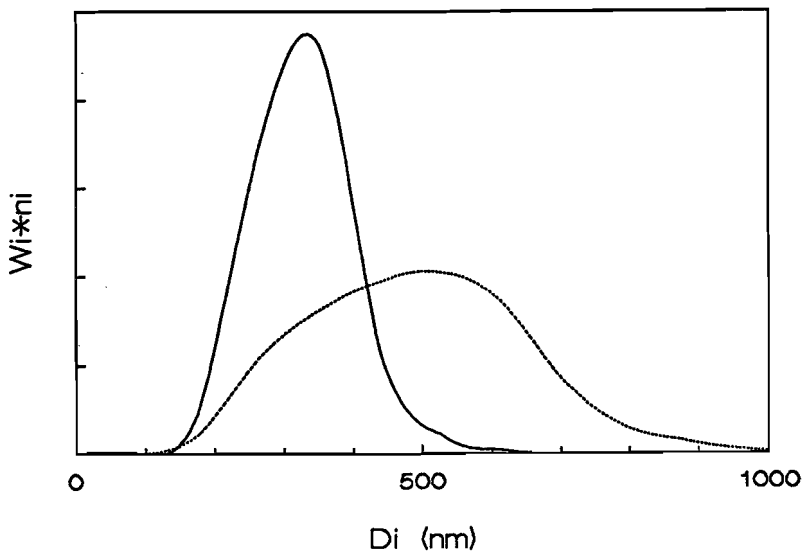


Figure 4: Original and fractioned TiO_2 -sample measured using the disc centrifuge particle sizer.
... original — fractioned

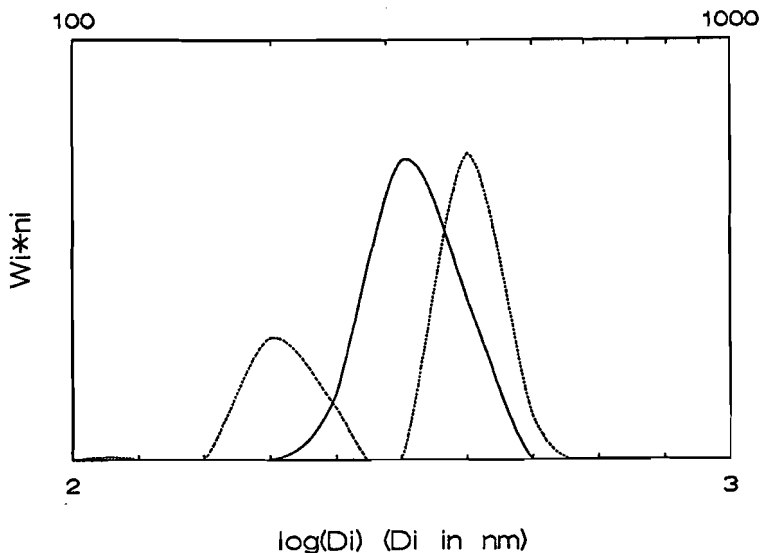


Figure 5: Original and fractionated TiO_2 -sample measured using the multi angle light scattering technique.
 original ——— fractionated

matched using the Malvern multi-angle software with a refractive index of the particles of 2.6. The range of 100 to 1000 nm was divided into 15 size-classes for this calculation. The samples were prepared in a dust-free flow cabinet using filtered water and filtered solutions. The suspension in the cuvettes was dispersed by ultrasonic treatment for 20 minutes. Samples with a bimodal distribution as a result were regarded as immeasurable. With the original rutile sample we obtained a bimodal distribution whereas the calculations of the fractionated TiO_2 sample resulted in one peak (see figure 5).

4) **Transmission electron microscopy (TEM)** pictures were taken of the original and fractioned TiO_2 samples. The particles were divided into the same size classes as above by measuring surfaces of projections of particles on TEM-photographs. In this way the size of about 100 particles was measured. It was difficult to distinguish between coagulated particles and sintered particles. We decided to count all more or less spherically shaped silhouettes on the picture as separate particles (figure 6), conscious of the fact that the mean radius obtained in this way is underestimated.

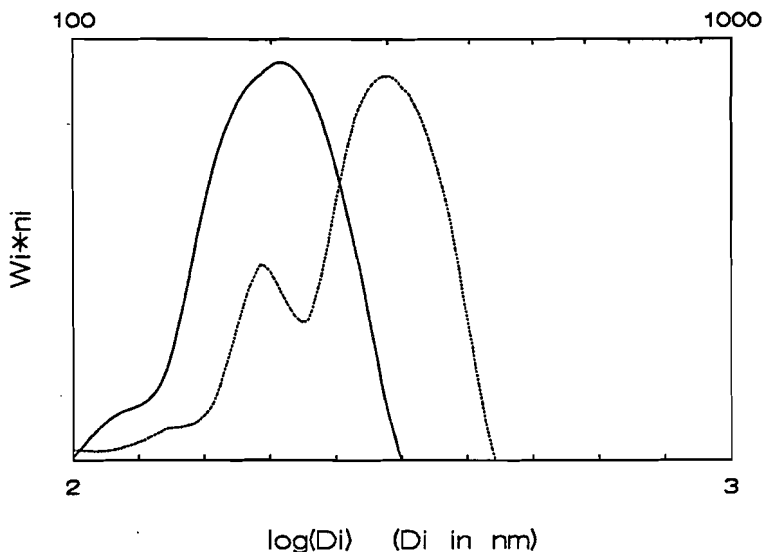


Figure 6: Size distributions obtained by measuring several TEM pictures.original, ——fractioned.

4.3 Results and discussion.

The result of six experiments with the counter flow centrifugation method is given in table 1:

exp	ω s ⁻¹	f1	f2	f3	$(Q1+Q2)/2$ m ³ /s	η_0 Pas	ρ_p kg/m	r_d μm	pol
Glass									
1	168	80	32	125	2.4×10^{-6}	0.9	2550	2.24	1.10
2	202	46	26	120	2.2×10^{-6}	0.9	2250	2.03	1.07
3	241	42	7	33	0.6×10^{-6}	0.9	2250	0.82	1.19
4	304	35	15	70	1.3×10^{-6}	0.9	2250	1.00	1.11
5	202	50	12	100	1.8×10^{-6}	0.9	2550	1.86	1.05
TiO ₂									
6	314	5.5	1.5	6.0	0.11×10^{-6}	1.2	4260	0.28	1.18

Table 1: Experiments with the counterflow centrifugation method. f1, f2, f3 refer to the volume rate of flow of the discharging tubes (figure 1). r_d is measured with the Coulter Counter (glass) or with the disc centrifuge (TiO₂) r_d is the number weighted particle radius. pol: polydispersity, defined as: D_w/D_n . D_w = mass average diameter, D_n = number average diameter

The radius of the TiO₂ particles were measured with three different methods. Table 2 shows the result of these measurements.

Method		D_n	D_w	polydisp.
disc centrifuge	original	332	488	1.47
	fractioned	280	329	1.18
dynamic light scat	original	(347)	(409)	(1.18)
	fractioned	306	318	1.04
transm. electr. micr	original	210	270	1.33
	fractioned	170	200	1.15

Table 2: The size of the original and fractionated TiO₂ dispersion. The result with dynamic light scattering was not reliable, a bimodal size distribution was calculated in this case.

4.4 Conclusions

With the counter flow centrifugation method it is possible to fractionate particles with a radius of 0.1 to 4 μm as long as the density difference with the continuous phase is sufficient. With particle radii of 1 μm to 4 μm the method is faster compared to the traditional sedimentation method. With particle radii of 0.1 to 1 μm the described method to fractionate the particles is the only available method. With this method we obtained a titanium dioxide dispersion with particles with a radius of about 0.15 μm . The polydispersity was about 1.15. In future research the fractionated titanium dioxide samples can be useful in coagulation experiments, rheological experiments and dynamic light scattering experiments. One important application is testing the ability of dispersing agents, for instance PAA-copolymers, to form sterically stabilizing layers. The hydrodynamic layer thickness can be measured either with rheological measurements (see chapter 6) or with dynamic light scattering. For the latter experiments monodisperse particles are essential(see figure 5 of this chapter), so perhaps the counter flow centrifugation technique can contribute to the search for a better dispersing agent in the future.

Literature

¹Barringer E.A.,The synthesis, interfacial electrochemistry, ordering and sintering of monodisperse TiO_2 Powders, Thesis, Massachusetts Institute of Technology, September 1983.

CHAPTER 5:

WETTING BEHAVIOUR OF OXIDES IN WATER.

5.1 Introduction

Traditionally the wetting behavior of oxide pigments is very important in the dispersing process for the production of solvent based paints. Surfactants were needed to convert the polar surface of the oxide to an apolar surface. Only with the aid of these surfactants were the pigments were wetted by the apolar solvent. In the case of the dispersion of oxide pigments in water it is obvious that the wetting is not obstructed by the different polarities as is the case of the apolar solvent. The contact angle is probably smaller than 90° , but the exact value of the contact angle is not known, neither is the possibility investigated of decreasing the contact angle in order to enhance the dispersion process. To gain insight into the wetting behavior of pigment particles an imbibition method was used to measure the contact angle. With this method the dynamic advancing and receding contact angle can be measured but the experiments are very laborious especially with small particles. Another drawback of this experiment is that the surface cannot be cleaned after an experiment with one concentration of an adsorbed agent. For the above mentioned reasons and for comparison the contact angle was also measured on the surface of a titanium dioxide single crystal.

5.2.1 The theory of wetting of a sessile drop.

To describe the influence of adsorbed agents on the contact angle it is convenient to consider the forces on a point of the contact line between the three phases:

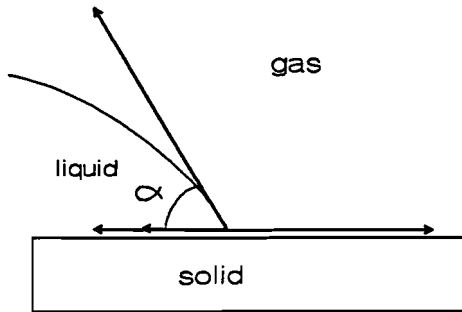


Figure 1: surface tensions at the liquid/gas/solid contact line

The force alongside the liquid-gas surface can be resolved into one component alongside the solid surface and one perpendicular to the surface. In an equilibrium situation the sum of the three forces alongside the solid surface should be zero:

$$\gamma_{SG} = \gamma_{SL} + \gamma_{LG} \cos \theta \quad (1)$$

with: $\gamma_{SG}, \gamma_{SL}, \gamma_{LG}$: surface tension in respectively the solid-gas, solid-liquid, and liquid-gas interface.
 θ = contact angle

The surface tension is strongly dependent on the excess of chemical substances in the interface. A relation between the surface tension and the amount adsorbed in an interface is given by Gibbs Law which for a binary solution can be formulated in the following way:

$$(d\gamma_T = -\Gamma_2 d\mu_2 \quad (2)$$

with: γ : surface tension (N/m)
 Γ_2 : amount adsorbed (kmol/m²)
 μ_2 : chemical potential (J/kmol)

Differentiating 1 and combining with 2 gives:

$$d(\gamma_{LG} \cos \theta) = d\gamma_{SG} - d\gamma_{SL} = -(\Gamma_{SG} - \Gamma_{SL}) d\mu_2 \quad (3)$$

Also $d\mu_2 = -d\gamma_{LG} / \Gamma_{LG}$, substituting $d\mu_2$ in 3 results in¹:

$$\frac{d(\gamma_{LG} \cos \theta)}{d\gamma_{LG}} = \frac{\Gamma_{SG} - \Gamma_{SL}}{\Gamma_{LG}} \quad (4)$$

In the case of the wetting of a dry pigment the adsorption of species from the solution in the solid/liquid interface and in the gas/liquid interface should be considered. If the solid surface is cleaned adequately before the experiment and if there is no evaporation of species from the solution and adsorption in the solid/gas interface, then the change in surface tension of the solid/gas interface is of minor importance. In this special case with no adsorption in the solid/gas interface we may write 4 as:

$$\frac{d(\gamma_{LG} \cos \theta)}{d\gamma_{LG}} = \frac{-\Gamma_{SL}}{\Gamma_{LG}} \quad (5)$$

The above considerations are based on the equilibrium situation in every stage of the wetting process. That there is indeed an equilibrium situation during the experiments is very unlikely: The occurrence of hysteresis of the contact angle in the case of wetting (advancing contact angle) and dewetting (receding contact

angle) is an important indication of the absence of equilibrium. There are three possible explanations for the hysteresis:

- 1) The surface roughness resulting in a different macroscopic contact angle while the contact angle on microscopic scale is the same for the advancing and receding situation (see figure 2).
- 2) No equilibrium in the adsorption of species from the solution.
- 3) There are no adsorbed species on the solid-gas interface in the case of the advancing contact angle. Measuring the receding contact angle, adsorbed species are left on the solid surface while the liquid is receding.

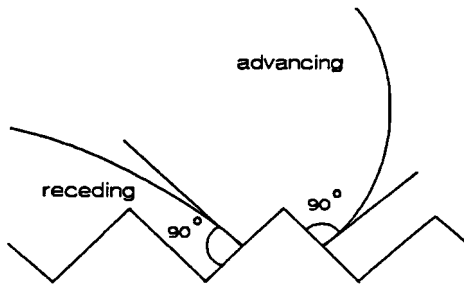


figure 2: schematic visualisation of the influence of surface roughness on the receding and advancing contact angle. The microscopic contact angle is 90° in both cases.

5.2.2 The theory of the wetting of powders.

For the wetting behavior of a dry aggregate it is also important to consider the fact that the wetting solution should penetrate the holes in the aggregate and substitute the air in these holes. One way to simplify this problem is to regard the holes as capillaries. If the contact angle is smaller than 90° the solution penetrates the aggregate through the smallest capillaries whereas the air leaves through the larger ones. The driving force for this process is the difference in Laplace pressure in the narrow and the wide capillaries. The Laplace pressure of a meniscus in a capillary can be calculated with:

$$\Delta P = \frac{2 \gamma_{LG} \cos \theta}{r} \quad (6)$$

with: ΔP : Laplace pressure (N/m^2)
 γ_{LG} : surface tension liquid-gas (N/m)
 θ : contact angle [rad]
 r : radius of the capillary (m)

This formula can in a simple way be derived from the Laplace law because the curvature radius(R) and the capillary radius(r) are related by the contact angle θ (see figure 3):

$$\cos \theta = \frac{r}{R}$$

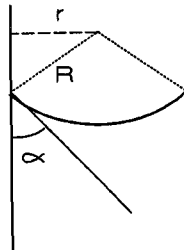


figure 3: curved interface in a capillary

If we substitute 1 in 6 we find:

$$\Delta P = \frac{2 (\gamma_{SG} - \gamma_{SL})}{r} \quad (7)$$

From 7 it is clear that if we use a surfactant which is only adsorbed at the solid-gas interface, the solid-gas interfacial tension is decreased and consequently the contact angle is decreased. However the effect on the penetration rate into the dry aggregate is probably very low. For a significant effect on the penetration rate we should alter the solid-gas or the solid liquid interfacial tension. As argued above the adsorption at the solid-gas interface of one of the substances present in the solution is not expected, so the only parameter that we can try to alter is the solid-liquid interfacial tension. This interfacial tension can decrease if an agent e.g. a surfactant is adsorbed from the solution in the solid-liquid interface.

Measuring the contact angle of a powder with polydisperse and non-spherical particles is very difficult. Neumann and Good² mentioned two techniques of measuring the contact angle of a powder: A) The sessile drop on a compressed powder cake. B) Several imbibition techniques in order to determine the Laplace pressure in the pores of a packed bed. From the Laplace pressure the contact angle can be calculated with formula 6. According to Neumann the sessile drop method is not very reliable for a number of reasons. So we chose the second method.

5.2.3 The theory of wetting a packed bed.

There are several ways to measure the Laplace pressure of the curved interface in the pores of a packed bed:

A) Pressure of displacement: The actual pressure necessary to balance the Laplace pressure is measured. The major drawback of

this technique is the polydispersibility of the pores in the packed bed, but the contact angle can be calculated in an easy way with 6 if an estimation of the pore radius can be made.

B) The rate of capillary penetration. A packed bed filled with one phase is penetrated by the other phase. The driving force for this process can be the Laplace pressure or a superimposed pressure. The rate of penetration in a capillary with only the Laplace pressure as driving force can be calculated with the Washburn equation. The formula is a combination of the Hagen-Poiseuille formula for the average velocity in a capillary with formula 6 for the Laplace pressure:

$$v_1 = \frac{r \gamma_{LG} \cos \theta}{4 \eta l} \quad (8)$$

with: v_1 : average velocity of the liquid (m/s)
 r : capillary radius (m)
 γ_{LG} : surface tension (N/m)
 θ : contact angle
 η : viscosity (Ns/m²)
 l : length of the liquid column (m)

In the above formula the viscosity of the third phase (gaseous) is neglected, but an equivalent formula can be derived in the case of an organic liquid as the apolar phase. In the case of a packed bed a similar formula can be derived using Darcy's law:

$$Q = \frac{K A \Delta P}{\eta l} \quad (9)$$

with: Q : volume flow of the liquid (m³/s)
 K : permeability (m²)
 A : cross section of the packed bed (m²)
 ΔP : pressure difference (N/m²)
 η : viscosity of the liquid (Ns/m²)
 l : length of the wetted part (m)

The pressure difference is the sum of the superimposed pressure

and the Laplace pressure: $\Delta P = \Delta P_s + \Delta P_L$. In combination with formula 6 this results in:

$$Q = \frac{K A}{\eta l} \left(\frac{2 \gamma_{LG} \cos \theta}{r} + \Delta P_s \right) \quad (10)$$

with: r : pore radius (m) ΔP : superimposed pressure (N/m^2)

This formula is difficult to use in the experimental situation because both Q and l are time dependent. If we note that:

$$Q = \frac{dV}{dt} = \frac{d(l\epsilon A)}{dt} = \epsilon A \frac{dl}{dt} \text{ we can form the integral:}$$

$$\int l \, dl = \int \frac{K A}{\epsilon \eta} \left(\frac{2 \gamma_{LG} \cos \theta}{r} + \Delta P_s \right) dt \quad (11)$$

Solving this integral results in:

$$l^2 = \frac{2 K A}{\epsilon \eta} \left(\frac{2 \gamma_{LG} \cos \theta}{r} + \Delta P_s \right) t \quad (12)$$

with: time $t = 0$ as the liquid starts penetrating the packed bed ($l = 0$)

Formula 12 predicts a linear relation between the square of the penetration length and the time. For a number of reasons this relation is not observed in most experiments with packed beds: A possible reason for this deviation might be that the kinetic processes during movement of a SLG-contact line result in local deviations of the surface curvature from the equilibrium value³. However this should not influence the value for ΔP obtained on extrapolating to $Q=0$. In addition the beds are not ideally packed. The consequence is that the pores in the plug are not

equalized. This causes preferential streaming of the fluid in the packed bed. The velocity of the liquid in the wider canals is higher than in the narrow pores. For this reason there will be some air which is not replaced by liquid in the time that is necessary for the majority of the fluid to pass through the packed bed. This effect is even more important in the case of the liquid being replaced by air (in the case of a contact angle $< 90^\circ$). In the case of a receding contact angle with a wetting liquid the Laplace pressure in the narrow pores can be higher than the driving pressure. So the liquid/air interface is fixed in these narrow pores and the preferential streaming patterns are very pronounced. This process of preferential streams of an interface in a packed bed is a well-known problem in many technological processes. In our own experiments (contact angle $< 90^\circ$) it has been frequently observed that the total volume displaced was higher when measuring the advancing contact angle (displacement of air by water) than when measuring the receding contact angle (displacement of water by air). In the case of displacing the water by air the water is not forced through the narrow pores because the Laplace pressure is higher than the driving pressure. The liquid is only pushed through the wider canals and the air leaves the packed bed on the other side after dewatering only the widest channel.

The effect of partial displacement of one phase by the other is more pronounced when the particles are polydisperse and the packed bed is not homogeneous because the pore size distribution is wider compared to the homogeneous packed bed of monodisperse particles.

In figure 4 the volume of liquid displaced by air (receding contact angle) is plotted as a function of time. One curve is calculated from the packed bed characteristics and one curve is measured experimentally (see later). Comparing these two curves it

is clear that the theoretical description can not be used to calculate the contact angle from one experiment.

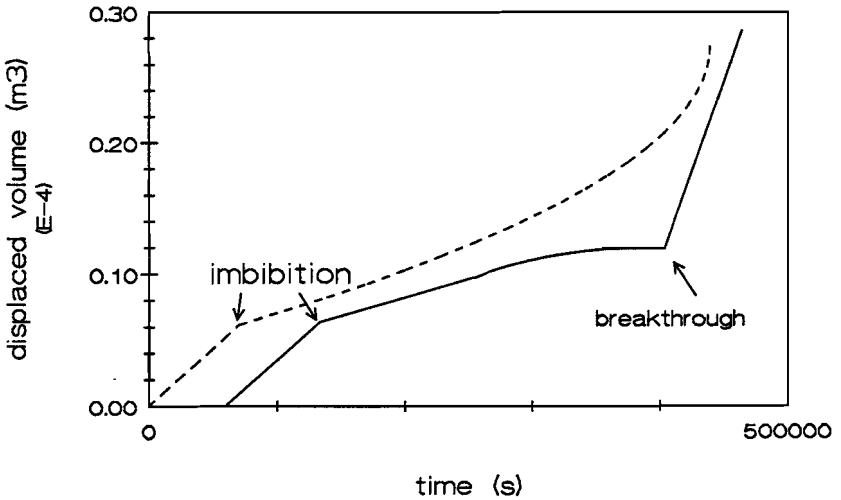


Figure 4: Displaced volume as a function of time when measuring the receding contact angle.
 — measured curve
 - - calculated curve. Parameters: $\xi=0.42$, $A=0.000491$ m, $L=0.0988$ m, $k=4.8$, $\Delta P_s=6$ N/m², $\Delta P_L=4$ N/m², $\eta=0.001$ Ns/m², $r_c = 37$ nm. The displaced volume is calculated using formula 12

There is another reason for the discrepancy between theory and experiment: In theory the imbibition of a liquid in a packed bed should start at a contact angle of 90° . In experiments⁴ this was found not to be true: The liquid imbibition of a water/ethanol mixture into packed beds of several materials only started at contact angles between 50 and 60° . This phenomenon could be explained by describing the packed bed not as a bundle of

capillaries but as packed spheres. If the contact angle is just smaller than 90° the penetration of the liquid in the pores stops when the interface is flattened (see figure 5). In the absence of curvature (figure 5, right side) the Laplace pressure is zero and the imbibition stops. Only if the contact angle is small enough, the surface retains a curvature at all places between the spheres and the Laplace pressure is finite everywhere, so that the imbibition can proceed. A maximum contact angle of 50.7° was derived⁴ for the spontaneous imbibition of a phase into close packed spheres of equal size. In the case of heterodisperse spheres the maximum contact angle is in theory higher but this was not found in the experiments.

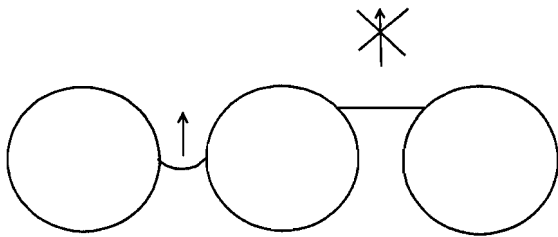


figure 5: Liquid/gas interface between two spheres. The curvature of the liquid/gas surface changes with the position between the spheres.

5.3 Results and discussion

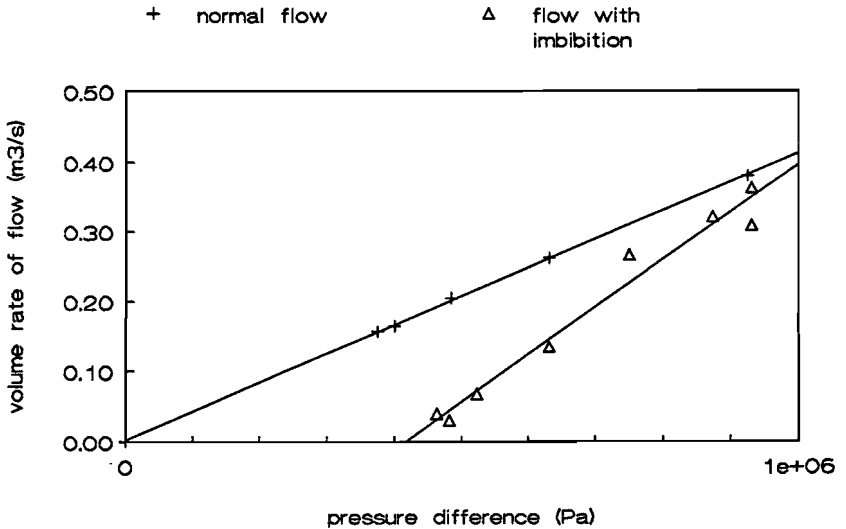


Figure 6: The results of experiments with the imbibition of air in a packed bed of water and titanium dioxide (A). $\epsilon=0.42$, $K=2.07 \times 10^{-17} [\text{m}^2]$

From the normal flow of water through the packed bed we can calculate a permeability in the packed bed with formula 9. From the permeability we can calculate a mean pore radius using the Blake-Kozeny equation (formula 10 chapter 3). If we extrapolate the imbibition rate at different pressures to imbibition rate=0 we obtain the Laplace pressure in the pores of the packed bed. Knowing the mean pore radius and the Laplace pressure we can calculate the contact angle with equation 6. From figure 6 we calculate a mean pore radius of 31 nm and a contact angle of 84° .

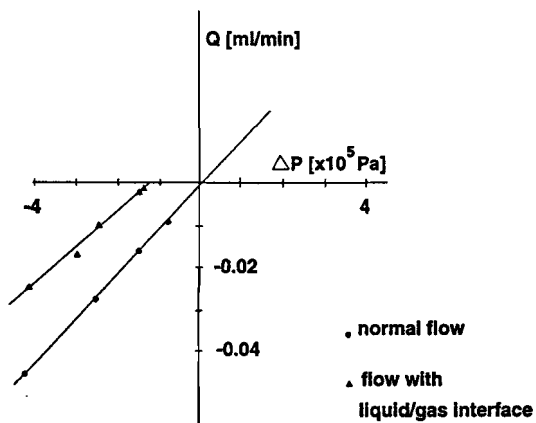


Figure 7: Imbibition of air in a packed bed of water and titanium dioxide (sample B). $\epsilon=0.59$, $K=2.46 \times 10^{-16}$

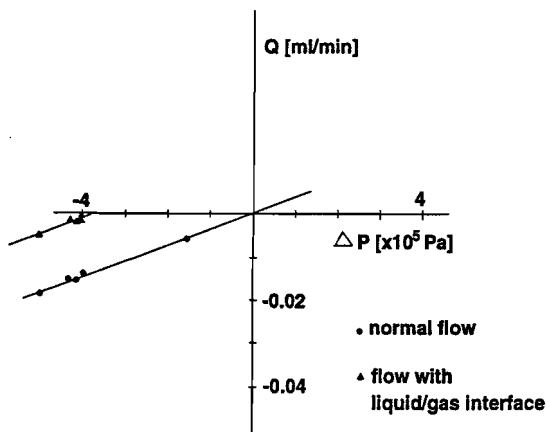


Figure 8: The imbibition of air in a packed bed of titanium dioxide (sample B) and 10 g/l polyacrylate solution (sample B). $\epsilon=0.59$, $K=1.35 \times 10^{-16}$.

From the normal flow in figure 7 we can calculate a mean pore radius of 91 nm and from the imbibition flow a contact angle of 85° .

From the normal flow in figure 8 we can calculate a mean pore radius of 68 nm and from the imbibition flow a contact angle of 79° .

The receding contact angle had decreased as a result of the adsorption of PAA on the oxide surface. The permeability of the packed bed had decreased as a result of the polyelectrolyte adsorption (see chapter 3).

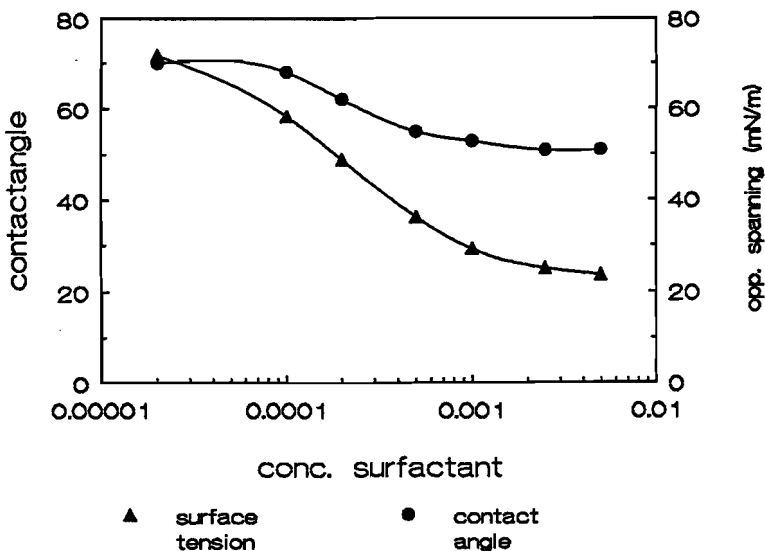


Figure 9: The influence of the CTAB concentration on both the surface tension liquid/air and the contact angle rutile/liquid/air. The sessile drop method on a one crystalline rutile surface was used.

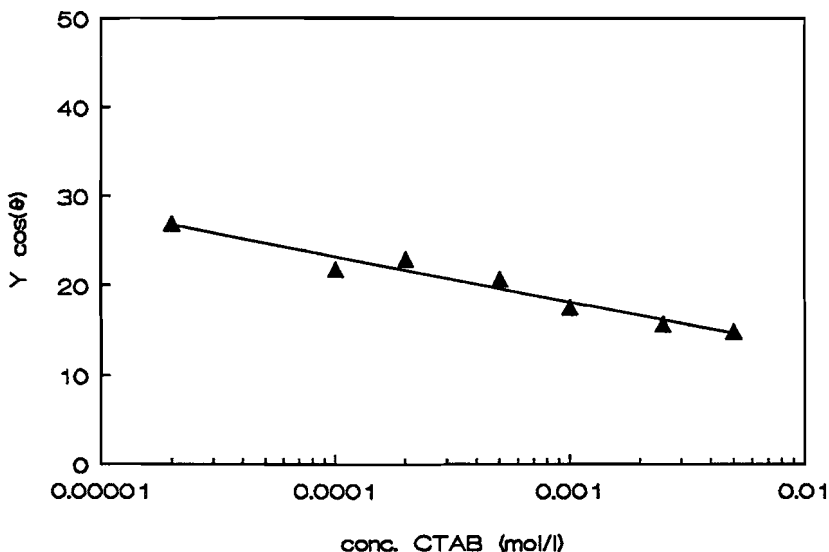


Figure 10: The influence of the CTAB concentration on $\gamma_{LG} \cos(\theta)$. There is a decrease of this value with increasing concentrations of CTAB.

Although the contact angle decreases with increasing concentrations of CTAB the Laplace pressure is decreasing. This is an indication that the driving force of the wetting of agglomerates of oxides particles by water is not enhanced by using a traditional surfactant.

5.4 Conclusions

- As expected the contact angle of the oxide/water/air system was less than 90° .
- It is not to be expected that the wetting of the oxide with water is a limiting factor in the dispersion process of TiO_2 in water.
- The contact angle can be decreased with a traditional

surfactant but the dispersion process of aggregates is not enhanced in this way.

- Measuring the Laplace pressure of the water/air interface in a packed bed of titanium dioxide particles is possible but the interpretation is difficult. The calculated receding contact angles are larger than measured with the sessile drop method on a monocrystalline surface of titanium dioxide.
- The advancing contact angle cannot be measured with the packed bed method if an adsorption process is involved. The concentration of the adsorbed species decreases in the first injected fluid until the adsorption plateau is reached.

¹Van Voorst Vader, J.Coll. Int. Sci. (1970)

²A.W. Neumann, R.J. Good, Techniques of measuring contact angles, Surface and Science, Volume 11, experimental methods edited by R.J. Good and R.R. Stromberg, Plenum Press, New York

³van der Zanden A.J.J., The hydrodynamics of a moving fluid-liquid contact line, Ph.D. thesis Eindhoven (1992).

⁴S. Bán, E. Wolfram, S. Rohrsetzer, The conditioning of starting liquid imbibition in powders. Colloids and surfaces, 22 (1987) 301-309.

CHAPTER 6:

THE STABILITY OF TITANIUM DIOXIDE/WATER DISPERSIONS.

6.1 Introduction

In order to investigate the colloidal stability of a dispersion light-transmission experiments are often used. In the first part of this chapter the influence of the polyacrylic acid concentration and the electrolyte concentration on the colloidal stability are evaluated using such experiments. The effect of the polyacrylic acid is investigated because an increase of the colloid stability is expected as a result of the adsorption of PAA on the oxide surface. The effect of the electrolyte concentration is investigated because this provides information about the mechanism of stabilization and because high salt concentrations may occur during the drying process of a paint film.

However the light-transmission experiments are only applicable to dispersions with low volume fractions of oxide particles. Since the volume fractions used in the paint industry in the dispersion process of an oxide pigment are about 20 to 26 vol% (\approx 50 to 60 wt%), there is a need for an experiment which monitors the stability of the dispersion at these high volume fractions. In the paint industry viscosity experiments are often used for this purpose. The interpretation of viscosity experiments with pigment concentrations of 50 wt% or more is not unambiguous^{1,2}. In these experiments a minimum in viscosity is found using a polyelectrolyte as a dispersing agent. Starting from concentrations of polyelectrolyte=0, the viscosity first increases

with the increase of the polyelectrolyte concentration, then passes through a maximum, decreases, passes through a minimum, finally increases again (see figures 5 and 6). The maximum in viscosity is an indication of the destabilization of the dispersion at these polyelectrolyte concentrations. One of the unanswered questions is whether:

A) The PAA-concentration found at the minimum in viscosity does in fact correspond with the optimal dispersing agent concentration, or

B) The dispersion is in fact more stable at a higher PAA-concentration despite the higher viscosity of the dispersion at this concentration.

To draw conclusions from rheological experiments some additional colloid chemical information is useful. In the second part of this chapter we give an interpretation of the observed phenomena.

In the third part of this chapter the possibility of a synergistic mechanism between both the steric and the electrostatic stabilization is proposed. The experimentally found hydrodynamic layer thickness of about 3 nm (see chapter 3) is in fact rather thin for steric stabilization of a dispersion. From calculations it will be seen, however, that even such a thin layer can have a large influence on electrostatic stabilization (see 6.5).

6.2 Stability of dilute titanium dioxide suspensions.

Experimental setup

The stability of a dilute oxide dispersion can be followed by measuring light transmission as a function of time. From such measurements we can calculate a stability factor W , defined as: the coagulation rate of the dispersion divided by the coagulation rate in the absence of any kind of stabilization. The stability of

the dispersion is measured as a function of the salt concentration (KNO_3) and as a function of the polyacrylic acid concentration. Before measurement the titanium dioxide was dispersed using an Ystral colloid mill (X40/38) during two periods of 5 minutes. It appeared that a third period of 5 minutes had no influence on the light-transmission of the dispersion. The concentration of titanium dioxide was 0.114 g/l (volume fraction= 2.7×10^{-5}). The electrolyte concentration was raised at time=0 in the stirred cylindrical vessel. The light transmission was followed using a Vitatron MPS spectrometer. The data were collected by a computer.

Results and discussion

As the stability factor W is measured and calculated as a function of the electrolyte concentration we find for low polyacrylic acid concentrations a graph typical for electrostatic stabilization³: At electrolyte concentrations above 0.15 M KNO_3 the stability factor is 1, indicating that there is no stabilization (neither electrostatic nor steric). At lower electrolyte concentrations the stability increases (higher W) as a result of an increasing electrostatic repulsion. This increase is not very pronounced when no PAA has been added (see figure 1) because the suspension is very near its isoelectric point. At low PAA concentration the stability at electrolyte concentrations below 0.15 M increases as a result of the higher zeta potential (in absolute sense). The stability at electrolyte concentrations above 0.15 M does not change. But with increasing polyacrylic acid concentrations, stability factors significantly higher than 1 are obtained even at electrolyte concentrations of 0.4 M.. Even in this polyacrylic acid concentration range, the $\log(W)$ versus $\log(c)$ graph (c =electrolyteconcentration) turns upwards with decreasing c values (figure 1). Under these circumstances, the stability surpasses the values found for electrostatic stabilization. This

indicates that under these circumstances, both steric and electrostatic stabilization occur simultaneously.

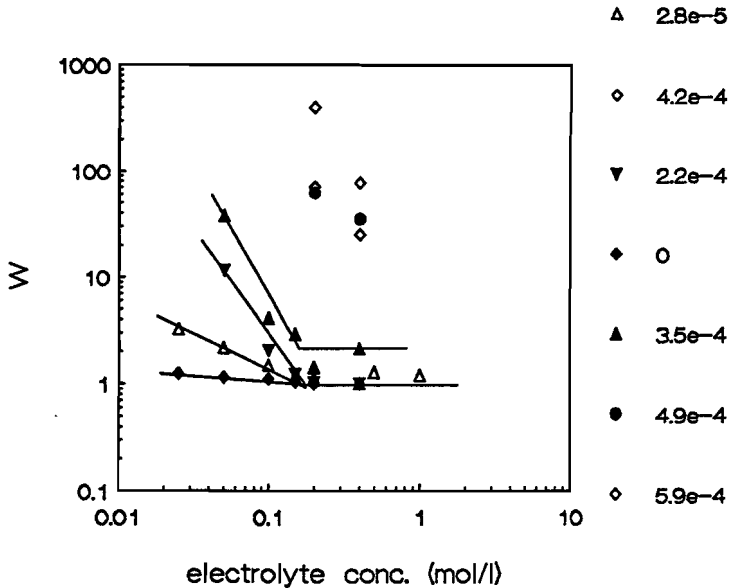


Figure 1: Stability of a titanium dioxide dispersion with a low volume fraction ($\phi=2.7 \times 10^{-5}$). The stability factor W is measured at different salt concentrations and with different amounts of polyacrylic acid added, pH=6.0. Polyacrylic acid concentration in g per m² pigment surface. Titanium dioxide sample= A; PAA=A;

The total stability could be expected to be the sum of both separate $\log(W)$ values. The results of our experiments suggest that this is in fact the case. It is not clear yet whether there is also a synergistic effect of both stabilization mechanisms. In that case the resulting stability is larger than the sum of both electrostatic and steric stability.

As the polyacrylic acid concentration is raised further the stability of the dispersion is enhanced to such an extent that the slope of the light-transmission versus time curve can no longer be measured.

In order to compare the PAA concentrations with other experiments the PAA concentration is expressed as the total initial concentration divided by the surface area of the oxide in the suspension.

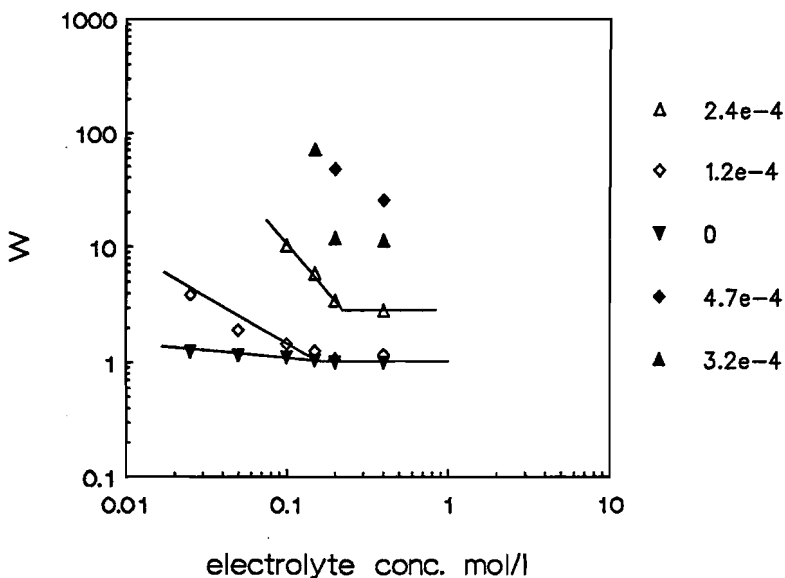


Figure 2: Stability of a titanium dioxide dispersion with a low volume fraction of solids ($\phi=2.7 \times 10^{-3}$). The stability factor W is measured at different salt concentrations and with different amounts of SERVO FX 508 added, pH=6.0. Polyacrylic acid concentration in g/m^2 . Titanium dioxide sample= A; PAA=C.

Unfortunately it is not possible to give an equilibrium concentration for this experiment because the amount adsorbed changes with the salt concentration (see chapter 2). At low PAA concentrations ($<2 \times 10^{-4} \text{ g/m}^2$) the PAA added to the solution is indeed nearly totally adsorbed (see chapter 2). At higher concentrations there is a division of the total amount over the oxide surface and the bulk solution.

Almost the same results are obtained with a polyacrylic acid co-polymer used in the paint industry for stabilizing pigment dispersions as used in water based paints (figure 2).

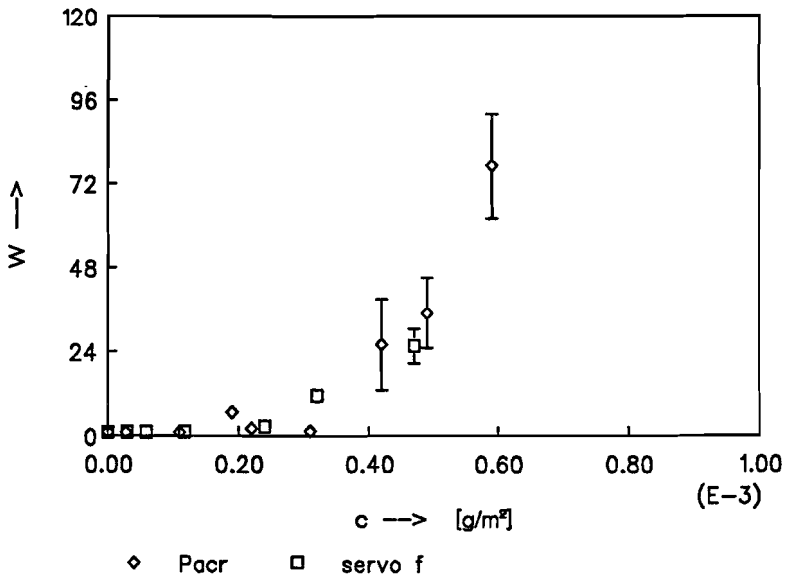


Figure 3: The measured stability as a function of the concentration of polymer. The salt concentration is 0.4 M KNO_3 . At this electrolyte concentration the electrostatic stabilization is absent. Titanium dioxide sample A; PAA:A and C. pH=6.0.

We found that a concentration of 2×10^{-4} g PAA per square meter oxide surface (at pH=6) is a characteristic concentration: It is the concentration at which the zeta potential reaches its most negative value and becomes constant (see figure 5 and 6 and chapter 2). Furthermore the viscosity shows a minimum at this PAA-concentration (see figure 5 and 6) and at a concentration higher than 2×10^{-4} g/m² there is an increase in the steric stabilization of the oxide dispersion (see figure 3).

6.4 Stability of TiO₂ dispersions at high volume fractions ($\phi=0.16$).

At high volume fractions light transmission experiments cannot be used for measuring the stability. We therefore use rheological experiments to measure the stability of dispersions with volume fractions of 0.16 to 0.19 (44 to 50 wt%).

Experimental setup.

About one liter of suspension was mixed and dispersed for one minute in an Ystral colloid mill before measurement. The viscosity of a sample of this dispersion was measured at 20°C using a Contraves Rheomat 115 with a coaxial cylinder type of viscosimeter (rotating bob, thermostated cub, DIN 145). The shear stress is measured going from the lowest shear rate to higher shear rates (343 s^{-1}) and back. The measured dispersion was then added to the bulk dispersion and polyacrylic acid was added. After mixing and dispersing with the colloid mill the above mentioned procedure was repeated. From the measurements an apparent viscosity was calculated assuming a shear rate distribution in the viscosimeter as for a Newtonian liquid.

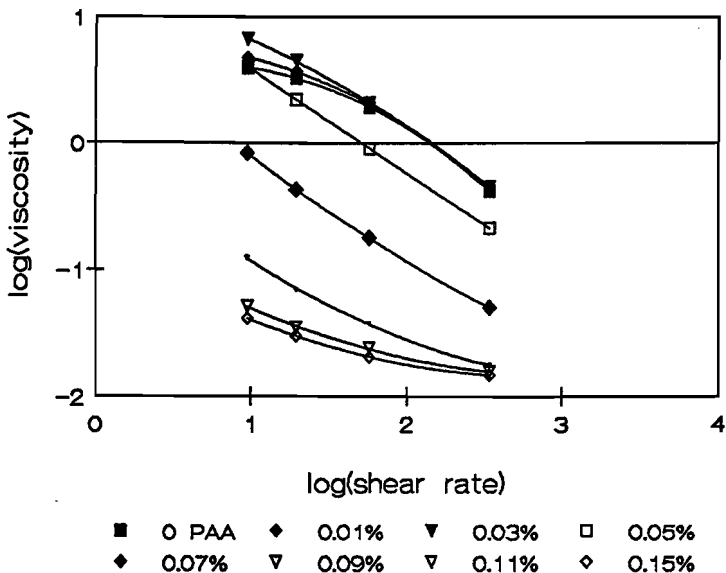


Figure 4: A dispersion of titanium dioxide in water shows a shear thinning behavior. At the higher PAA concentration the shear thinning behavior is less pronounced. The PAA concentration is expressed as wt% PAA added to the dispersion, 0.2 wt% corresponds with 2×10^{-4} g PAA/m². Titanium dioxide sample=D PAA=B pH=6.1.

Results and discussion.

In most cases titanium dioxide dispersions show a shear thinning behavior (see figure 4). The apparent viscosity decreases at higher shear rates as a result of the breaking up of the flocks under these conditions. At lower shear rates flocks are formed again and the viscosity increases. Some thixotropy is observed during the measurements. Especially with the lower concentrations of polyacrylic acid the time effect was pronounced.

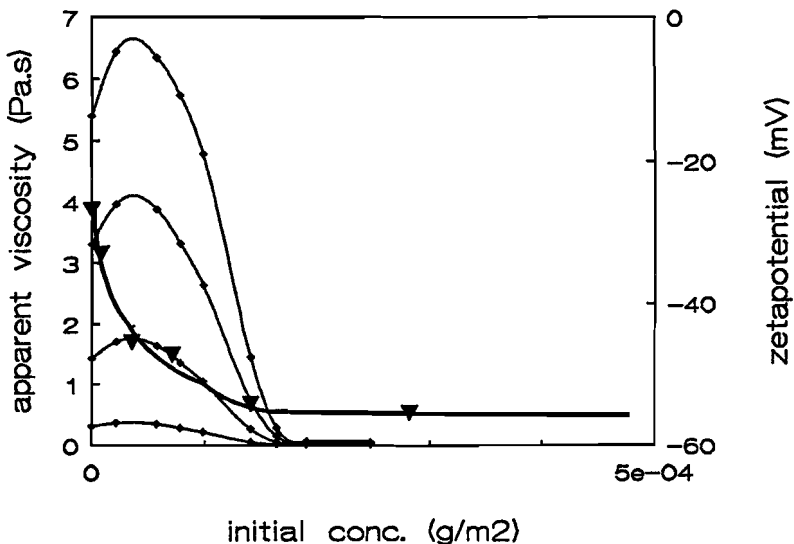


Figure 5: At lower polyacrylic acid concentrations the viscosity goes through a maximum as the PAA concentration increases. At medium PAA concentrations the viscosity decreases by a factor of about 100. The concentration of PAA at this point is about 2×10^{-4} g/m². This is also the concentration with the lowest zeta potential (as an absolute value). The concentration PAA is expressed as the amount of PAA per square meter oxide surface.
Titanium dioxide sample=B; PAA=B; pH=7.4

In figure 5 and 6 the influence of the amount of PAA added to the dispersion on both the apparent viscosity and the zeta potential is shown. The maximum in viscosity is either caused by the bridge-forming properties of the polymer or the adsorbed charged polymer causing a neutralization of the surface charge and thus a destabilization of the dispersion. The viscosity decreases at higher PAA concentrations and reaches a minimum value as the zeta potential reaches a maximum value (in absolute sense).

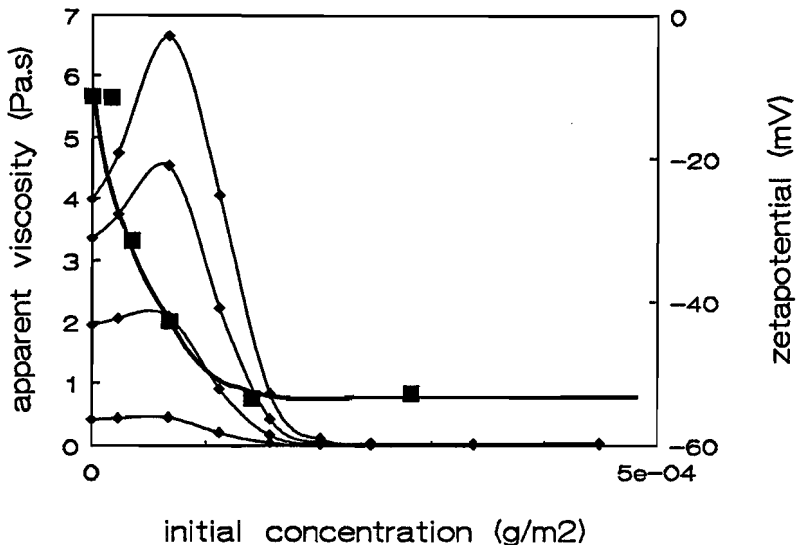


Figure 6: Same as figure 5 but at another pH value and with a different titanium dioxide sample. It is striking that although the specific surface of this oxide is about 4 times smaller than that of the sample used in figure 5, the concentration of 2×10^{-4} g/m² is also the concentration at which the viscosity reaches a minimum. Titanium dioxide sample=D; PAA=B; pH=6.1

An increase in viscosity is observed (figure 7, 8 and 9) at concentrations above 2×10^{-4} g/m² PAA. This increase in viscosity can be caused by :

- 1) a destabilization of the dispersion. This is not very likely because the light transmission experiments show a tendency to higher stability at higher PAA concentrations.
- 2) an increase in viscosity of the continuous fluid caused by the dissolved polyacrylic acid. This was not the case: an experiment

with the continuous phase and increasing amounts of PAA showed no significant change in viscosity in the concentration range tested.

3) The first or second electroviscous effect (see also chapter 3): The zeta potential does not change in the PAA concentration-range (0.2 to 1.0 w/w%) so there is no reason to suppose an influence of either the first or the second electroviscous effect.

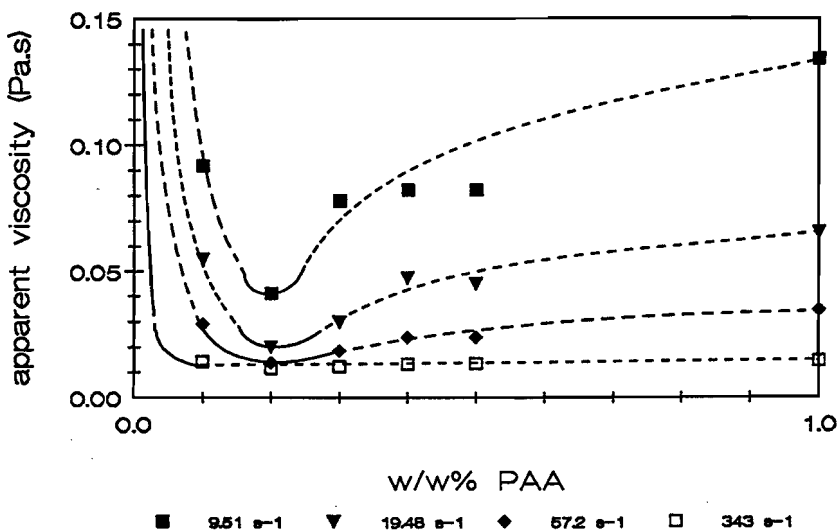


Figure 7: The viscosity of a 44 wt% titanium dioxide dispersion shows a minimum at 0.2 wt% added PAA. The increase in viscosity after the minimum is attributed to an increase in effective solid volume fraction due to the polymer layer on the surface. pH=6.1; Titanium dioxide sample=D; PAA=B.

4) The third electroviscous effect (see also chapter 3): If the amount of adsorbed PAA still increases at these higher concentrations the formation of a hydrodynamically stagnant

polymer layer (further referred to as the hydrodynamic layer) is possible. The formation of a hydrodynamic layer can be interpreted as an increase in volume fraction of the solid phase in the dispersion. Consequently the viscosity of the dispersion increases.

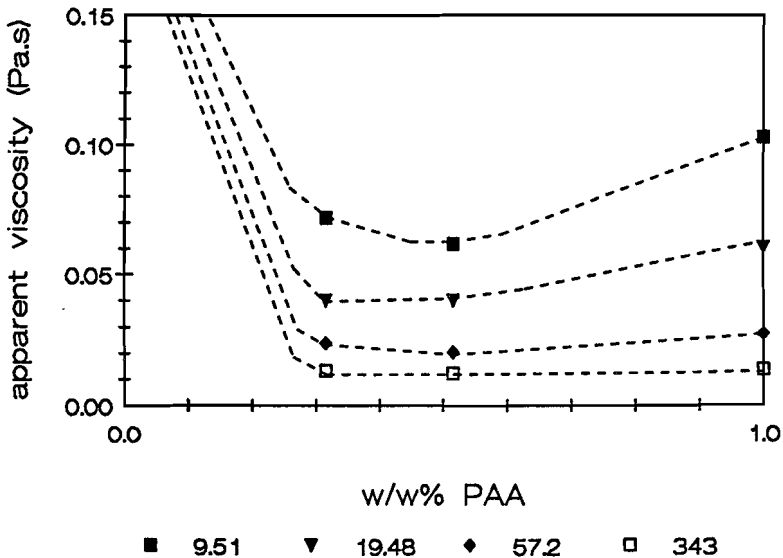


Figure 8: Same as figure 7 but at pH 4. The minimum is shifted to a PAA-concentration of 0.4 wt%. This is explained by the fact that the charge of the oxide surface is more positive at this pH and the charge of PAA is smaller. As a consequence more PAA is needed to (over)compensate the surface charge.

In chapter 3 we calculated a layer thickness of 3 nm at 0.01 M KNO_3 on the basis of experiments with a packed bed of titanium dioxide particles. If we want to check whether the increase in the viscosity in figure 7, 8 and 9 is also caused by the hydrodynamic layer thickness there is unfortunately no generally accepted

theory to predict the viscosity of a heterodisperse paste with a high volume fraction of non spherical particles and possible aggregates in it.

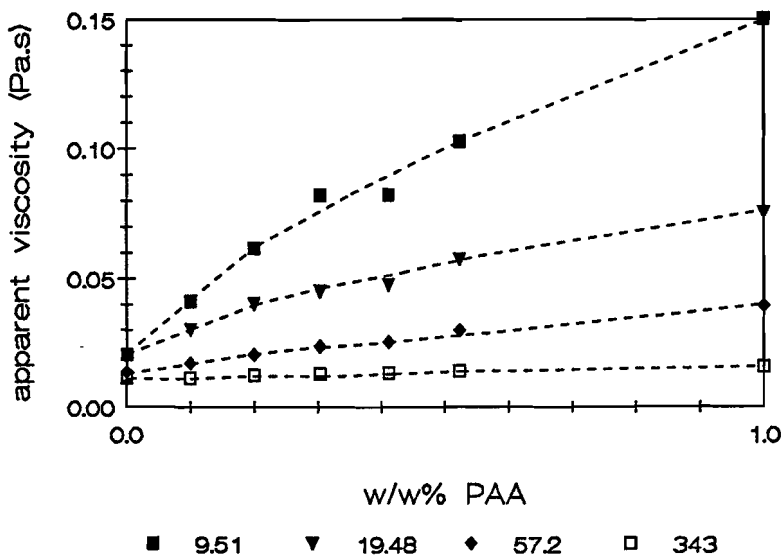


Figure 9: Same as figure 7 and 8, but at pH=10.5. The dispersion is already stable in the absence of PAA.

The only information we can possibly derive from these rheological experiments is whether the hydrodynamic layer thickness we can calculate with for instance the Dougherty-Krieger formula⁴ (see formula 1) is in the same order of magnitude as calculated from the packed-bed experiments. This formula is only valid for spherical particles in a dispersion not containing aggregates. While we are aware that in the systems discussed here some deviations from this model occur we expect that the values found

can be considered as an indication of the hydrodynamic layer thickness, especially since we are discussing relatively small viscosity changes in a dispersion.

$$\eta_r = \left(1 - \frac{\phi}{\phi_{\max}}\right)^{-[\eta] \phi_{\max}} \quad (1)$$

with: $[\eta]$ = intrinsic viscosity $\cong 2.5$
 ϕ_{\max} = maximum volume fraction $\cong 0.6$
 ϕ = volume fraction of the solids
 η_r = relative viscosity

The formula can be transformed to:

$$\phi = \frac{\eta_r^{0.67} - 1}{\eta_r^{0.67} / 0.6} \quad (2)$$

If the number of particles is constant and a polymer adsorbs as a layer on these particles the volume fraction increases with the third power of the radius. $\phi \cong r^3$. So:

$$\frac{r_1^3}{r_2^3} = \frac{\phi_1}{\phi_2} = \frac{(\eta_{r,1}^{0.67} - 1) \eta_{r,2}^{0.67}}{(\eta_{r,2}^{0.67} - 1) \eta_{r,1}^{0.67}} \quad (3)$$

with: η_1 = relative viscosity without polymer layer
 η_2 = relative viscosity with polymer layer

In the minimum in figures 7, 8 and 9, the polyacrylic acid is adsorbed as a flat layer on the surface only enhancing the electrostatic stabilization. As the radius of the particles we propose a value of 150 nm taken from size-experiments with a disc-centrifuge (see chapter 4). The viscosity in the minimum without the polymer layer (or with only a flat layer) is compared with the situation where 0.6 wt% more PAA is added to the dispersion.

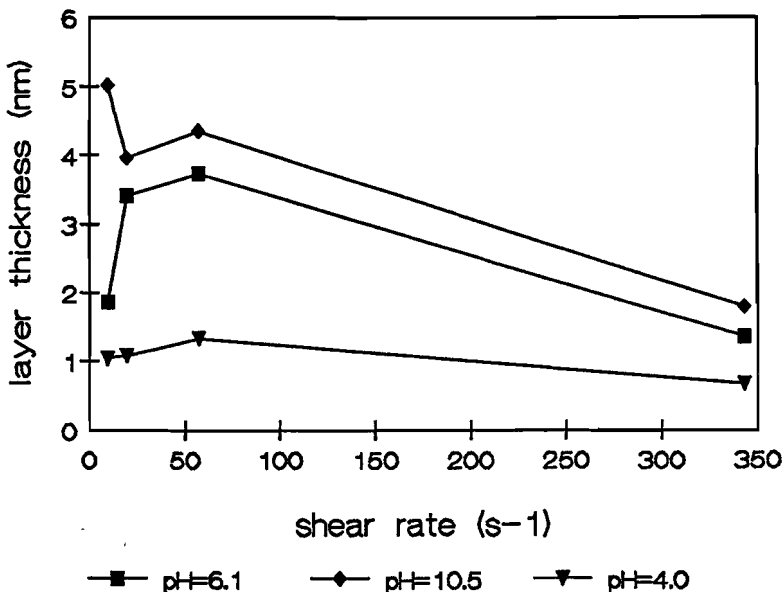


figure 10: Hydrodynamic layer thickness calculated from figure 7, 8 and 9. The calculated values vary from 1 to 5 nm and are in the same range as the hydrodynamic layers calculated from the packed bed experiments. There is a tendency to smaller layers at lower pH's

In figure 10 the calculated layer thickness is presented at different shear rates and at different pH's. For these calculations the viscosity of the dispersion in the minimum was taken as the viscosity ($\eta_{r,1}$ in formula 3) without a polymer layer (0, 0.2 and 0.4 wt%. respectively at pH 10.5, 6.1 and 4.0). This viscosity is compared with the viscosity ($\eta_{r,2}$) after addition of 0.6 wt% additional PAA (0.6, 0.8 and 1 wt% respectively at pH 10.5, 6.1 and 4.0). For these calculations we used a maximum volume fraction of 0.6. For hetero-disperse systems maximum volume fractions of up to 0.8 were sometimes reported. Using this value

hydrodynamic layer thicknesses varying from 1 to 8 nm were calculated. So the calculation is not sensitive to changes in this variable. The calculated hydrodynamic layers are similar to those calculated from the packed bed experiment (chapter 3). The calculated hydrodynamic layer thickness is small compared to the layer thicknesses obtained after the adsorption of uncharged polymers on oxide surfaces⁵. For charged polymers the measured adsorption has always been far less than the adsorption measured with an uncharged polymer. Consequently a thin hydrodynamic layer was expected. Theoretical models⁶ predict a small hydrodynamic layer in the case of the adsorption of a charged polymer unless the salt concentration is very high. In this case the polyelectrolyte behaves like an uncharged polymer. The layer thickness obtained in this chapter is a realistic one: The volume fraction of PAA in this layer is about 17% (calculated with: $\rho_{\text{paa}}=1200 \text{ kg/m}^3$, $5 \times 10^{-4} \text{ g PAA /m}^2$ adsorbed in a layer of 3 nm). At low shear rates a layer of 1 nm is calculated at pH=4 whereas at pH 10.5 4 nm is calculated. This is a rather surprising result because the adsorption of PAA at a low pH is higher than at high pH's. An acceptable explanation is that the polymer chains are more rigid at a high pH as a result of the higher charge in the polymer chain (see chapter 1).

6.5 The influence of a thin polymer layer on the colloidal stability.

Theory: Calculation of the stability of a dispersion

In order to get an idea of the effect of the obtained layer thickness on the stability of the dispersions we calculated the stability ratio W as a function of the salt concentration. The complete problem, including hydrodynamic interaction and

interparticle potentials was solved by Spielman⁷ and Honig c.s.⁸. They calculated the stability ratio W in the absence of shear with:

$$W \equiv \frac{J_0}{J} = \frac{\int_0^{\infty} \frac{\beta(u)}{(2+u)^2} \exp\left(\frac{V_a + V_r}{kT}\right) du}{\int_0^{\infty} \frac{\beta(u)}{(2+u)^2} \exp\left(\frac{V_a}{kT}\right) du} \quad (4)$$

with u : shortest distance between particle surfaces divided by the particle radius.

J_0 : flux of particles towards a central particle if $V_r=0$ (fast coagulation)

J : as J_0 but with $V_r>0$ (slow coagulation)

$\beta(u)$: hydrodynamic correction factor from tables.

V_a : Van der Waals attraction energy (J)

V_r : repulsion energy (J)

For the attraction energy the formulas of Clayfield⁹ were used. These formulas are the result of the double integration of the attraction forces between all places on two spheres taking into account the retardation at large distances. These formulas gave nearly the same result as the formulas of Schenkel and Kitchener¹⁰.

In order to calculate an attraction energy either a constant potential model or a constant charge model can be used¹¹. If the adsorption and desorption of potential determining ions is relatively slow, the charge is constant during the coagulation of two particles. On the other hand if this process is very rapid the potential is constant. It does not seem to make any significant difference whether the constant potential or the constant charge model is used as long as the distance between the particles is not too small ($ua \ll 0.4$). A constant potential is easier to use because we can use the measured zeta potential. The Derjaguin formula can be used in the case of low potentials ($\psi < 25$ mV) and thin double layers ($\kappa a > 10$) to calculate the repulsion energy:

$$V_r = 2\pi \epsilon_0 \epsilon_r \psi_0^2 a \ln(1 + e^{-\kappa a u}) \quad (5)$$

with ψ_0 : potential at the surface
 a : particle radius
 κ : reciprocal debeye length
 u : shortest distance between the particles divided by the radius.

For the higher potentials ($\psi > 25\text{mV}$) the attraction energy is calculated applying the method introduced by Derjaguin and also described by Overbeek¹². The repulsion energy of two spherical particles is calculated by adding the repulsion energy of pairs of rings with the radius r to either of the two particles. Each ring is regarded as a flat plate with a surface of $2\pi r dr + \pi dr^2$. For the interaction energy of a flat plate we used Overbeek's¹³ tables. These tables give a repulsion energy per m^2 flat plate surface as a function of the potential at the plate (converted into the dimensionless form as $ze_0 \psi/kT$) and as a function of the distance of the plates (converted into a dimensionless form as κa). The repulsion energy is tabulated for discrete values of $ze_0 \psi/kT$. As a function of the distance the table was interpolated with a spline. Between the successive $ze_0 \psi/kT$ values a linear interpolation was used.

It is very important to define the electrokinetic slipping plane for these calculations because we take the measured zeta potential for the potential used to calculate the repulsion energy. We assume that the distance between the electrokinetic slipping plane and the surface of the particle is about the same size as the hydrodynamic layer thickness measured in the packed bed. If the shortest distance between the particle surfaces is twice the hydrodynamic layer thickness the particles are regarded in the context of the present calculations as coagulated.

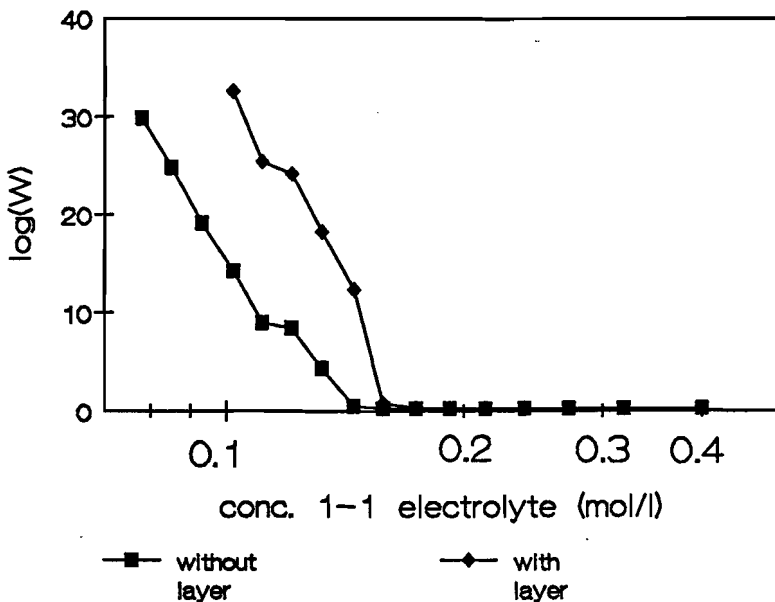


Figure 12: Calculation of the stability W as a function of the salt concentration. The stability was calculated with and without a theoretical layer of polymer.

The second line was calculated in the same way but in this case a polymer layer was assumed varying from 1 \AA at 0.4 M to 10 \AA at 0.1 M electrolyte (see figure 11 chapter 3). The zeta potential was in this case assumed to be the potential at the outer boundary of the hydrodynamic layer.

The calculations show an important influence of the rather thin layer on the colloid stability. An explanation for this influence is: The diffuse double layer repulsion is of the same magnitude both with and without the polymer layer at a given salt concentration (the zeta potential is the same!), but in the case of a polymer layer it starts further away from the oxide surface. At this distance the influence of the attraction force is not as

strong as very close to the surface. The attraction force is a short distance force. So the result of both attraction and repulsion forces acting simultaneously is a better stability in the case of a thin polyacrylic acid layer.

In these calculations the steric stabilization was not taken into account because we defined two particles as coagulated if the distance between two particles became twice the hydrodynamic layer thickness. The repulsion of the polymer layer becomes important as the distance becomes smaller. So this calculation does not show the influence on the steric stabilization of the polymer layer.

One of the unsolved problems in colloid chemistry is that the calculated stabilities can not yet be compared with measured stabilities¹⁴. Regarding this gap in the theory we did not try to compare figure 12 with figures 2 and 3.

6.6 Consequences for the dispersion process of pigments in water.

The experiments in this chapter show that both steric and electrostatic stabilization can occur as polyacrylic acid adsorbs on an oxide surface. The steric stabilization is only important at the higher concentrations of PAA. The increase in viscosity often observed at these higher PAA-concentrations can be explained by the polymer layer formed on the surface. Consequently the increase in viscosity can be used as an indicator of the capability of a polyelectrolyte to form such layers. Because a viscosity experiment is a widely spread technique in the paint industry it is perhaps useful to do some more research on this subject.

From calculations it is clear that a thin polyelectrolyte layer can enhance the electrostatic stability. This is a very important conclusion because the electrostatic stabilization vanishes with the increase of the salt concentration. To get an idea of the

electrolyte concentration of a water-based paint system we centrifuged a paint (FLEXA H₂O-Oké) in an ultra centrifuge (40.000 rpm). The conductivity in the clear supernatant was about 7 mS/cm with a pH of 8.3. If the solution contains a 1-1 electrolyte the salt concentration is about 0.04 M. The oxide particles covered with PAA have a zeta potential of about -40 mV at this electrolyte concentration which should be enough for a normal electrostatic stabilization. But in a drying paint film the concentration of salt increases as the water evaporates. In this water based paint the water fraction is 77 vol% ($\phi=33\%$). The water content decreases with a factor 3.5 before the volume fraction of solids becomes too high ($\phi=0.6$) to allow any movement. The salt concentration is then increased to 0.14 M and thus approaches the critical coagulation concentration (CCC) of 0.15 M of a 1-1 electrolyte above which no electrostatic stabilization is possible. Under these circumstances it is very important that the declining electrostatic stabilization is backed up by the steric stabilization.

There is also a possibility that the oxide particles are "excluded" from the bulk of binding material and as a consequence are consequently concentrated in the remaining water pockets. The barrier against coagulation must be higher in that case. It is therefore important to enhance the stabilization at salt concentrations of about 0.1 M. Such an additional stabilization under these circumstances is probably only possible with the influence of the polymer layer as described above.

6.7 Conclusions

- Stability experiments in dilute dispersions show a steric stabilization in addition to the electrostatic stabilization. The weak polyelectrolyte (PAA) is probably capable of

enhancing both stabilization mechanisms.

- Stability experiments in dispersions with high volume fractions of solids indicate the existence of a polymer layer on the oxide particle at higher concentrations of PAA.
- Calculations show the influence of charged groups at some distance from the oxide surface on the stability of the dispersion at medium electrolyte concentrations (0.05-0.15 M of a 1-1 electrolyte).
- The electrolyte concentration in water based paint is about 0.04 M of a 1-1 electrolyte. During the drying of the paint film the salt concentration reaches the critical coagulation concentration (CCC). An additional stabilization is necessary at these salt concentrations in order to prevent coagulation.

¹Strauss H., Heegn H., Strienitz I., Effect of PAA adsorption on stability and rheology of TiO₂ dispersions. Preprints of the conference: "The preparation of dispersions", IACIS-conference Veldhoven, The Netherlands, 14-16 October 1991.

²Seivard and Downey, Pigmentation and formulation variables affecting gloss in latex paints, J. of Paint Technology, vol 40, nr 522, 1968.

³Lyklema J. and Fleer G.J., Electrical contributions to the effect of the electrolyte colloid stability, Colloid and Surfaces, 25 (1987) 357-368.

- ⁴Krieger I.M., Rheology of mono disperse latices, *Advan. Colloid Interface Science*, 3 (1972) 111-136.
- ⁵Pandou A., Siffert B., Polyethyleneglycol adsorption at the $\text{TiO}_2\text{-H}_2\text{O}$ interface: Distortion of ionic structure and shear plane position. *Colloids and Surfaces*, 24(1987) 159-172.
- ⁶Schee H.A. van der, Ph.D.-Thesis, Wageningen 1984.
- ⁷L.A. Spielman, Viscous interactions in brownian coagulation, *J. of Colloid and Interface Science*, Vol 33, No.4,(1970),p 562-571.
- ⁸E.P.Honig , G.J. Roeberson, P.H. Wiersema, Effect of hydrodynamic interaction on the coagulation rate of hydrophobic colloids, *J. of Colloid and Interface Science*, Vol. 36. No. 1, May 1971, p 97-109.
- ⁹Clayfield E.J., Lumb E.C., Mackey P.H., *J. Colloid Interface Science*, 37 1971) 382.
- ¹⁰J.H.Schenkel, J.A. Kitchener, A test of the Derjaguin- Verwey-Overbeek theory with a colloidal suspension, *Trans. Faraday Soc.*, 56, 161 (1960).
- ¹¹G.Frens and J.T.G. Overbeek, Repeptization and the theory of electrocratic colloids, *J.Colloid and Interface science*, 38(1972)376.
- ¹²Th. Overbeek, in H.R. Kruyt (ed), *Colloid Science I*, p257

¹³Th.Overbeek, in H.R. Kruyt(ed), Colloid Science I, p.254

¹⁴Overbeek Th., Strong and weak points in the interpretation of colloid stability, Advances in Colloid and Interface Science, 16 (1982) p17-30.

CHAPTER 7:

POSSIBLE IMPROVEMENTS IN THE DISPERSION PROCESS OF PIGMENTS IN WATER: PRELIMINARY INVESTIGATION.

7.1 Introduction

The fundamental research in colloid chemistry and the applied research in the industrial research environment are far apart if we consider the approach to problems concerning colloids. But the materials investigated in those disciplines are often the same and that makes it interesting to work in between these two fields of research . From fundamental research certain behaviour of a material can be predicted or explained. The applied research can use such predictions to select the right experiments and to search more effectively for solutions. On the other hand there are many problems in the applied research which are of interest for the fundamental research. So a mutual stimulation of both fields of research is possible. But there is an important barrier between the two fields. The systems investigated in the applied research are complex compared to the systems used in the fundamental research. A full water based paint system for instance contains more than 10 components

Most important ingredients in water based paints:

Binder: latex particles dispersed in water. These particles build the paint film after the latex particles coalesce as the water evaporates.

Water: The continuous phase in which all the particles are dispersed.

Coalescing agents: organic low molecular weight molecules dissolved in the binder particles to speed up the coalescence process.

Anti-foam agents: preventing the formation of stable foam during the application of the paint.

Thickener: large polymers dissolved in the water phase and probably partly adsorbed on the binder particles in order to improve the rheological behaviour of the paint

Titanium dioxide pigment: to give opacity to the paint.

Colored pigment: to give a color to the paint, sometimes these pigments are also oxides (iron oxide), but frequently organic pigments are used.

Dispersing agent: to improve the dispersion degree of the pigment particles.

Fungicides: to prevent the growth of fungicides in the paint.

Anti-blocking agents: The time necessary for drying between painting and piling up is shortened by this agent.

In the fundamental colloid science the oxide/water system is investigated thoroughly and although there are some problems with the theoretical description (see chapter 1), most properties can be explained. In the case of the three component system (oxide/water/polyacrylic acid) as investigated in our work, the number of published experiments is increasing and in recent years even the number of theoretical explanations has increased. But the findings with a three component system cannot be projected on a 15-component system without making mistakes. For this reason the suggestions for a more efficient dispersion process can at best only be intelligent guesses.

The basic problem of a dispersion of oxide pigment in water based paint can be formulated as: The gloss and the opacity of a water based paint is not as good as the gloss and the opacity of the solvent based paint systems. Because the gloss and the opacity of the paint is mainly influenced by the degree of dispersion of the pigment particles, it is important to disperse the pigment agglomerates into the primary particles. There are three approaches to improve the dispersion degree of the pigment in the paint film:

- 1) The wetting of the pigment agglomerates by water could be improved (see chapter 5).
- 2) During the dispersion process the stability of the particles against flocculation is important to prevent reagglomeration under influence of the shear in the milling device. It is also important that the dispersion process is not interfered with by the bridge forming properties of the dispersing agent.
- 3) After the application of the film a number of occurrences can influence the gloss of the dry film: In some paint systems a 'clear layer' is important for the gloss of the dry film. This clear layer is a binder layer at the binder/air interface where no pigment particles are present. For some reason (as yet unknown) the pigment particles avoid the presence of the binder/air interface. Another important factor during the drying process is the 'wetting' of the pigment by the binder. It is possible that, if the pigment is hardly wetted by the binder, the pigment particles are pressed against each other to form aggregates and in so doing decrease the contact area with the binder.

7.2 Theoretical considerations

In this chapter we want to focus attention on the possible interference by the bridge-forming properties of the polyacrylic acid during the dispersion process. Polyacrylic acids are used in various industrial processes as a flocculation agent. The polymer can effect a selective flocculation of positively charged particles by being adsorbed on two particles simultaneously.

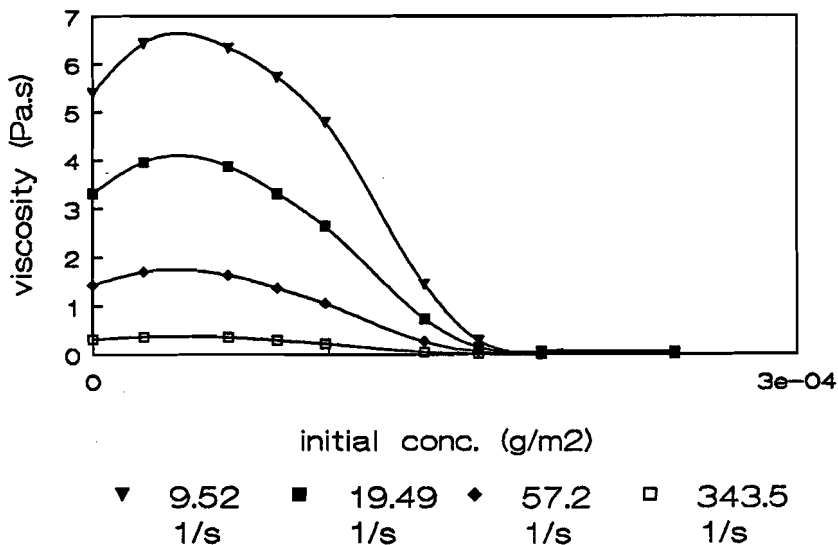


Figure 1: Apparent viscosity of a pigment paste (50 wt%) as a function of the PAA concentration. The PAA concentration is expressed as the total initial concentration (g/l) divided by the surface area of the pigment m²/l. The maximum in viscosity at PAA= 0.5×10^{-4} can be explained by the bridge forming properties of PAA. Titanium dioxide sample=B; PAA=B; pH=7.4

The positive particles can be separated in this way from the negative or uncharged particles. The polyacrylic acids used for this purpose have a molecular weight of about 1,000,000 and are used in low concentrations. The polyacrylic acids used in water based paints have molecular weights of about 10,000. At higher molecular weights the bridging properties are probably too strong, at lower molecular weights the advantages of a polymer decrease (slow desorption from a surface, ability to form loops and tails). But even with a molecular weight of 10,000 bridge forming properties occur (see figure 1). The effect is most striking at low concentrations of polyacrylic acid ($<2 \times 10^{-4}$ g/m³).

At low concentrations the surface is only partly covered with polyacrylic acid and the dangling tails are able to adsorb on the surface of another particle. If the concentration is higher the surface is totally covered with polyacrylic acid and the number of polymers adsorbing on two particles at the same time is decreases. When a pigment dispersion is made in the paint industry the concentration is high enough to cover the whole surface with polyacrylic acid. So in the ideal situation no bridge forming will occur. But in the mixing procedure the situation is far from ideal: The polyacrylic acid is added before all particles are well dispersed, so the polymer molecules adsorb on aggregates. Also concentration gradients can play a role while adding a polymer solution to the dispersion. In a practical situation areas with a low polymer concentration cannot be avoided during a certain period. This period of time may be enough for the polymer to form bridges in the dispersion, because the adsorption process of polymers is fast compared to the desorption process. If the formed bridges are strong enough they will reduce the quality of the pigment dispersion. If the bridge-forming properties of the polymer are an important factor in the dispersion process it would be worthwhile to try to avoid the formation of these bridges.

7.3 Experimental setup

In order to avoid bridge formation during the dispersion process we can take four precautions:

- 1) Disperse the particles before the polyacrylic acid is added. This will prevent the adsorption of polyacrylic acid on aggregates.
- 2) Add the polyacrylic acid under low shear conditions. The higher the frequency of the collisions of particles the higher the change of bridge formation between two particles. At low shear conditions only the collisions caused by the Brownian motion are important.
- 3) Add the polyacrylic solution to a diluted dispersion of the pigment. A normal pigment dispersion contains 50-60 wt% of pigment. The collision rate is very high in such concentrated suspensions. After the diluted dispersion is stabilized with polyacrylic acid, the suspension must be concentrated before it can be used for the further paint formulation.
- 4) Add the polyacrylic acid solution to a dispersion with negative oxide particles. The polyacrylic acid is not adsorbed in large amounts under these conditions and the concentration gradients can be balanced by stirring the dispersion. Then the particles are made positive and the polyacrylic acid adsorbs. With the pigments used in water based paint the particles can be made negative by increasing the pH to 11. The titanium dioxide particles are coated with a layer of Al_2O_3 . The iso-electrical point for this kind of pigment is around pH 8 (see figure 2). After the polyacrylic acid solution is well mixed with the dispersion, the adsorption of the polyacrylic acid takes place as the pH is brought to pH 7. The

particles remain negative during this process because the adsorbed polyacrylic acid overcompensates the positive charge of the oxide. (see figure 2).

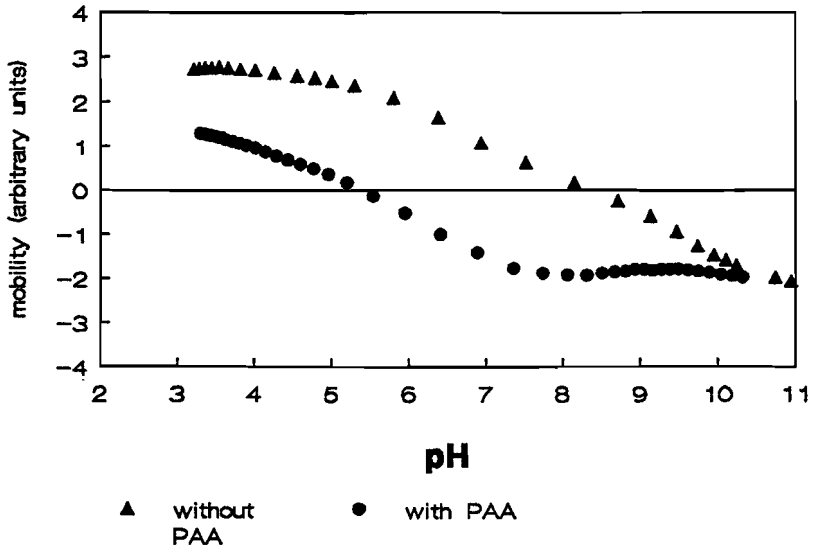


Figure 2: The mobility of the pigment dispersion as used in the experiments in this chapter. The zeta potential of the uncovered particles (triangles) changes from positive at a low pH to zero at pH=8.3 (=iso-electrical point) to negative at high pH's. At a high pH PAA was added to the dispersion and the zeta potential is more negative over the whole pH-range.

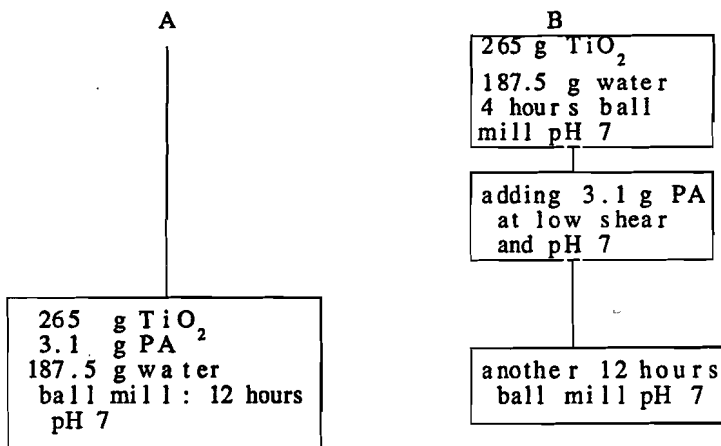
If all four precautions were to be checked on their importance a large number of experiments would be necessary. We only want to do some preliminary experiments and we decided to choose four combinations:

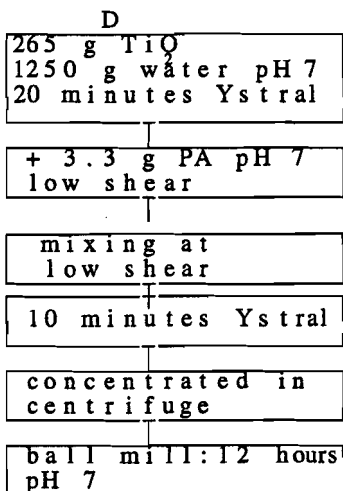
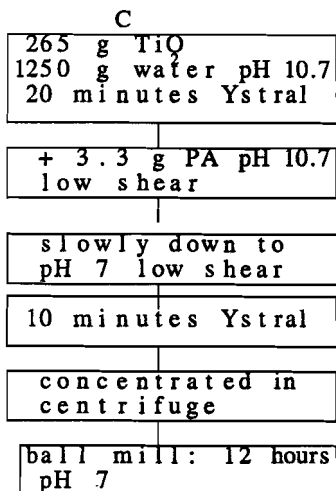
A) Pigment, polyacrylic acid and water are mixed and dispersed at pH 7 in a ball mill for 12 hours.

B) The pigment is dispersed in a concentrated form in a ball mill for 4 hours at pH 7. The solution of polyacrylic acid is added at a low shear rate (only stirring). After the addition the pigment is dispersed in a ball mill for another 12 hours.

C) The pigment is dispersed in a diluted solution at pH 11. The polyacrylic acid is added at low shear rate and the pigment dispersion is brought to pH 7. Then the dispersion is concentrated in a centrifuge and dispersed in a concentrated form in a ball mill for 12 hours.

D) As in C) but the pigment was dispersed at pH 7 and the polyacrylic acid was added at pH 7.





After the dispersion process with only three components other components are added: 39.7 g 1-2 propanediol. 0.7 g biocide 1.3 g anti-foaming agent. The concentrations used correspond with a formula of AKZO-coatings for pigment dispersions with the maximum amount of water. The only variation on this formula was the PAA concentration in pigment dispersion C and D: some extra PAA was added in order to compensate the loss of PAA after concentrating the dilute pigment dispersion. The extra amount of PAA was based on the equilibrium concentration of PAA in the adsorption isotherms in Chapter 2.

7.4 Materials

The materials used for this experiment were all purchased by AKZO-coatings Vilvoorde (Belgium). The materials are normally used as a standard for the dispersion process in testing a new dispersing technique.

The dispersing agent used was probably a co-polymer of acrylic acid and an uncharged monomer. This may be concluded if we compare the titration curve of this polyelectrolyte with the titration curve of a homo-polymeric PAA (figure 3). The maximum charge of the dispersion agent used is about 30 % of the maximum charge possible for a homo-polymer (see chapter 1).

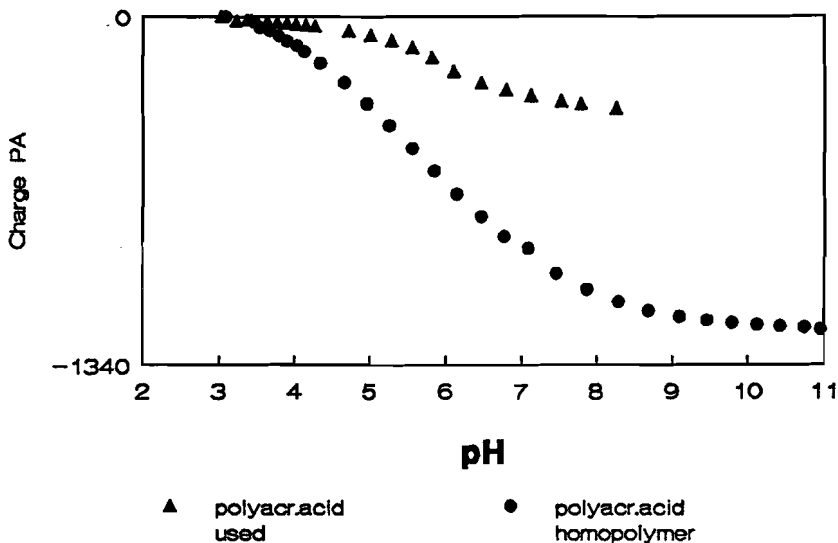


Figure 3: The charge of the polymer used in this chapter compared to the charge of a homo polymer of polyacrylic acid. The charge is expressed as C/g of polymer. Obviously there are less carboxylic acid groups in the chain.

The loops and the tails of such a co-polymer are perhaps more extended compared to the loops and tail of a homo-polymer. More extended loops and tails can increase the stability of the dispersion and so improve the quality of the paint (see chapter 6).

The dispersing agent was purchased as the ammonium salt of the polyacrylic acid (35 wt% solution in water). The titanium dioxide was coated with $\text{Al}_2\text{O}_3/\text{SiO}_2$. But the amount of Al_2O_3 was predominant. The iso-electrical point was 8.3 (figure 2). The 1,2 propanediol was from Merck (>99%). The pH was adjusted with Ammonium hydroxide (13.6 M) and Nitric acid (1 M). The biocide and the anti foaming agent were commercial products used in the paint industry about which no specifications are available.

7.5 Equipment

The concentrated pigment pastes (58 wt%) were dispersed in a agate jar of 250 ml with agate balls. The diluted suspensions (17 wt%) were dispersed in a 1.5 liter double-walled baffled vessel. The vessel was cooled with ethanol of -15°C . The dispergator was a colloid mill (Ystral X40/38 with generator X41/G1 S) used at full speed (22000 rpm). The generator was built of a stator and a rotor with a slit-width of 1 mm a slit-height of 25 mm and a diameter of 35 mm. The mean shear rate in this generator can be estimated by measuring the rate of temperature change in a certain volume of water when the colloid mill is used in an isolated jar. The increase in temperature was 0.2K/s in a volume of 1.2 liter of water. The increase in temperature is also caused by the agitation in the vessel. But this is only a minor contribution. The majority of the energy is dissipated in the slit of the generator. From this energy dissipation a mean shear rate can be estimated with:

$$\bar{\gamma}^2 = \frac{\rho c_p \Delta T V/v}{\eta_0 \Delta t}$$

with ρ : density of the fluid (kg/m^3)
 c_p : specific heat capacity ($\text{J Kg}^{-1}\text{K}^{-1}$)
 $\Delta T/\Delta t$: rate of temperature change (K/s)
 V : total volume of the fluid (m^3)
 v : volume in the slit (m^3)
 η_0 : viscosity of the fluid (Pa s)

With $V/v \approx 500$ and $\Delta T/\Delta t = 0.2 \text{ K/s}$ (measured) the mean shear rate in the slit is about $6 \times 10^5 \text{ s}^{-1}$. Because the transport of the fluid through the generator was about $10^{-4} \text{ m}^3/\text{s}$ the fluid remains in the slit for only 30 ms. For a dispersing time of 20 minutes the number of passages is about 100. So the particles are exposed to the shear of $6 \times 10^5 \text{ s}^{-1}$ for about 3 seconds.

7.6 Results and discussion

The pigment dispersions were formulated to a paint by AKZO-coatings in Vilvoorde (Belgium). The paint only contained the purchased pigment pastes and a pure acrylate binding dispersion. The four paints were tested in a number of experiments. After 5 months the experiments were repeated. The results are presented in tabel 1 Although these experiments are only preliminary some conclusions can be drawn: The most sensitive experiment is the measurement of the gloss at 20° . The viscosity experiments show no significant difference between the four paints. The viscosity of these paints is probably determined by the binder particles and therefore a small difference in aggregation of the pigment particles does not alter the viscosity of the paint. The most

important difference in gloss is obtained between the paints A and B on the onehand and C and D on the other.

	A	B	C	D
Viscosity ICI	2.3	2.2	2.3	2.4
Viscosity KU	114	115	117	116
pH	9.0	9.0	9.0	9.0
Aspect	+	+	+	+
Gloss 20°	59	57	66	67
Gloss 60°	82	82	84	84
After 5 months:		some sediment- ation		
Viscosity ICI	2.0	2.0	2.2	2.0
Viscosity KU	108	111	115	111
Gloss 20°	59	59	64	64
Gloss 60°	80	80	81	81

Tabel 1: Four pigment pastes dispersed according to four different methods are formulated to a paint (only a binder was added). The paint was tested in a number of experiments related to the quality of the pigment dispersion. ICI= viscosity at high shear rates
 KU= viscosity at low shear rates ($\pm 100 \text{ s}^{-1}$). A paint formulated in the same way but using a standard dispersed pigment (AKZO standard procedure) gives a gloss 20°/60° of 68/84.

The better performance of paints C and D is a result of a better dispersed pigment. This result can be explained in three ways:

- The shear rate in the ball mill is not high enough.
- The dispersion time in the ball mill was not long enough.
- The dispersion in a dilute suspension is more efficient compared to a dispersion in a concentrated suspension.

From the limited experiments it is not possible to discriminate between these three explanations.

7.7 Conclusions

Because there is no difference in gloss of paints C and D we may conclude that:

-either the bridge formation is not important and the formed bridges are destroyed at high shear rates.

-or we did not prevent the formation of bridges in case C as we intended to do.

Another result of our experiments is that it is possible to disperse the pigment in a dilute suspension. The dispersing agent (a polyacrylic acid) covers the particles. The pigment can be concentrated by centrifugation to a pigment paste of about 70 wt%. The pigment particles are separated by the adsorbed polymer and the redispersion of this paste is expected to be very easy.

Although these preliminary experiments did not result in a better gloss compared to the gloss obtained with paint formulated according to normal procedures in the paint industry, the experiments are encouraging enough to extend these experiments in the future. Experiments with higher molecular weight PAA-co polymers are particularly promising. High molecular weight PAA-co polymers can provide a more extended hydrodynamic layer on the oxide particles and thus a better steric stabilization of the dispersion. With these high molecular weight polymers bridge formation should be avoided. A first move in this direction has been made in this chapter.

CHAPTER 8:

THE INFLUENCE OF THE DISPERSING AGENT POLYACRYLIC ACID ON TITANIUM DIOXIDE IN WATER BASED PAINTS.

8.1 Introduction

Gloss and opacity of a paint is strongly dependent on the degree of agglomeration of the pigment particles. The commercially available pigments have primary particles with an optimal size for the scattering of light¹. The light scattering will decrease if these particles coagulate. On the other hand aggregates of pigments at the surface of a dry paint film are the most important cause of the loss of gloss of the dry paint. So an optimal dispersion of the pigment in the dry paint film will also give an optimal paint regarding these two parameters. However, before basic chemicals become dry paint film, much occurs that can cause coagulation of pigment particles.

In the case of water based paints the following events are important:

- a) The wetting of the dry pigment aggregate by the water phase during the dispersion process. (see figure 1).
- b) The milling process
- c) The stabilization of the pigment during the dispersion process.
- d) Coagulation by bridge-forming properties of polymers
- e) Coagulation under the influence of Brownian motion during the maintenance of the paint.
- f) Coagulation during the drying process of a paint film.

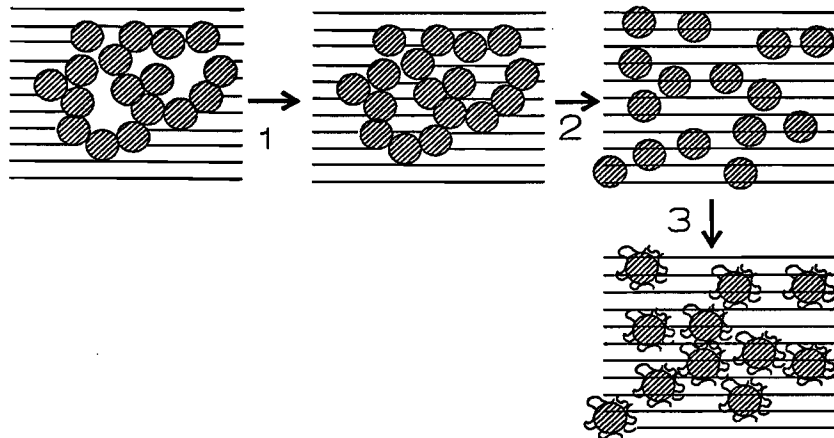


Figure 1: Schematic representation of the dispersion process.

- 1) The wetting of the dry aggregate
- 2) The dispersion of the aggregates
- 3) The stabilization of the single particles against coagulation.

In this chapter we shall discuss the above mentioned events and show the relationship with the rest of the chapters in this thesis.

8.2 The wetting of the dry aggregate by the water phase.

In the case of a water based paint the wetting process of the pigment involves the substitution of air by water in the pigment aggregates. The contact angle solid(S)/liquid(L)/gas(G) (see chapter 5) is an important parameter in describing the wetting behaviour.

All the experiments in chapter 5 gave a contact angle of less than

90° for both the receding as well as the advancing contact angle. The wetting of the aggregates is a spontaneous process² with an advancing contact angle between 0° and about 55°. For contact angles between ±55° and 90° some extra pressure is necessary but if the particles are wetted the process is not spontaneously reversed. In general, therefore, the wetting of oxide pigments in water is not a problem, but perhaps the wetting process and simultaneously the dispersion process can be enhanced by decreasing the contact angle.

Theoretical considerations in chapter 5 suggest that if the contact angle is decreased by an adsorption of the surface active agent in the liquid/gas interface, the decrease of the contact angle has no effect on the driving force of the wetting process. So the usual surfactants like soaps are no candidate. On the otherhand an adsorption of molecules at the liquid/solid interface can increase the driving force in order to enhance the imbibition of water in an aggregate. Polyacrylic acid is such a molecule that adsorbs in the liquid/solid interface (see chapter 2) and is therefore in theory able to decrease the contact angle without adsorption in the liquid/gas interface. The advantage of the use of such a surface active agent is that the PAA is already used in water based paint and that PAA does not increase the foam stability, which is very important during the application of paint. Experiments with PAA in a packed bed with titanium dioxide as well as on a flat surface of titanium dioxide show however that the effect of PAA on the contact angle is not significant.

8.3 The milling process.

Since the milling process is mainly a physical problem we did not pay much attention to this field of research. In chapter 7 some

considerations are written down about dispersing in a dilute or in a concentrated dispersion and a method is described to calculate the mean shear rate in a dispergator by measuring the warming of the dispersion during the dispersion process.

8.4 The stabilization of the pigment during the dispersion process.

In a sheared dispersion of oxide particles both coagulation and separation of particles occur simultaneously. After a certain time an equilibrium situation is obtained. A well dispersed pigment paste is obtained by preventing coagulation during the dispersion process in order to achieve an equilibrium with as many primary particles as possible. In concentrated dispersions the collision frequency is high so in this case the stabilization of the particles against coagulation is very important. There are two mechanisms known in colloid science: electrostatic and steric stabilization (see figure 2).

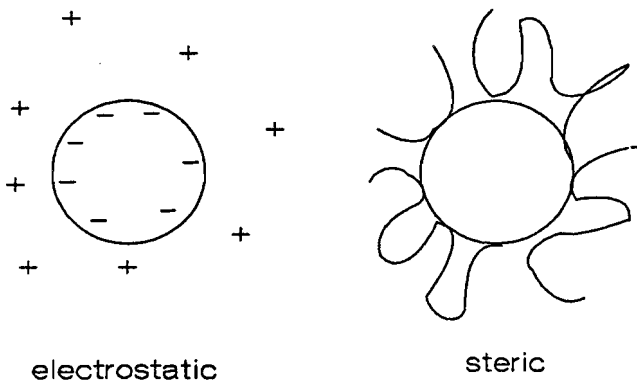


Figure 2: Electrostatic and steric stabilization of a pigment particle.

In the paint industry the effect of the dispersing agent polyacrylic acid on the quality of a pigment dispersion is well known. But it is not clear what mechanism is responsible for this success. In this thesis we hope to contribute to the discussion about the mechanism of stabilization. Insight into the mechanism will make more direct research possible in order to find a better dispersing agent.

Electrostatic stabilization:

As PAA is adsorbed on the surface the charge of the surface is (over) compensated. In the case of an alumina coated pigment particle the zeta potential is changed from positive without adsorbed PAA to negative with polyacrylic acid. The negative charge on the surface is restricted to a maximum value. An increase in the amount of PAA adsorbed does not increase the negative charge on the surface because the extra PAA is adsorbed as an uncharged unit on the surface if a certain coverage of the surface is exceeded (see chapter 2). The zeta potential is for this reason limited to a certain (negative) value. The zeta potentials obtained with PAA can also be obtained using other adsorbing negative ions such as poly phosphates. The performance of paint with pigments dispersed with the aid of poly phosphates is inferior compared to the paints which contain PAA as a dispersing agent. This indicates that the electrostatic stabilization is not the only stabilization mechanism involved. In the literature many attempts have been made to find a relationship between the zeta potential of the pigment particles and the quality of the paint produced with the pigment paste. The fact that the correlation was never satisfactory is another indication that the electrostatic stabilization is not the only mechanism involved. A correlation was found between the concentration needed to obtain a maximum (negative) zeta potential and the minimum in viscosity of a concentrated pigment paste (see chapter 6).

Regarding the limitation in the zeta potential we assume that there is no method to enhance the electrostatic stabilization of the pigment particles using the adsorption of negative polyelectrolytes.

Steric stabilization

In chapter 6 a steric stabilization is found at the higher PAA concentrations. Steric stabilization is caused by a polymer with trains adsorbed on the surface and loops and tails protruding into the solution. In chapter 3 a rather thin layer (3 nm) was found using permeability data of a packed bed of pigment particles. In our opinion this layer causes the increase in the viscosity at concentrations of PAA above the concentration with the minimum in viscosity. Calculations from rheological experiments show an estimated layer thickness of 1 to 5 nm (see chapter 6) which is in the same range as the layer thickness found in chapter 3. This increase in viscosity can in the future perhaps lead to a screening technique for the steric stabilization properties of dispersion agents. But more (fundamental) research is necessary before this technique can be used for this purpose. In the paint industry there is a tendency to use copolymers of acrylic acid with uncharged monomers (see chapter 7). These copolymers are a compromise between the uncharged polymers which adsorb with extended loops and tails and which are therefore suitable for steric stabilization and the charged polyelectrolytes (like PAA) which produce a rather small hydrodynamic layer. The copolymer is probably able to give a more extended layer than the 3 nm found for PAA on titanium dioxide. In further research it will be fruitful to investigate the relation between the performance in paint, the ability to increase the viscosity in the high concentration area and the number of charged and uncharged groups in the polymer.

In chapter 6 the possibility of a synergistic effect of the

hydrodynamic layer on the electrostatic stabilization is discussed. We think that it is plausible that a small hydrodynamic layer has a great influence on the electrostatic stabilization before a real steric stabilization exists. In figure 3 the simultaneous occurrence of electrostatic and steric stabilization is called electrosteric stabilization.

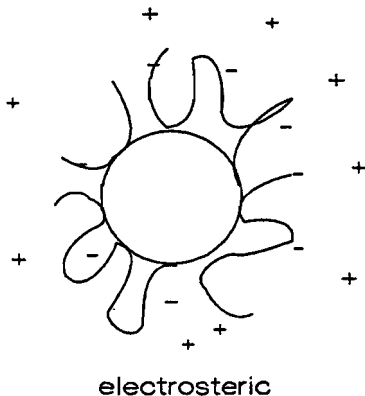


Figure 3: Simultaneous electrostatic and steric stabilization of a pigment particle by a charged polymer.

Some of the dispersing agents used for water based paints are copolymers of PAA and uncharged groups (see chapter 1 and 7). Perhaps these dispersing agents have a better performance because of the combination of the steric stabilization and the electrostatic stabilization.

8.5 Bridge forming properties of polyacrylic acid.

Polyelectrolytes like polyacrylic acid are used in waste water treatment to enhance the flocculation of the solid particles. The

mechanism involved is thought to be the formation of bridges as a polymer adsorbs on two particles simultaneously. The polymers used for this purpose have a high molecular weight (10^6) and are used in small amounts (for example: 3 g/kg dry solid).

The rheological experiments in chapter 6 show an increase in viscosity at the lower PAA concentrations. Although the length of the chain is about 1/10 of the diameter of the particles the dispersion is destabilized by the added PAA. The formed bridges can not be very strong: Even at low shear rates the flocks break up as more PAA is added. At medium and high concentration of PAA the possibility for one polymer molecule to adsorb on two particles at the same time decreases (see figure 4) as a consequence of the higher surface coverage.

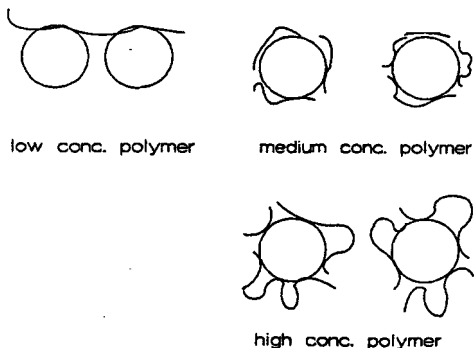


Figure 4: Adsorption of polyelectrolytes at different concentrations. At medium and high concentrations of the polyelectrolyte the change to adsorb on two particles at the same time is decreased.

If higher molecular weights were used the bridges could be so strong that the pigment could not be optimally dispersed even at higher concentrations of PAA. This is probably the reason why a polymer with a molecular weight of about 10.000 is popular as a dispersing agent: This molecular weight is a compromise between

the very low molecular weight PAA without the properties of a polymer and the high molecular weight PAA with the unwanted bridge forming properties. The research for other dispersing agents will therefore be restricted to such medium molecular weight polyelectrolytes unless a molecule is developed that adsorb with one part (anchor) and does not adsorb with the other parts (tails).

8.6 Coagulation under influence of brownian motion

After the dispersion process (high shear) the paint is stored for a long period. During this period coagulation under the influence of brownian motion is possible. The measured ionic strength is about 0.04 M KNO_3 in a water based paint as commercially available (see chapter 6). Under conditions investigated in a pigment/PAA/water system this ionic strength would result in a zeta potential of about -40 mV which is sufficient for electrostatic stabilization. But a water based paint contains over 10 components. In such a complex system it is possible that there are components which influence the stability of the pigment particles. Our investigation was restricted to a three component system. But in the future it would be worth measuring the influence of other components on both the zeta potential as an indication of the electrostatic stabilization and the hydrodynamic layer thickness as an indication of the steric stabilization.

8.7 Coagulation during the drying process of a paint film.

As the water evaporates the ionic strength in the dispersion increases. The starting ionic strength of 0.04 M found in a

commercial water based paint can be increased to such an extent that the electrostatic stabilization is insufficient. Especially under these circumstances it is important that there is another barrier against coagulation like steric stabilization. In chapter 2 the influence of the salt concentration on the adsorption is measured. The adsorption is increased at higher salt concentrations. In chapter 3 the influence of the salt concentration on the layer thickness is measured. The layer thickness decreases with increasing salt concentration. Calculations in chapter 6 however show an important contribution of such a small layer to the stability of the particles at ionic strength between 0.01 and 0.15 M. During the drying process the salt concentration is increased from 0.04 M (24 vol%) to about 0.12 M (50 vol%) before all particles are immobilized. So during the drying of the paint film the synergistic effect of the (small) layer on the electrostatic stabilization is probably important.

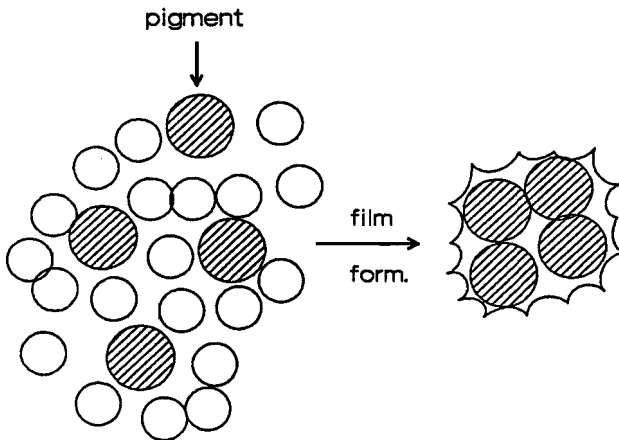


Figure 5: Incorporation of pigment particles in water pockets in the dry paint film.

There is also a possibility that the pigment particles are concentrated in water pockets during the drying process (see figure 5). This process can raise the salt concentration to an even higher level and give an increase in the clustering of the pigment particles. Stability experiments in very dilute systems (chapter 6) show even an increase in stability at an ionic strength at which no electrostatic stabilization is to be expected. At these salt concentrations the only possible stabilization mechanism is the steric stabilization. In chapter 6 a screening technique for the ability of polyelectrolytes to form hydrodynamic layers is proposed.

8.8 Conclusions

- The wetting of the pigment by the water phase is not the limiting factor in the dispersion process of the pigment.
- There are no indications that the wetting can be enhanced.
- The increase in electrostatic stabilization after addition of PAA is limited as a result of the restriction of charged groups of the polymer on the surface. As a consequence additional adsorption of PAA does not result in an increase in zeta potential.
- In a system with only three components (water/pigment/PAA) the electrostatic stabilization of the oxide particles is sufficient to keep the particles apart. The influence of other additives on the electrostatic stabilization is not investigated.
- A simultaneous electrostatic and steric stabilization is observed in dilute dispersions of titanium dioxide/water/PAA systems.
- The formation of a hydrodynamic layer on the oxide particles

- can be the reason for the increase in viscosity at higher concentrations of PAA in concentrated pigment dispersions.
- The layer thickness calculated from the rheological experiments with the concentrated pigment dispersions is of the same order as the hydrodynamic layer obtained from the experiments with a packed bed of titanium dioxide.
 - The rheological experiments can be used as a screening technique for the steric stabilization properties of polyelectrolytes.
 - Especially at the higher electrolyte concentrations the combination of both stabilization mechanisms is important. High electrolyte concentrations are to be expected during the drying process of a paint film.

Literature

¹Stein H.N., Het dekkend vermogen van pigmenten, Verfkroniek, jaargang 59, (1986), nr 12, p 468-471

²Bán S., Wolfram E., Rohrsetzer S., The conditioning of starting liquid imbibition in powders. Colloid and Surfaces, 22 (1987) 301-309.

LIST OF SYMBOLS

A	cross section area of a packed bed [m^2]
A_{sp}	specific surface area [$1/m$]
a	radius of an ion or a particle [m]
b	triangle side length [m]
C_s	capacitance of the stern layer [$C/(Vm^2)$]
c_p	specific heat capacity water [$J/(kg K)$]
e	elementary charge [$1.602 \times 10^{-19} C$]
F	Faraday constant [$9.65 \times 10^7 C/kmol$]
h	slit width [m]
J, J_0	flux of particles towards a central particle (slow coagulation and fast coagulation)
k	Boltzmann constant [$1.38 \times 10^{-23} J/K$]
k	kozeny constant [≈ 4.2]
K, K'	permeability of a packed bed [m^2]
K_a	dissociation constant carboxylic acid [$kmol/m^3$]
L	length of a packed bed [m]
N_{av}	Avogadro constant [$6.022 \times 10^{26} 1/kmol$]
n_0	concentration in the bulk solution [$kmol/m^3$]
PZC	point of zero charge [pH-units]
Q	volume rate of flow [m^3/s]
Q_c	volume rate of flow in one capillary [m^3/s]
R	molar gas constant [$8314.41 J/(K kmol)$]
R (chapter 5)	curvature radius (m)
r_c, r_p	capillary and particle radius [m]
T	absolute temperature [K]
u	particle distance divided by particle radius []
v_l, v_p	velocity of liquid and particles [m/s]
V	total volume [m^3]
v	volume in slit [m^3]
V_a, V_r	attraction energy, repulsion energy [J]
W	stability constant []
x	distance to rotor axis [m]
z	valency of counterions []

LIST OF GREEK SYMBOLS

α	number of charged groups divided by the total number of carboxylic acid groups []
ΔP	pressure difference [Pa]
ΔT	temperature difference [K]
Δt	time difference [s]
ε	porosity= void volume/total volume []
ε_0	permittivity of vacuum [8.8542x10 ⁻¹² F/m]
ε_r	relative permittivity []
ϕ	volume fraction solids [1- ε]
ϕ_{max}	maximum volume fraction of solids [\approx 0.6]
γ	surface tension [N/m]
Γ	amount adsorbed [kmol/m ²]
η	viscosity [Pa s]
η_r	relative viscosity []
η_0	viscosity fluid [Pa s]
[η]	intrinsic viscosity [\approx 2.5]
ψ	potential [V]
ψ_0	surface potential [V]
ψ_d	diffuse double layer potential [V]
λ_0	electrical conductivity fluid
μ	chemical potential [J/kmol]
κ	reciprocal Debye length [1/m]
θ	contact angle [rad]
ρ	particle density [kg/m ³]
ρ_0	fluid density [kg/m ³]
σ_0	surface charge [C/m ²]
σ_d	diffuse charge [C/m ²]
σ_{PAA}	charge calculated from PAA-adsorption [C/m ²]
σ_{pHstat}	charge calculated from pHstat-experiment [C/m ²]
ω	rotation speed [1/s]
ζ	zeta potential [V]
[H ⁺]	concentration of H ⁺ [kmol/m ³]

DANKWOORD

Het is vrijwel ondoenlijk om een complete opsomming te geven van personen, bedrijven en instanties die een bijdrage hebben geleverd bij het tot stand komen van dit proefschrift. In dit dankwoord zal ik daarom voornamelijk de meer formele bijdragen noemen. De personen die een informele bijdrage hebben geleverd hoop ik op een meer informele manier te bedanken.

Mijn beide promotoren Prof.dr. H.N. Stein en Prof.ir. E.L.J. Bancken ben ik zeer erkentelijk voor de begeleiding van de voltooiing van dit proefschrift.

De Onderzoekstimuleringscommissie Verf (OSV) heeft dit onderzoek begeleid namens het Ministerie van Economische Zaken en de Nederlandse verfindustrie, die samen dit onderzoek financieel mogelijk maakten.

Verder dank ik:

De heren M.W.M. Tielemans en R.J. Vis van TDF Tiofine B.V. voor het ter beschikking stellen van pigmenten.

De heer Thys en mevrouw Legros van AKZO Coatings Vilvoorde voor het verwerken van mijn "maalsels" tot complete verven en het uittesten van deze verven met betrekking tot de glans.

Stan Holten en Wies van Diemen voor de experimentele ondersteuning van mijn onderzoek.

Anita Buijs, Peter Maessen en Henk van den Berg die als onderdeel van hun studie een bijdrage leverden aan dit onderzoek.

Mijn ouders hebben via de opvoeding mij een bepaalde dosis eigenwijsheid en vasthoudendheid meegegeven, eigenschappen die niet gemist kunnen worden zeker niet tijdens de schrijffase.

Mijn vrouw Gonda en mijn kinderen Heeltsje en Allard die op bepaalde momenten de moeilijkheden tot de juiste proporties terug wisten te brengen.

CURRICULUM VITAE

Ik ben geboren op 21 juli 1958 te Heerlen. Na het behalen van het VWO-diploma in Maastricht ben ik in 1976 begonnen met de studie Moleculaire Wetenschappen aan de Landbouw Universiteit (toen nog Landbouw Hogeschool) te Wageningen. Als hoofdvakken heb ik Fysische- en Kolloïdchemie en Toxicologie gekozen. Na mijn doctoraal examen in 1985 heb ik anderhalf jaar scheikunde gedoceerd aan de Middelbare Tuinbouwschool te Nijmegen. In 1987 ben ik aangesteld als Toegevoegd Onderzoeker aan de Technische Universiteit Eindhoven. Bij de vakgroep Colloïdchemie en Thermodynamica mocht ik vier jaar onderzoek doen dat uiteindelijk geresulteerd heeft in dit proefschrift. Sinds 1991 ben ik in dienst bij KIWA NV te Nieuwegein.

SUMMARY:

Oxide pigments are important components in paint: The opacity of a dry paint film is determined by the scattering of light of these inert particles. Subsequently the particles contribute to the color of the paint. Pigments are synthesized with an optimal particle size. Coagulation and aggregation of the particles causes a decrease of opacity and a decrease of gloss of the dry paint film. In water-based paints gloss and opacity are improved by addition of a dispersing agent. Frequently ionic poly-electrolytes as polyacrylic acid are used.

In our research the effect of this type dispersing agents on the stability against coagulation of titanium dioxide particles in water is investigated. Because polyacrylic acid is a charged polymer, two mechanism are important: electrostatic stabilization and steric stabilization. Theoretical calculations show a possible synergistic effect of the layer thickness of the adsorbed polymer on the electrostatic stabilization. At low salt concentrations the electrostatic stabilization is the most important mechanism. During the drying process of the paint film the ionic strength is increasing and consequently the electrostatic stabilization is decreasing. Under these circumstances the additional steric stabilization is necessary to prevent coagulation.

Two methods are evaluated in order to measure the hydrodynamic layer thickness of the adsorbed polymer layer. Because the layer is relatively thin (3 nm) the methods normally used to measure the hydrodynamic layer thickness are not applicable. The hydrodynamic layer thickness is an indication for the steric stabilization properties of a dispersing agent. De electrostatic stabilization of the pigment dispersion can be quantified by measuring the zeta potential of the dispersion. A combination of both parameters gives an indication of the working mechanism of a dispersing agent.

A method to obtain monodisperse pigment from a polydisperse sample was found in the so called counter flow centrifugation method.

Some experiments were done in order to measure the contact angle titanium dioxide/solution/air (wetting of the pigment).

SAMENVATTING:

Oxyde-pigmenten zijn belangrijke componenten in verf: het dekkend vermogen van een droge verffilm wordt bepaald door het lichtverstrooiend vermogen van deze inerte deeltjes. Bovendien dragen de deeltjes bij tot de kleur van de verf. De pigmentdeeltjes worden voor dit doel met een optimale deeltjesgrootte gefabriceerd. Treedt er om wat voor reden dan ook een samenklontering (coagulatie en aggregatie) van de deeltjes op, dan neemt het dekkend vermogen van de verf af. Bovendien zorgen aggregaten van pigmenten aan het oppervlak van een droge verffilm voor een vermindering van de glans. In waterverdunbare verf worden glans en dekkend vermogen bevorderd door het toevoegen van een disperseermiddel aan de verf. Vaak worden anionische polyelectrolyten als polyacrylzuur voor dit doel gebruikt.

In dit proefschrift wordt onderzoek beschreven naar het effect van dit type disperseermiddel op de colloïdale stabiliteit van TiO_2 -deeltjes in water. Omdat polyacrylzuur een geladen polymeer is zijn twee mechanismen belangrijk: elektrostatische en sterische stabilisatie. Theoretische berekeningen maken het zeer waarschijnlijk dat de laagdikte van het geadsorbeerde polyelectrolyt voor extra elektrostatische stabilisatie zorgt. Bij lage zoutconcentraties speelt de elektrostatische stabilisatie een overheersende rol. Bij het droogproces van de verf neemt de zoutconcentratie toe en wordt sterische stabilisatie steeds belangrijker.

In dit proefschrift worden twee methoden beschreven voor het meten

van de hydrodynamische laagdikte van de geadsorbeerde polymeer moleculen op het oxyde-oppervlak. Deze laagdikte is vooral belangrijk voor het kwantificeren van een mogelijke sterische stabilisatie van verschillende dispergeermiddelen. De elektrostatische stabilisatie kan in de praktijk van de verbereiding goed gekwantificeerd worden door het meten van de zetapotential. Een combinatie van beide parameters geeft een indruk van de stabiliserende werking van een dispergeermiddel.

Een methode om monodispers pigment af te scheiden uit een heterodispers monster werd gevonden in de zogenaamde "counterflow centrifugation method".

Tenslotte worden nog enkele experimenten met betrekking tot de contacthoek TiO_2 /water/lucht beschreven (bevochtiging pigment).

Stellingen

behorende bij het proefschrift van

S.G.J. Heijman

1. Geadsorbeerde polyacrylzuur-moleculen zorgen niet alleen voor sterische stabilisatie maar versterken ook de electrostatische stabilisatie. (pagina 6-16 tot 6-21 van dit proefschrift)
2. Het "site-binding" model mag niet worden toegepast indien het oxyde een onbekende kwaliteit en kwantiteit aan specifiek geadsorbeerde ionen als verontreiniging bevat. (Acid-base properties of inorganic coated TiO₂ pigments, U. Gesenhues Proceedings XIX Fatipec Kongress Aachen 1988)
3. De hogere viscositeit van oxyde-pigment pasta's bij hogere polyacrylzuur concentraties kan worden verklaard door een polymeerlaag op het pigmentdeeltje van de orde van grootte van de in dit proefschrift gemeten hydrodynamische laagdikte. (Hoofdstuk 3 en 6 van dit proefschrift)
4. Het verbeteren van de bevochtiging van pigmenten door water door middel van het verlagen van de contacthoek levert geen voordelen op voor het dispergeerproces. (hoofdstuk 5 van dit proefschrift)
5. Het inpakken van anorganische pigmentdeeltjes in een organische omhulling door middel van emulsiopolimerisatie dient eerder als het verplaatsen dan als het oplossen van het dispergeerprobleem te worden opgevat. (C.H.M. Caris, Polymer encapsulation of inorganic submicron particles in aqueous dispersion, Ph.D.thesis Eindhoven 1990)

6. Bij het verklaren van verschillen in schuimstabiliteit gemeten bij verschillende temperaturen dient terdege rekening gehouden te worden met de viscositeiten bij deze temperaturen. (S. Ross, Langmuir, volume 1, 1985, p145)
7. Een verklaring van de permeabiliteits vermindering van alumina membranen bij pH 11 kan gevonden worden in het vernielen van de membraan structuur bij deze pH. (M.J. Gieselmann, Langmuir 1992, vol 8, p1342)
8. Enige vorm van projectplanning en tijdsbewaking zou ook voor promotie-onderzoek wenselijk zijn.
9. Omdat dyslexie te maken heeft met een asymmetrische ontwikkeling van de taalcentra in de linker en rechter hersenhelften kan een oorzaak gezocht worden in een asymmetrisch stimulatie van deze centra in het eerste levensjaar. Om deze reden zou het verschil tussen flesgevoede (asymmetrisch stimulatie) en langdurig borstgevoede baby's (symmetrische stimulatie) onderzocht moeten worden.
10. Het gebruik van zeer grote hoeveelheden radioactieve tracers in open proefbasins met het doel deze tracers in het grondwater terug te vinden is verwerpelijk. (Proefstortproject Geuzenhoek, Gent. bezoek in het kader van het CATS-congres maart 1991).
11. Denken in termen van reductie, recyclen en nuttige inzet vóór de productie van een proefschrift levert niet alleen voordelen op voor het milieu maar kan de promovendus ook geld besparen. (bladzijde 0-2 van dit proefschrift)
12. Rugby is better than science (sometimes)